

Version: 000  
May 2017

## Contents

<b>1</b>	<b>Introduction</b>	<b>1</b>
<b>2</b>	<b>TMDs and WW-type approximation</b>	<b>4</b>
2.1	Definition and notation for TMDs and FFs	4
2.2	The classic WW approximation for PDFs	6
2.3	WW-type approximations for TMDs	6
2.4	WW-type approximations for FFs	8
2.5	Tests of classic WW approximation for PDFs in theory	8
2.6	Tests of classic WW approximation for PDFs in DIS experiments	8
2.7	Tests of WW-type approximations for TMDs in effective models	10
2.8	Tests of WW-type approximations for TMDs on the lattice	11
2.9	Tests of WW-type approximations for FFs in models	14
2.10	Limitations of WW-type approximation	14
2.11	Basis functions	14
<b>3</b>	<b>SIDIS in WW-type approximation</b>	<b>15</b>
3.1	The SIDIS process	15
3.2	Phenomenological information on the basis functions	18
3.3	Leading structure functions amenable to WW-type approximations	20
3.4	Subleading structure functions in WW-type approximations	20
<b>4</b>	<b>Leading twist asymmetries and basis functions</b>	<b>20</b>
4.1	Gauss Ansatz and $F_{UU}$ structure function	21
4.2	Leading twist $A_{UU}$ : first test of intrinsic $\mathbf{k}_\perp$ beyond unpolarized case	22
4.3	Leading twist $A_{UT}^{\sin(2\phi_h - \phi_S)}$ Sivers asymmetry	23
4.4	Leading twist $A_{UT}^{\sin(\phi_h + \phi_S)}$ Collins asymmetry	24
4.5	Leading twist $A_{UU}^{\cos(2\phi_h)}$ Boer-Mulders asymmetry	25
4.6	Leading twist $A_{UT}^{\sin(3\phi_h - \phi_S)}$ asymmetry	25
<b>5</b>	<b>Leading twist asymmetries in WW approximation</b>	<b>26</b>
5.1	Leading twist $A_{LT}^{\cos(\phi_h - \phi_S)}$	26
5.2	Leading twist $A_{UL}^{\sin 2\phi_h}$ Kotzinian-Mulders asymmetry	27
<b>6</b>	<b>Subleading twist azimuthal asymmetries in WW-type approximation</b>	<b>28</b>
6.1	Subleading twist $A_{LU}^{\sin \phi_h}$	29
6.2	Subleading twist $A_{LT}^{\cos \phi_h}$	31
6.3	Subleading twist $A_{UL}^{\cos \phi_h}$	32
6.4	Subleading twist $A_{LL}^{\cos(2\phi_h - \phi_S)}$	33
6.5	Subleading twist $A_{UL}^{\sin \phi_h}$	34
6.6	Subleading twist $A_{UU}^{\cos \phi_h}$	35

**ABSTRACT:** We present the complete cross-section for pion production in Semi-Inclusive Deep Inelastic Scattering (SIDIS) in the Wandzura-Wilczek-type approximation up to power-suppressed  $\mathcal{O}(1/Q^2)$  terms. We compute all twist-2 and twist-3 SIDIS structure functions and the corresponding asymmetries. We discuss the applicability of the Wandzura-Wilczek-type approximations on the basis of available data, and make predictions which can be tested by data from Jefferson Lab, COMPASS, HERMES, and the future EIC. The results of this paper can be readily used for phenomenology and for event generators for SIDIS.

**KEYWORDS:** Wandzura-Wilczek-type approximation, semi-inclusive deep inelastic scattering, transverse momentum dependent distribution functions, spin and azimuthal asymmetries, leading and subleading twist

6.7 Subleading twist $A_{UT}^{\sin \phi s}$	37
6.8 Subleading twist $A_{UT}^{\sin(2\phi) - \phi s}$	38
<b>7 Conclusions (0 % okay, PS)</b>	39
<b>8 Acknowledgments</b>	40
<b>A The “minimal basis” of TMDs and FFs</b>	41
A.1 Unpolarised distribution function $f_1^a(x, k_\perp)$ , unpolarised fragmentation function $D_1(z, P_\perp)$	41
A.2 Helicity distribution function $g_1^a(x, k_\perp)$	42
A.3 Sivers function $f_{1T}^{1q}(x, k_\perp)$	42
A.4 Transversity $h_1^q(x, k_\perp)$ and Collins fragmentation function $H_1^{\perp q}(x, P_\perp)$	43
A.5 Boer-Mulders function $h_1^\perp(x, k_\perp)$	44
A.6 Pretzelosity distribution $h_{1T}^\perp(x, k_\perp)$	45
<b>B Convolution integrals and expressions in Gaussian Ansatz</b>	45
B.1 Notation for convolution integrals	46
B.2 Gaussian factors	46

*Chiral factor*

## 1 Introduction

A great deal of what is known about the quark-gluon structure of nucleon is due to studies of parton distribution functions (PDFs), in deeply inelastic reactions. Leading-twist PDFs tell us how likely it is to find an unpolarized parton (described by PDF  $f_1^a(x)$ ,  $a = q, \bar{q}, g$ ) or a longitudinally polarized parton (described by PDF  $g_1^a(x)$ ,  $a = q, \bar{q}, g$ ) in a fast-moving unpolarized or longitudinally polarized nucleon, which carries the fraction  $x$  of the nucleon momentum. This information depends on the “resolution (renormalization) scale” associated with the hard scale  $Q$  of the process. ~~which we will not indicate for notational simplicity.~~ Although the PDFs  $f_1^a(x)$  and  $g_1^a(x)$  continue being the subject of intense research (small- $x$ , large- $x$ , helicity sea and gluon distributions), they can be considered as rather well-known, and the frontier has been extended in the last years to go beyond the one-dimensional picture offered by PDFs.

One way to do this consists in a systematic inclusion of transverse parton momenta  $k_\perp$ , which manifest themselves in certain reactions. It is customary to speak about “intrinsic” transverse momenta, if  $k_\perp \ll Q$ . The formal description is given in terms of transverse momentum dependent distribution functions (TMDs) and fragmentation functions (FFs) which are defined in terms of quark-quark correlators [1–4], and depend on two independent variables: the fraction  $x$  of nucleon momentum carried by parton, and intrinsic transverse momentum  $k_\perp$  of the parton. Being a vector in the plane transverse with respect to the light-cone direction singled out by the hard momentum flow in the process,  $k_\perp$  allows us to access novel information on the spin structure of the nucleon through correlations of  $k_\perp$  with the nucleon spin and/or the parton spin. The latter is a well-defined concept for leading-twist TMDs interpreted in the infinite momentum frame.

*One*

*The* powerful tool to study TMDs are measurements of the SIDIS process. By exploring various possibilities for electron beam and target polarizations unambiguous information can be accessed on the 8 leading-twist TMDs [2] and, if one assumes factorization, on certain linear combinations of the 16 subleading-twist TMDs [3, 4]. Complementary information can be obtained from the Drell-Yan process [5], and  $e^+e^-$  annihilation [6].

In QCD there are no relations among TMDs, and each TMD contains independent information on a different aspect of the nucleon structure. Twist-2 TMDs have clear partonic interpretations, while twist-3 TMDs give valuable insights on quark-gluon correlations in the nucleon [7–9]. ~~besides positivity constraints [10]~~ there is little model-independent information on TMDs. An interesting question with important practical applications at present is whether there exist any useful approximations ~~among~~ TMDs. Experience from the collinear (“ $k_\perp$ -integrated”) PDF case encourages to explore this possibility: the twist-3 PDFs  $g_T^a(x)$  and  $h_T^a(x)$  can be expressed in terms of the twist-2 PDFs  $g_1^a(x)$  and  $h_1^a(x)$ , and additional quark-gluon-quark correlations or current quark mass terms [11, 12]. We shall refer to the latter generically as  $\bar{q}qg$ -terms, but it is important to keep in mind that one deals in different cases with matrix elements of different operators. The  $\bar{q}qg$ -correlations contain new insights on hadron structure which are worthwhile exploring for their own sake, see [13] for the case of  $g_T^a(x)$ . But the striking observation is that the  $\bar{q}qg$ -terms in  $g_T^a(x)$  and  $h_T^a(x)$  are small: theoretical mechanisms predict this [14–17], and in the case of  $g_T^a(x)$  data confirm or are compatible with these predictions [18, 19].

This approximation (“neglect of  $\bar{q}qg$ -terms”) is commonly known as Wandzura-Wilczek (WW) approximation [11]. The possibility to apply this type of approximation also to TMDs has been explored in [20–25]. Both in the case of PDFs and TMDs one basically neglects  $\bar{q}qg$ -terms, but the nature of the omitted matrix elements is different, and one often prefers to speak about WW-type approximations.

In this note we shall address the question what can be said at present about the reliability of WW-type approximations, on the basis of results from theoretical approaches, models, and experiment. We shall in particular address the question to which extent forthcoming or planned experiments will be capable of resolving  $\bar{q}qg$ -terms. Or, to rephrase the question: how far will we be able to arrive with WW-type approximations?

In this paper we will apply WW-type approximations to TMDs, and evaluate the SIDIS cross-section up to twist-3. We will calculate structure functions and the corresponding asymmetries using WW-type approximations. Our results will be spelled out for simplicity assuming Gaussian type behavior in transverse momentum. The results can be modified for other models of transverse momentum dependence. All structure functions computed could be used both in phenomenology to test the validity of WW-type approximations and for event generators for future experiments [26].

The paper is organized as follows: In Subsection 2.2 we briefly remind the reader of the classic WW approximations. In Section 3 we apply WW-type approximations to the complete SIDIS cross-section for pion production. WW-type approximations are listed in Subsection 2.4, theory of WW-type approximations is discussed in Subsection 2.5, models

are discussed in Subsection 2.7 lattice QCD and WW-type approximations are discussed in Subsection 2.8. Classic WW approximations and experimental results are discussed in Subsection 2.6. We derive and discuss the minimal TMD basis for implementation of WW-type approximations in Subsection 3.2. In Subsections 3.3 and 3.4 we derive formulas for leading and subleading structure functions in WW-type approximations.

## 2 TMDs and WW-type approximation

### 2.1 Definition and notation for TMDs and FFs

TMDs are defined in terms of light-front correlators

$$\Phi(x, \mathbf{k}_\perp; ij) = \int \frac{d\xi^- d^2 \xi_T}{(2\pi)^3} e^{i k_\perp \cdot \xi} \left. \langle N(P, S) | \bar{\psi}_j(0) \mathcal{W}_{(0, \infty)} \mathcal{W}_{(\infty, \xi)} \psi_i(\xi) | N(P, S) \rangle \right|_{\xi^+ = 0, k^+ = -P^+} \quad (2.1)$$

where the convention for light-cone coordinates  $a^\pm = (a^0 \pm a^3)/\sqrt{2}$  is used. The symbolically indicated Wilson-link refers to the SIDIS process [27] where the light-cone direction is singled out by the momentum of the virtual photon, and transverse vectors like  $\mathbf{k}_\perp$  are perpendicular to it. In the nucleon rest frame the polarization vector is given by  $S = (0, \mathbf{S}_T, \mathbf{S}_L)$  with  $\mathbf{S}_T^2 + \mathbf{S}_L^2 = 1$ .

The eight leading-twist TMDs [2] are projected out from the correlator (2.1) as follows (color online: red: T-odd; blue: T-even; we suppress flavor and renormalization scale dependence for brevity)

$$\frac{1}{2} \text{Tr} \left[ \gamma^+ \Phi(x, \mathbf{k}_\perp) \right] = f_1 - \frac{\epsilon^{ijk} k_\perp^i S_T^k}{M_N} f_T^\perp \quad (2.2)$$

$$\frac{1}{2} \text{Tr} \left[ \gamma^+ \gamma_5 \Phi(x, \mathbf{k}_\perp) \right] = S_L g_1 + \frac{\mathbf{k}_\perp \cdot \mathbf{S}_T}{M_N} g_T^\perp \quad (2.3)$$

$$\frac{1}{2} \text{Tr} \left[ i \sigma^{ij+} \gamma_5 \Phi(x, \mathbf{k}_\perp) \right] = S_T^j h_1 + S_L \frac{k_\perp^j}{M_N} h_L^\perp + \frac{(k_\perp^j k_\perp^k - \frac{1}{2} \mathbf{k}_\perp^2 \delta^{jk}) S_T^k}{M_N} h_T^\perp + \frac{\epsilon^{ijk} k_\perp^i}{M_N} h_T^\perp \quad (2.4)$$

and the 16 subleading twist TMDs [1, 4] are given by

$$\frac{1}{2} \text{Tr} \left[ 1 \Phi(x, \mathbf{k}_\perp) \right] = \frac{M_N}{P^+} \left[ e - \frac{\epsilon^{ijk} k_\perp^i S_T^k}{M_N} e_T^\perp \right] \quad (2.5)$$

$$\frac{1}{2} \text{Tr} \left[ i \gamma_5 \Phi(x, \mathbf{k}_\perp) \right] = \frac{M_N}{P^+} \left[ S_L e_L + \frac{\mathbf{k}_\perp \cdot \mathbf{S}_T}{M_N} e_T^\perp \right] \quad (2.6)$$

$$\frac{1}{2} \text{Tr} \left[ \gamma^j \Phi(x, \mathbf{k}_\perp) \right] = \frac{M_N}{P^+} \left[ \frac{k_\perp^j}{M_N} f^\perp + \frac{\epsilon^{ijk} S_T^k}{M_N} f_T^\perp + S_L \frac{\epsilon^{ijk} k_\perp^i}{M_N} f_L^\perp + \frac{(k_\perp^j k_\perp^k - \frac{1}{2} \mathbf{k}_\perp^2 \delta^{jk}) \epsilon^{klm} S_T^l}{M_N^2} f_T^\perp \right] \quad (2.7)$$

$$\frac{1}{2} \text{Tr} \left[ \gamma^j \gamma_5 \Phi(x, \mathbf{k}_\perp) \right] = \frac{M_N}{P^+} \left[ S_T^j g_T + S_L \frac{k_\perp^j}{M_N} g_L^\perp + \frac{(k_\perp^j k_\perp^k - \frac{1}{2} \mathbf{k}_\perp^2 \delta^{jk}) S_T^k}{M_N^2} g_T^\perp + \frac{\epsilon^{ijk} k_\perp^i}{M_N} g_L^\perp \right] \quad (2.8)$$

$$\frac{1}{2} \text{Tr} \left[ i \sigma^{jk} \gamma_5 \Phi(x, \mathbf{k}_\perp) \right] = \frac{M_N}{P^+} \left[ \frac{S_T^j k_\perp^k - S_T^k k_\perp^j}{M_N} h_T^\perp - \epsilon^{jk} h_L^\perp \right] \quad (2.9)$$

$$\frac{1}{2} \text{Tr} \left[ i \sigma^{+-} \gamma_5 \Phi(x, \mathbf{k}_\perp) \right] = \frac{M_N}{P^+} \left[ S_L h_L + \frac{\mathbf{k}_\perp \cdot \mathbf{S}_T}{M_N} h_T^\perp \right] \quad (2.10)$$

with the indices  $j, k$  referring to the plane transverse with respect to the light-cone and  $\epsilon_T^{ij} \equiv \epsilon^{-+ij}$  with  $\epsilon^{0123} = +1$ . The Dirac-structures not listed in Eqs. (2.2-2.10) are twist-4

[3]. Integrating out transverse momenta in the correlator (2.1) leads to the ‘‘usual’’ PDFs known from collinear kinematics [12, 28], namely at twist-2 level

$$\frac{1}{2} \text{Tr} [\gamma^+ \Phi(x)] = f_1 \quad (2.11)$$

$$\frac{1}{2} \text{Tr} [\gamma^+ \gamma_5 \Phi(x)] = S_{L,gl} \quad (2.12)$$

$$\frac{1}{2} \text{Tr} [i\sigma^{j+} \gamma_5 \Phi(x)] = S_T^j h_1 \quad (2.13)$$

and at twist-3 level

$$\frac{1}{2} \text{Tr} [1 \Phi(x)] = \frac{M_N}{P_+} e \quad (2.14)$$

$$\frac{1}{2} \text{Tr} [\gamma^j \gamma_5 \Phi(x)] = \frac{M_N}{P_+} S_T^j g_T \quad (2.15)$$

$$\frac{1}{2} \text{Tr} [i\sigma^{j+} \gamma_5 \Phi(x)] = \frac{M_N}{P_+} S_L h_L. \quad (2.16)$$

Other structures drop out either due to explicit  $k_\perp$ -dependence, or due to the sum rules [4]

$$\int d^2 k_\perp f_T(x, k_\perp^2) = \int d^2 k_\perp e_L(x, k_\perp^2) = \int d^2 k_\perp h(x, k_\perp^2) = 0, \quad (2.17)$$

which are imposed by time reversal constraints.

The fragmentation functions are similarly defined in terms of the correlator

$$\Delta(z, \mathbf{P}_\perp)_{ij} = \sum_X \int \frac{d\xi^- d^2 \xi_T}{2z(2\pi)^3} e^{i\xi^- (0) |N_{(-\infty, \xi)} \psi_i(\xi)|_h, X \rangle \langle h, X | \bar{\psi}_j(0) N_{(0, \infty)} |0\rangle} \Big|_{\xi^- = 0, p^- = P_h, z \mathbf{P}_\perp = \mathbf{P}_\perp}. \quad (2.18)$$

In this work we will consider only unpolarized hadrons in the final state. In that case there are 2 leading-twist FFs. If the produced hadron moves fast in the ( $-$ ) light cone direction, the twist-2 FFs are projected out as follows

$$\frac{1}{2} \text{Tr} [\gamma^- \Delta(z, \mathbf{P}_\perp)] = D_1, \quad (2.19)$$

$$\frac{1}{2} \text{Tr} [i\sigma^{j-} \gamma_5 \Delta(z, \mathbf{P}_\perp)] = -e^{jk} \frac{P_h^k}{m_h} H_1^\perp + \frac{\mathbf{P}_\perp^k}{zm_h} \quad (2.20)$$

and at twist-3 level

$$\frac{1}{2} \text{Tr} [1 \Delta(z, \mathbf{P}_\perp)] = \frac{M_h}{P_h} E \quad (2.21)$$

$$\frac{1}{2} \text{Tr} [\gamma^j \Delta(z, \mathbf{P}_\perp)] = \frac{P_h^j}{P_h} D^\perp \quad (2.22)$$

$$\frac{1}{2} \text{Tr} [\gamma^j \gamma_5 \Delta(z, \mathbf{P}_\perp)] = -e^{jk} \frac{P_h^k}{P_h} G^\perp \quad (2.23)$$

$$\frac{1}{2} \text{Tr} [i\sigma^{jk} \gamma_5 \Delta(z, \mathbf{P}_\perp)] = -e^{jk} \frac{M_h}{P_h} H \quad (2.24)$$

where in addition to the scale and flavor dependence we also ~~omit~~ the type of hadron  $h$  for brevity. Integration over transverse hadron momenta leaves us with  $D_1(z), E(z), H(z)$  while the other structures drop out due to their  $P_\perp$  dependence.

## 2.2 The classic WW approximation for PDFs

Having established the notation we now turn to the discussion of the WW-approximation. In principle all three collinear twist-3 PDFs in Eqs. (2.14, 2.15, 2.16) are amenable to this approximation which was established first for  $g_T^a(x)$  in [11], and derived for  $h_L^a(x)$  in [12]. The situation for  $e^a(x)$  is somewhat special, see below and Ref. [29] for a review.

The basis of these approximations is the following. The operators defining  $g_T^a(x)$  and  $h_L^a(x)$  can be decomposed by means of the QCD equations of motion into twist-2 parts, and pure twist-3 (“interaction dependent”)  $\bar{q}qg$ -terms and current quark mass terms. We will denote  $\bar{q}qg$ -terms and mass-terms collectively by functions with a tilde. Such decompositions are possible because  $g_T^a(x)$  and  $h_L^a(x)$  are “twist-3” not according to the “strict QCD definition of twist” (mass dimension of the associated operator minus its spin). Rather they are classified according to the “working twist-definition” of Ref. [30] (a function is “twist  $t$ ” if its contribution to the cross section is suppressed, in addition to kinematic factors, by  $(M/Q)^{t-2}$  with  $Q$  the hard scale in the process and  $M$  the nucleon mass or other generic hadronic scale). In this way one obtains [11, 12]

$$g_T^a(x) = \int_x^1 \frac{dy}{y} g_1^a(y) + \tilde{g}_T^a(x) \stackrel{\text{WW}}{\approx} \int_x^1 \frac{dy}{y} g_1^a(y), \quad (2.25)$$

$$h_L^a(x) = 2x \int_x^1 \frac{dy}{y^2} h_1^a(y) + \tilde{h}_L^a(x) \stackrel{\text{WW}}{\approx} 2x \int_x^1 \frac{dy}{y^2} h_1^a(y), \quad (2.26)$$

where the WW approximations in the last steps result from neglecting the tilde-terms. The case of  $e^a(x)$  is special in the sense that it receives no twist-2 contribution, i.e.

$$xe^a(x) = x\tilde{e}^a(x) \stackrel{\text{WW}}{\approx} 0 \quad (2.27)$$

where a prefactor of  $x$  is provided to cancel a  $\delta(x)$ -type singularity in  $e^a(x)$  [29]. Below we will review theoretical predictions in favor of Eqs. (2.25, 2.26) and experimental results supporting (2.25). Before that we will however introduce the WW-type approximations for TMDs and FFs.

### 2.3 WW-type approximations for TMDs

Analog to the WW approximations discussed in Sec. 2.2, also certain TMDs can be decomposed in twist-2 terms and tilde-terms and one may assume the latter to be negligible in a first approximation [4], keeping in mind one of course deals with different types of  $\bar{q}qg$ -correlations.

In the T-even case one obtains the following approximations, where the terms on the left-hand-side are twist-3, those on the right-hand-side (if any) are twist-2,

$$xe^q(x, k_1^2) \underset{\text{WW-type}}{\approx} 0, \quad (2.28)$$

$$xf^{\perp q}(x, k_1^2) \underset{\text{WW-type}}{\approx} f^{\perp}(x, k_1^2), \quad (2.29)$$

$$xg_L^{\perp q}(x, k_1^2) \underset{\text{WW-type}}{\approx} g^q(x, k_1^2), \quad (2.30)$$

$$xg_T^{\perp q}(x, k_1^2) \underset{\text{WW-type}}{\approx} g_{IT}^{\perp q}(x, k_1^2), \quad (2.31)$$

$$xg_T^{\perp q}(x, k_1^2) \underset{\text{WW-type}}{\approx} g_{IT}^{\perp(1)q}(x, k_1^2), \quad (2.32)$$

$$xh_L^q(x, k_1^2) \underset{\text{WW-type}}{\approx} -2h_{LU}^{\perp(1)q}(x, k_1^2), \quad (2.33)$$

$$xh_T^q(x, k_1^2) \underset{\text{WW-type}}{\approx} -h_T^q(x, k_1^2) - h_{IT}^{\perp(1)}(x, k_1^2), \quad (2.34)$$

$$xh_T^{\perp q}(x, k_1^2) \underset{\text{WW-type}}{\approx} h_T^{\perp}(x, k_1^2) - h_{IT}^{\perp(1)}(x, k_1^2). \quad (2.35)$$

In the T-odd case one obtains the approximations

$$xe_L^q(x, k_1^2) \underset{\text{WW-type}}{\approx} 0, \quad (2.36)$$

$$xe_T^q(x, k_1^2) \underset{\text{WW-type}}{\approx} 0, \quad (2.37)$$

$$xe_T^{\perp q}(x, k_1^2) \underset{\text{WW-type}}{\approx} 0, \quad (2.38)$$

$$xg^{\perp q}(x, k_1^2) \underset{\text{WW-type}}{\approx} 0, \quad (2.39)$$

$$xg_L^{\perp q}(x, k_1^2) \underset{\text{WW-type}}{\approx} 0, \quad (2.40)$$

$$xg_T^{\perp q}(x, k_1^2) \underset{\text{WW-type}}{\approx} f_{IT}^{\perp q}(x, k_1^2), \quad (2.41)$$

$$xf_T^{\perp q}(x, k_1^2) \underset{\text{WW-type}}{\approx} -f_{IT}^{\perp(1)q}(x, k_1^2), \quad (2.42)$$

$$xh_T^q(x, k_1^2) \underset{\text{WW-type}}{\approx} -2h_1^{\perp(1)}(x, k_1^2), \quad (2.43)$$

where the superscript “(1)” denotes the unintegrated transverse moments of TMDs defined generically as

$$f^{(1)}(x, k_1^2) = \frac{k_1^2}{2M^2} f(x, k_1^2), \quad f^{(1)}(x) = \int d^2k_{\perp} f^{(1)}(x, k_1^2). \quad (2.44)$$

Two very useful WW-type approximations follow from combining WW-type approximations (2.32, 2.33) with WW approximations (2.25, 2.26). This yields [1, 23, 31]

$$g_{IT}^{\perp(1)q}(x) \underset{\text{WW-type}}{\approx} x \int_x^1 \frac{dy}{y} g_1^q(y), \quad (2.45)$$

$$h_1^{\perp(1)q}(x) \underset{\text{WW-type}}{\approx} -x^2 \int_x^1 \frac{dy}{y^2} h_1^q(y). \quad (2.46)$$

~~Several~~ theoretical aspects and phenomenological applications of the above WW-type approximations were discussed in [1, 20–25, 31].

## 2.4 WW-type approximations for FFs

No WW-relations exist for the 2 unpolarized twist-2 FFs. However twist-3 FFs can, in analogy to twist-3 TMDs, be approximated as follows [4]

$$E(z, P_\perp^2) \underset{\text{WW-type}}{\approx} 0 \quad (2.47)$$

$$G^\perp(z, P_\perp^2) \underset{\text{WW-type}}{\approx} 0 \quad (2.48)$$

$$D^\perp(z, P_\perp^2) \underset{\text{WW-type}}{\approx} z D_1(z) \quad (2.49)$$

$$H^\perp(z, P_\perp^2) \underset{\text{WW-type}}{\approx} z \frac{P_\perp^2}{M_h^2} H_1^\perp(z, P_\perp) \quad (2.50)$$

In the remainder of this section we will review the results from theory, models, and experiment which support some WW- and/or WW-type approximations.

## 2.5 Tests of classic WW approximation for PDFs in theory

Nonperturbative calculations in the instanton model of the QCD vacuum predict  $\tilde{g}_T^q(x)$  [14] and  $\tilde{h}_T^q(x)$  [15] in (2.25, 2.26) to be strongly suppressed. This semi-classical approach explores that the properties of the QCD vacuum are dominated by instantons that form a strongly interacting but dilute medium: the ratio of the average instanton size  $\rho_{\text{av}}$  and the average instanton separation  $R_{\text{av}}$  is a small parameter. Numerically it is found  $\rho_{\text{av}}/R_{\text{av}} \sim 1/3$  [32, 33], see also [34]. Calculations in the instanton vacuum have shown that the matrix elements of the  $\bar{q}qg$  operators defining  $\tilde{g}_T^q(x)$  [14] or  $\tilde{h}_T^q(x)$  [15] are strongly suppressed by powers of the instanton packing fraction  $\rho_{\text{av}}/R_{\text{av}}$  and negligible with respect to the contributions from the respective twist-2 parts which are of the order  $(\rho_{\text{av}}/R_{\text{av}})^0$ . The instanton calculus has not yet been applied to the case of  $\tilde{g}^q(x)$ .

Also calculations in lattice QCD in the quenched approximation [16] and with  $N_f = 2$  flavors of light dynamical (sea) quarks [17] have given results on Mellin moments on  $\tilde{g}_T^q(x)$  compatible with a small  $\tilde{g}_T^q(x)$ . Below we shall report a test of the WW approximation (2.26) on the basis of recent lattice data, see Sec. 2.8.

We remark that quark models such as the bag model [12, 35–37], spectator models [38], chiral quark-soliton model [23, 39, 40], and light-cone constituent quark models [41] support the approximations (2.25, 2.26) within an accuracy of (10–30) %. It is though difficult to judge to what extent quark model approaches are capable to simulate reliably the effects of the quark-gluon dynamics [12]. Remarkably, in the covariant parton model approach with intrinsic 3D-symmetric parton orbital motion [42, 43] all quark-gluon correlations are absent because the quarks are non-interacting (“parton model”). The phenomenological success of this approach [42] could hint at a general smallness of quark-gluon correlations in parton distribution functions and TMDs, although many of the predictions of this model in the context of TMDs have yet to be tested [43].

## 2.6 Tests of classic WW approximation for PDFs in DIS experiments

The presently available phenomenological information on  $g_T^q(x)$  is due to measurements of the structure function  $g_2(x)$  in DIS off various transversely polarized targets. In the Bjorken

limit  $g_2(x)$  is given by (for brevity we do not indicate the  $Q^2$  dependence)

$$g_2(x) = \frac{1}{2} \sum_a \epsilon_a^2 g_1^a(x) - \frac{1}{2} \sum_a \epsilon_a^2 g_1^a(x). \quad (2.51)$$

Remarkably so far all data on  $g_2(x)$  are compatible with the approximation in Eq. (2.25). At valence- $x$  the data support the WW-approximation within 40 % or better [18, 19]. In the less well measured small- $x$  region a larger violation cannot be excluded. Notice that in this approximation  $g_2(x)$  can be written as a total derivative

$$g_2(x)_{WW} = \frac{d}{dx} \left[ x \int_x^1 \frac{dy}{y} \left( \frac{1}{2} \sum_a \epsilon_a^2 g_1^a(y) \right) \right]. \quad (2.52)$$

The function in  $\left[ \dots \right]$  is defined in terms of the experimentally well known structure function  $\frac{1}{2} \sum_a \epsilon_a^2 g_1^a(x)$  exhibiting a maximum at  $x \sim (0.2\text{--}0.4)$  for  $Q^2 \sim (2\text{--}5)\text{ GeV}^2$  such that  $g_2(x)_{WW}$  has a zero in that region of  $x$ . We present calculations of  $g_2(x)_{WW}$  in Fig. 1.

How well does  $g_2(x)_{WW}$  describe the data with the “error band” of about 40 % deduced in [44]? In order to investigate this, we split the error in two parts  $\varepsilon_1 = \pm 20\%$  and  $\varepsilon_2(x) = \pm 20\% (1-x)$  with a small  $\varepsilon > 0$  and estimate the impact of this uncertainty as

$$g_2(x)_{WW} = (1 \pm \varepsilon_1) \frac{d}{dx} \left[ x \int_x^1 \frac{dy}{y} \left( \frac{1}{2} \sum_a \epsilon_a^2 g_1^a(y(1 \pm \varepsilon_2)) \right) \right]. \quad (2.53)$$

The effect of  $\varepsilon_1$  is to change the magnitude of  $g_2(x)_{WW}$  while  $\varepsilon_2$  varies the position of its zero (the  $x$ -dependence of  $\varepsilon_2$  is necessary to preserve  $g_2(x) \rightarrow 0$  for  $x \rightarrow 1$ ; choosing e.g.  $\varepsilon = 0.05$  ensures that  $\varepsilon_2 \approx 20\%$  up to the highest measured  $x$ -values). These two sources of uncertainty “simulate” the fact that in  $\bar{q}q$  type operators are neglected. The good agreement of  $g_2(x)_{WW}$  with data does not necessarily mean that  $\bar{q}q$  correlations are small, and could also be due to cancellations of possibly more sizable contributions [44]. We also remark that our estimates with the splitted uncertainties  $\varepsilon_{1,2}$  may overestimate the possible (not excluded) violations up to 40 % from [44] in certain  $x$ -regions, but it serves our purpose to give a conservative estimate of possible uncertainties.

Presently no phenomenological information is available on  $h_2^q(x)$ . With phenomenological information on  $h_1^q(x)$  [45–47], the WW approximation (2.26) for  $h_2^q(x)$  could be tested experimentally in the Drell-Yan process [48].

To start with, let us point out [24, 25] that in quark models without gauge field degrees of freedom certain relations among TMDs hold, namely the so-called (quark model) Lorentz-invariance relations (qLIRs). These relations were originally thought to hold in QCD [1, 31]. After hints from models [49, 50] it was realized they are not valid in QCD [51]. The qLIRs are based on decomposing the (completely unintegrated) quark correlator in terms of Lorentz-invariant amplitudes. TMDs are expressed as certain integrals over those amplitudes. Originally, the correlator was decomposed into 12  $A_\mu$  amplitudes [1, 31], i.e. fewer amplitudes than TMDs known at that time, see the review [4], implying relations among TMDs, the qLIRs. In [51] it was shown that the correct Lorentz decomposition requires to consider the effects of gauge links, which generate additional amplitudes [50, 51]. As a result there are as many amplitudes as TMDs and no relations exist. In quark models without explicit gluon degrees of freedom qLIRs must [24, 25] and do [37, 38] hold. In QCD qLIRs do not hold, but “can be justified” in the WW-type approximation [24]. One consequence is that in quark models supporting the classic WW approximations (2.25, 2.26) the WW-type approximations are automatically supported (2.45, 2.46) [24].

The “best tested” WW-type approximations in quark models are in fact (2.45, 2.46). This is so because these approximations involve only the more studied twist-2 objects (systematic studies of all twist-2 and twist-3 TMDs were presented only in few models). The bag, spectator and light-cone constituent quark models support the approximations (2.45, 2.46) within an accuracy of (10–30)% [37, 38, 40, 41]. It is hard to tell how reliably these approaches can model quark-gluon interactions. The bag model supports all WW-type approximations for T-even TMDs within (10–30)% [37]. In the covariant parton model of [43] the (2.45, 2.46) hold exactly, since  $\bar{q}q$ -terms absent in that model [43].

Let us finally discuss quark-target models, where gluonic degrees of freedom are included and WW(-type) approximations typically badly violated [49, 50, 52, 53]. This is a very natural consequence in this class of models for two reasons. First, the neglected terms include quark-mass insertions of  $\mathcal{O}(m_q/M_N)$  negligible in the case of the nucleon, but of  $\mathcal{O}(100\%)$  in a quark target where  $m_q$  plays the role of  $M_N$ . Second, even if one refrains from mass terms the approximations are not supported, see also the discussion in [54] in the context of the classic WW-approximation (2.25). This can be interpreted as ‘perturbative QCD does not support the WW-approximation’. While true, it is difficult to judge what such ‘perturbative insights’ imply for TMDs of real hadrons. What is crucial in this context are dynamical reasons for the smallness of the matrix elements of certain  $\bar{q}q$ -operators. This requires the consideration of chiral symmetry breaking effects reflected in the hadronic spectrum — which is considered in the instanton vacuum model [14, 15], but is out of the scope of quark-target models. We conclude that the violation of WW(-type) approximations in quark-target models implies that these approximations are certainly not preserved under evolution, but such scaling violations do not need to be large and do not need to invalidate the approximations.

## 2.7 Tests of WW-type approximations for TMDs in effective models

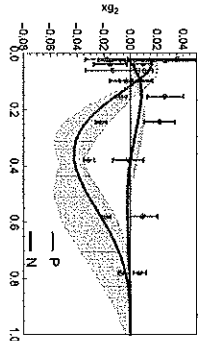


**Figure 1.**  $g_2$  structure function in WW-approximation, Eq. (2.32), for the proton and neutron. The error band procedure is described in the text.

## 2.8 Tests of WW-type approximations for TMDs on the lattice

In recent years, lattice studies of TMD quantities focused on improvements with regard to rigor, realism and methodology [Proceedings of Science LATTICE 2015 (2016) 116, Phys.Rev. D93 (2016) no.5, 054501, Phys.Rev. D91 (2015) 074009, Phys.Rev. D85 (2012) 094510]. However, numerical results from recent calculations are only available for a subset of observables, and the quantities calculated are not in a form that lends itself to straightforward tests of the WW-type relations as presented in this paper. Details about recent works and future perspectives are discussed at the end of this section.

For the time being, we content ourselves with rather crude comparisons based on the data published in Refs. [Phys.Rev. D83 (2011) 094507][55]. These early works explored all nucleon and quark polarizations, but they used a gauge link that does not incorporate the final or initial state interactions present in SIDIS or Drell-Yan experiments. In other words, the transverse momentum dependent quantities that were thus computed on the lattice are not precisely the TMDs measurable in experiment. More caveats will be discussed along the way.

Let us now translate the approximations (2.45, 2.46) into expressions for which we have a chance to compare them with available lattice data. For that we multiply the Eqs. (2.45, 2.46) by  $x^N$  with  $N = 0, 1, 2, \dots$  and integrate over  $x \in [-1, 1]$  which yields

$$\begin{aligned} \int_{-1}^1 dx x^N g_T^{\perp(1)q}(x) &\stackrel{\text{WW-type}}{\approx} \frac{1}{N+2} \int_{-1}^1 dx x^{N+1} g_1^q(x), \\ \int_{-1}^1 dx x^N h_{1L}^{\perp(1)q}(x) &\stackrel{\text{WW-type}}{\approx} -\frac{1}{N+3} \int_{-1}^1 dx x^{N+1} h_1^q(x). \end{aligned} \quad (2.55)$$

with the understanding that negative  $x$  refer to antiquark distributions  $g_1^q(-x) = +g_1^q(-x)$ ,  $h_1^q(-x) = -h_1^q(-x)$ ,  $g_T^{\perp(1)\bar{q}}(-x) = -g_T^{\perp(1)q}(-x)$ ,  $h_{1L}^{\perp(1)\bar{q}}(-x) = +h_{1L}^{\perp(1)q}(-x)$  according to the  $C$ -parity of the involved operators [1]. The right hand sides of Eqs. (2.54, 2.55) are  $x$ -moments of parton distributions, and those can be obtained from lattice QCD using well-established methods based on operator product expansion. The left hand sides are moments of TMDs in  $x$  and  $\mathbf{k}_\perp$ . We have to keep in mind that TMDs diverge for large  $\mathbf{k}_\perp$ . Therefore, without regularizing these divergences in a scheme suitable for the comparison of left and right hand side, a test of the above relations is meaningless, even before we get to address the issues of lattice calculations. Let us not give up at this point and take a look at the lattice observables of Ref. [Phys.Rev. D83 (2011) 094507]. Here, the TMDs are obtained from amplitudes  $\tilde{A}_i(\ell^2, \dots)$  in Fourier space, where  $\mathbf{k}_\perp$  is encoded in the Fourier conjugate variable  $\ell_\perp$ , which is the transverse displacement of quark operators in the correlator evaluated on the lattice. In Fourier-space, the aforementioned divergent behavior for large  $\mathbf{k}_\perp$  translates into strong lattice scale and scheme dependences at short distances  $\ell_\perp$  between the quark operators. The  $\mathbf{k}_\perp$  integrals needed for the left hand sides of Eqs. (2.54, 2.55) correspond to the amplitudes at  $\ell_\perp = 0$ , where scheme and scale-dependence is greatest. In Ref. [Phys.Rev. D83 (2011) 094507], Gaussian fits have been performed to the amplitudes *excluding* data at short quark separations  $\ell_\perp$ . The Gaussians describe the long range data quite well and bridge the gap at short distances  $\ell_\perp$ . Taking the Gaussian fit at  $\ell_\perp = 0$ , we get a value

which is (presumably) largely lattice scheme and scale independent. We have thus swept the problem of divergences under the rug. The Gaussian fit acts as a crude regularization of the divergences that appear in TMDs at large  $\mathbf{k}_\perp$  and manifest themselves as short range artefacts on the lattice. Casting this line of thought into Mathematics, we get

$$\begin{aligned} \int_{-1}^1 dx g_T^{\perp(1)q}(x) &= \int_{-1}^1 dx \int d^2 \mathbf{k}_\perp \frac{\mathbf{k}_\perp^2}{2M^2} g_T^{\perp q}(\mathbf{x}, \mathbf{k}_\perp) = -2\tilde{A}_{1q}(\ell = 0) \stackrel{\text{Gaussian}}{=} -c_{1q}/(2\pi) \\ \int_{-1}^1 dx h_{1L}^{\perp(1)q}(x) &= \int_{-1}^1 dx \int d^2 \mathbf{k}_\perp \frac{\mathbf{k}_\perp^2}{2M^2} h_{1L}^{\perp q}(\mathbf{x}, \mathbf{k}_\perp) = -2\tilde{A}_{10q}(\ell = 0) \stackrel{\text{Gaussian}}{=} -c_{10q}/(2\pi). \end{aligned}$$

We have thus expressed the left hand side of Eqs. (2.54, 2.55) in terms of amplitudes  $c_{7,q}$  and  $c_{10,q}$  of the Gaussian fits on the lattice. Before quoting numbers, a few more comments are in order. The overall multiplicative renormalization had been fixed by setting the Gaussian integral  $c_{2,u-d}$  of the unpolarized TMD  $f_1$  in the isovector channel (u-d) to the nucleon quark content, namely, to 1. The validity the assumption that renormalization is multiplicative and flavor-independent for the non-local lattice operators is under investigation [see Michael Engelhardt's upcoming paper, to be published]. The gauge link that goes into the evaluation of the quark-quark correlator introduces a power divergence that has to be subtracted. The subtraction scheme that was chosen on the lattice is not known to have a clear relation to a "real world" subtraction scheme designed for experimental TMDs and the corresponding gauge link geometry. The gauge link renormalization mainly influences the width of the Gaussian fits; the amplitudes are only slightly affected, so it may not play a big role for our discussion. Altogether, the significance of our numerical "tests" of WW-relations should be taken with a grain of salt.

For the test of Eq. (2.54, we take the following numbers from [Phys.Rev. D83 (2011) 094507]:  $\int dx g_T^{\perp(1)q}(x) \stackrel{\text{Gaussian}}{=} c_{7,q} = 0.1041(85)$  and  $\int dx g_{1T}^{\perp(1)u}(x) \stackrel{\text{Gaussian}}{=} c_{10,u} = -0.0232(42)$

Lattice data for  $\int dx x^N g_1^q(x)$  [56, 57] and  $\int dx x^N h_1^q(x)$  [58] are available for  $N = 0, 1, 2, 3$ . These values have been computed using (quasi-) local operators which have been renormalized to the  $\overline{MS}$  scheme at the scale  $\mu^2 = 4 \text{ GeV}^2$ . According to [57] (data set 4, with  $am_{u,d} = 0.020$  with  $m_\pi \approx 500 \text{ MeV}$ ) one has  $\int dx x g_1^{u+d}(x) = 0.257(10)$  and  $\int dx x g_1^{u+d}(x) = 0.159(14)$ . Decomposing the results from [57] into individual flavors, and inserting them into Eq. (2.54) we obtain

$$\begin{aligned} \underbrace{\int dx g_T^{\perp(1)u}(x)}_{=0.1041(85) \text{ Ref. [cite new]}} &\approx \frac{1}{2} \underbrace{\int dx x g_1^u(x)}_{=0.104(9) \text{ Ref. [57]}}, \\ \underbrace{\int dx g_T^{\perp(1)d}(x)}_{=-0.0232(42) \text{ Ref. [cite new]}} &\approx \frac{1}{2} \underbrace{\int dx x g_1^d(x)}_{=-0.025(9) \text{ Ref. [57]}}, \end{aligned} \quad (2.58)$$

which confirms the approximation (2.54) for  $N = 0$  within the statistical uncertainties of the lattice calculations. In order to test (2.55) we use  $\int dx h_{1L}^{\perp(1)u}(x) = -0.0931(73)$  and

$\int dx h_{1L}^{\perp(1)u}(x) = 0.0130(40)$  from [55] and the lattice data from QCDSF [58]<sup>1</sup>,  $\int dx x h_1^u(x) = 0.28(1)$  and  $\int dx x h_1^g(x) = -0.054(4)$ . Inserting these numbers into (2.55) for the case  $N=0$  we obtain

$$\underbrace{\int dx h_{1L}^{\perp(1)u}(x)}_{=-0.031(73) \text{ Ref. [55]}} \approx -\frac{1}{3} \underbrace{\int dx x g_1^u(x)}_{=-0.093(3) \text{ Ref. [57]}} , \quad \underbrace{\int dx h_{1L}^{\perp(1)d}(x)}_{=0.0130(40) \text{ Ref. [55]}} \approx -\frac{1}{3} \underbrace{\int dx x h_1^u(x)}_{=0.018(1) \text{ Ref. [57]}} . \quad (2.59)$$

which again confirms the WW-type approximation within the statistical uncertainties of the lattice calculations.

Several more comments are in order concerning tle, at first glance, remarkably good confirmation of the WW-type approximations by lattice data in Eqs. (2.58, 2.59).

First, the relations refer to lattice parameters corresponding to pion masses of 500 MeV, but we do not need to worry about that too much. The lattice results do provide a valid test of the approximations in a “hadronic world” with somewhat heavier pions and nucleons, and all that matters in our context is that the relative size of  $\bar{q}q$ -matrix elements is small with respect to  $\bar{q}q$ -matrix elements. (Other lattice artifacts, such as finite lattice spacing and finite volume effects could potentially play a role, but in the context of TMDs such effects are presently beyond systematic control, and we assume the associated uncertainties to be not larger than the statistical error bars of the lattice data.)

Second, we have to revisit carefully which approximations the above lattice calculations actually test. As mentioned above, in the lattice study [57] a specific choice for the path of the gauge link was chosen, which is actually different from the paths required in SIDIS or DY. With the path choice of [57] there are effectively only (T-even)  $A_t$  amplitudes, the  $B_t$  amplitudes are absent. Therefore, see [24, 25] and Sec. 2.7, the test (2.58) of the WW-type approximation (2.54) actually constitutes a test of the WW-approximation (2.25) and confirms earlier lattice work [16, 17]. Similarly, the test (2.59) of the WW-type approximation (2.55) actually constitutes a test of the WW-approximation (2.26). The latter however has not been reported previously in literature, and is a new result.

Third, to be precise: (2.53, 2.59) test the first Mellin moments of the WW approximations (2.25, 2.26), which corresponds to the Burkhardt-Cottingham sum rule for  $g_T^u(x)$  and an analog sum rule for  $h_T^g(x)$ , see [30] and references therein. In view of the long debate on the validity of those sum rules [29, 59, 60], this is an interesting result in itself.

It is important to stress that in view of the pioneering and exploratory status of the TMD lattice calculations [57], this is already a remarkable and very interesting result. Thus, apart from the instanton calculus [15] also lattice data provide support for the validity of the WW approximation (2.26). At the same time, however, we also have to admit that we do not really reach our goal of testing the WW-type approximations on the lattice. With the presently available lattice data this is not yet possible. Future lattice data on higher <sup>1</sup> These numbers are read off from a figure in [58], and were computed on a different lattice. We interpolate them to a common value of the pion mass  $m_\pi \approx 500$  MeV, and estimate the error conservatively in order to take systematic effects into account due to the use of a different lattice.

Mellin moments will provide further insights. Meanwhile we may try to gain insights into the quality of WW-type approximations from experiment.

## 2.9 Tests of WW-type approximations for FFs in models

FFs have been studied in models, but we are not aware of systematic tests of WW-type approximations. One information worth mentioning in this context is that in spectator models [38] tilde-contributions to FFs are proportional to the offshellness of the partons, in complete analogy to the case of TMDs [61, 62]. This natural feature may indicate that in the region dominated by effects of small  $p_T$  the tilde-contributions might be small. On the other hand, in the spectator model the quarks have sizable constituent masses of the order of few hundred MeV and the mass-terms are not small. The applicability of WW-type approximations to the case of FFs remains the least tested point in this approach.

## 2.10 Limitations of WW-type approximation

The experiment will decide how well the WW-type approximations hold. In two instances, however, we already know that there might be limitations due to the sum rules in Eq. (2.17). Let us first discuss the case of  $f_T^u(x, k_\perp)$ . The WW-type approximation (2.42) implies  $x \int d^2 k_\perp f_T^u(x, k_\perp) = -f_{1T}^{\perp(1)u}(x)$  at variance with (2.17) as the Sivers function is not zero. According to the QCD equations of motion  $x f_T^u(x, k_\perp) = x \tilde{f}_T^u(x, k_\perp) - f_{1T}^{\perp(1)u}(x, k_\perp)$  [4] which is the basis for (2.42). The sum rule (2.17) arises because the integrated variant of  $f_T^u(x, k_\perp)$  would be a T-odd(!) PDF but such objects have a straight gauge link and vanish due to time-reversal and parity symmetry of QCD, which is what the sum rule (2.17) states. The resolution is of course that in this case it is essential to keep the tilde-function.

The situation for the chirally and T-odd twist-3 TMD  $h^a(x, k_\perp)$  is completely analogous. The third function in (2.17) is  $e_L^a(x, k_\perp)$  and causes no issues since  $e_L^a(x, k_\perp) = \tilde{e}_L^a(x, k_\perp) \approx 0$  in WW-type approximation. Does this mean WW-type approximations completely fail for  $f_T^a(x, k_\perp)$  and  $h^a(x, k_\perp)$ ? Not necessarily. One has to keep in mind the formal character of the sum rules (2.17) which include integration in the large- $k_\perp$  region where the TMD description does not apply. Thus, issues with the sum rules (2.17) do not need to exclude the possibility that the WW-type approximations for  $f_T^a(x, k_\perp)$  and  $h^a(x, k_\perp)$  in (2.42, 2.43) may work at small  $k_\perp$  where we use them in our TMD approach. Of course, one should keep an eye on all WW-type approximations, and especially for  $f_T^a(x, k_\perp)$  and  $h^a(x, k_\perp)$ .

## 2.11 Basis functions

We close this section by summarizing our findings. In view of the results reviewed in this section we observe that the ‘basis TMDs’  $f_1^u$ ,  $f_{1T}^{\perp u}$ ,  $g_1^u$ ,  $h_1^u$ ,  $h_{1T}^{\perp u}$  and the basis FFs  $D_1^u$ ,  $H_1^{\perp u}$  allow us to express all other TMDs and FFs under the assumption of the validity of the WW-type approximations. We will explore this fact to evaluate SIDIS structure functions in terms of the phenomenological information available on the basis functions.

fein?

### 3 SIDIS in WW-type approximation

In this section we consequently apply the WW-type approximation to SIDIS. It is important to remark that the generalized parton model approach of Ref. [63] provides a description, which is largely equivalent to ours.

#### 3.1 The SIDIS process

We first review the SIDIS process (see also [1, 4, 63] and references therein) sketched in Fig. 2, where  $l$  and  $P$  are momenta of incoming lepton and nucleon, and  $l$  and  $P_h$  are the momenta of the outgoing electron and produced hadron.

The virtual photon momentum  $q = l - l'$  points in the direction of the x-axis from which azimuthal angles are counted. The relevant kinematic invariants are

$$x = \frac{Q^2}{2P \cdot q}, \quad y = \frac{P \cdot P_h}{P \cdot l}, \quad z = \frac{P \cdot P_h}{P \cdot q}, \quad (3.1)$$

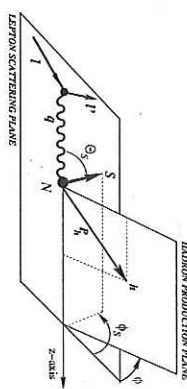
where  $Q^2 = -q^2$ . In addition to  $x, y, z$  the cross section is differential also in the azimuthal angle  $\phi_h$  of the produced hadron, and the square  $P_{hT}^2$  of its momentum component perpendicular to the virtual photon momentum (the cross section is also differential in an azimuthal angle characterizing the overall orientation of the lepton scattering plane, which we omit for simplicity). It is convenient to define the differential cross section as

$$\frac{d^6\sigma_0}{dx dy dz d\phi_h d\phi_h dP_{hT}^2} \equiv \frac{\alpha_{em}^2}{xyQ^2} \left(1 - y + \frac{1}{2}y^2\right) F_{UU}(x, z, P_{hT}^2) \quad (3.2)$$

where  $F_{UU}$  is the structure function due to transverse polarization of the virtual photon (sometimes denoted as  $F_{U,U,T}$ ), and we systematically neglect  $1/Q^2$  corrections due to known kinematic factors and a structure function arising from longitudinal polarization of the virtual photon which is poorly known in SIDIS (and sometimes denoted as  $F_{U,U,L}$ ). Structure functions also depend on the scale  $Q^2$  via scale dependence in TMD functions, we do not show this dependence explicitly in formulas.

To leading order in  $1/Q$  the SIDIS cross-section is then given by

$$\frac{d^6\sigma_{\text{leading}}}{dx dy dz d\phi_h d\phi_h dP_{hT}^2} = \frac{d^6\sigma_0}{dx dy dz d\phi_h d\phi_h dP_{hT}^2} \left\{ 1 + \cos(2\phi_h) p_1 A_{UU}^{\cos(\phi_h)} + S_L \sin(2\phi_h) p_1 A_{UL}^{\sin(2\phi_h)} + S_T \sin(\phi_h) p_3 A_{UT}^{\sin(\phi_h)} + S_T \sin(2\phi_h - \phi_S) p_3 A_{UT}^{\sin(2\phi_h - \phi_S)} + \lambda S_L \cos(\phi_h) p_4 A_{LL}^{\cos(\phi_h)} + \lambda S_T \cos(\phi_S) p_4 A_{LT}^{\cos(\phi_S)} + \lambda S_T \cos(2\phi_h - \phi_S) p_4 A_{LT}^{\cos(2\phi_h - \phi_S)} + \lambda S_T \cos(2\phi_h - \phi_S) p_4 A_{LT}^{\cos(2\phi_h - \phi_S)} \right\} \quad (3.4)$$



$$\text{where, } d\phi_l \simeq d\phi_S. \text{ Neglecting } 1/Q^2 \text{ corrections, the kinematic prefactors } p_i \text{ are given by}$$

$$p_1 = \frac{1-y}{1-y+\frac{1}{2}y^2}, \quad p_2 = \frac{y(1-\frac{1}{2}y)}{1-y+\frac{1}{2}y^2}, \quad p_3 = \frac{(2-y)\sqrt{1-y}}{1-y+\frac{1}{2}y^2}, \quad p_4 = \frac{y\sqrt{1-y}}{1-y+\frac{1}{2}y^2}. \quad (3.5)$$

and the asymmetries are defined as

$$A_{XY}^{\text{weight}} = \frac{F_{YY}^{\text{weight}}}{F_{UU}}. \quad (3.6)$$

Hereby the first index  $X = U(L)$  denotes the unpolarized beam (longitudinally polarized beam with helicity  $\Lambda$ ). The second index  $Y = U(L, T)$  refers to the target which can be unpolarized (or longitudinally, transversely polarized with respect to virtual photon). The superscript "weight" indicates a particular kind of angular  $\phi_h, \phi_S$ -distribution of produced hadrons with no index indicating an isotropic angular distribution. Note that sometimes experimental collaborations define the asymmetries in terms of counts  $N(\phi_h)$  proportional to cross sections. This means the kinematical prefactors  $1/(x; y; Q^2)$  and  $p_1, p_2, p_3$ , or  $p_4$  are included in the numerators or denominators of the asymmetries and averaging over  $y$  within experimental cuts is implied. We will call the corresponding asymmetries  $A_{XY}^{\text{weight}}$ . For instance, focusing on the  $\phi_h$ -dependence, one has in unpolarized case

$$N(\phi) = \frac{N_0}{2\pi} \left( 1 + \cos \phi A_{UU}^{\cos(\phi_h)} + \cos 2\phi A_{UU}^{\cos 2\phi_h} \right) \quad (3.7)$$

where  $N_0$  denotes the total ( $\phi_h$ -averaged) number of counts in the kinematic bin of interest. It would be preferable if the SIDIS asymmetries were analyzed with the known kinematical prefactors divided out on a event-by-event basis. One could then directly compare the  $A_{XY}^{\text{weight}}$  measured in different experiments with different beam energies, different acceptance cuts, etc. and focus on evolution and/or  $1/Q$  suppression for twist-3 observables. In practice, the data analysis is simpler if the kinematical prefactors are included so that most of the data show  $A_{XY}^{\text{weight}}$ . We will comment on this and define the explicit expressions as needed. The structure functions in Eqs. (3.3, 3.4) are described in the Bjorken limit at tree level in terms of convolutions of TMDs and fragmentation functions. We define the unit vector as  $\hat{n} = \mathbf{P}_{hT}/P_{hT}$  and use the following convolution integrals (see Appendix B.1 for details)

$$c \left[ \omega f D \right] = x \sum_a c_a^2 \int d^2 k_\perp d^2 P_\perp \delta^{(2)}(z k_\perp + P_\perp - P_{hT}) \omega \left( \frac{k_\perp}{z} - \frac{P_\perp}{z} \right) f^a(x, k_\perp^2) D^a(z, P_\perp^2). \quad (3.8)$$

**COMPASS** : beam polarized always.

if target long.  $\rightarrow$  also  $S_T \neq 0$  comp.

$$\begin{aligned} A_{LL} &= \sin 2\phi, \quad A_{UL} = \cos(\phi_h - \phi_S), \quad S_T = \sin(\phi_h + \phi_S), \quad A_{LU} = \sin(\phi_h - \phi_S), \\ A_{UU} &= \sin(\phi_h + \phi_S), \quad A_{UT} = \sin(\phi_h - \phi_S), \quad A_{TU} = \sin(\phi_h + \phi_S), \quad A_{TT} = \sin(\phi_h + \phi_S) \end{aligned}$$

The 8 leading in  $1/Q$  structure functions are then given by

The 8 subleading in  $1/Q$  structure functions are given by

$$F_{UU}^{\cos \phi_h} = \frac{2M}{Q} C \left[ \frac{\mathbf{h} \cdot \mathbf{P}_\perp}{zm_h} \left( x h H_1^\perp + \frac{m_h}{M} f_1 \frac{\tilde{D}^\perp}{z} \right) - \frac{\mathbf{h} \cdot \mathbf{k}_\perp}{M} \left( x f^\perp D_1 + \frac{m_h}{M} h_1^\perp \frac{\tilde{H}}{z} \right) \right] \quad (3.17)$$

$$F_{LU}^{\sin \phi_h} = \frac{2M}{Q} C \left[ \frac{\hat{\mathbf{h}} \cdot \mathbf{P}_\perp}{zm_h} \left( x e H_1^\perp + \frac{m_h}{M} f_1 \frac{\tilde{G}^\perp}{z} \right) + \frac{\hat{\mathbf{h}} \cdot \mathbf{k}_\perp}{M} \left( x g^\perp D_1 + \frac{m_h}{M} h_1^\perp \frac{\tilde{E}}{z} \right) \right] \quad (3.18)$$

$$F_{UL}^{\sin \phi_h} = \frac{2M}{Q} C \left[ \frac{\hat{\mathbf{h}} \cdot \mathbf{P}_\perp}{zm_h} \left( x h_L H_1^\perp + \frac{m_h}{M} g_1 \frac{\tilde{G}^\perp}{z} \right) + \frac{\hat{\mathbf{h}} \cdot \mathbf{k}_\perp}{M} \left( x g^\perp D_1 + \frac{m_h}{M} h_1^\perp \frac{\tilde{E}}{z} \right) \right] \quad (3.19)$$

$$F_{LL}^{\cos \phi_h} = \frac{2M}{Q} C \left[ -\frac{\hat{\mathbf{h}} \cdot \mathbf{P}_\perp}{zm_h} \left( x e_L H_1^\perp - \frac{m_h}{M} g_1 \frac{\tilde{D}^\perp}{z} \right) - \frac{\hat{\mathbf{h}} \cdot \mathbf{k}_\perp}{M} \left( x g_1^\perp D_1 + \frac{m_h}{M} h_1^\perp \frac{\tilde{E}}{z} \right) \right] \quad (3.20)$$

$$F_{UT}^{\sin \phi_S} = \frac{2M}{Q} C \left[ x f_T^\perp D_1 - \frac{m_h}{M} h_1^\perp \frac{\tilde{H}}{z} + \frac{\mathbf{P}_\perp \cdot \mathbf{k}_\perp}{2zMm_h} \left( x h_T H_1^\perp + \frac{m_h}{M} g_{1T} \frac{\tilde{G}^\perp}{z} - x h_T^\perp H_1^\perp - \frac{m_h}{M} f_{1T}^\perp \frac{\tilde{D}^\perp}{z} \right) \right] \quad (3.21)$$

$$F_{LT}^{\cos \phi_S} = \frac{2M}{Q} C \left[ -\frac{\mathbf{P}_\perp \cdot \mathbf{k}_\perp}{2zMm_h} \left( x e_T H_1^\perp - \frac{m_h}{M} g_{1T} \frac{\tilde{D}^\perp}{z} + x e_T^\perp H_1^\perp + \frac{m_h}{M} f_{1T}^\perp \frac{\tilde{G}^\perp}{z} \right) \right] \quad (3.22)$$

$$F_{UT}^{\sin(2\phi_h - \phi_S)} = \frac{2M}{Q} C \left[ \frac{2(\hat{\mathbf{h}} \cdot \mathbf{k}_\perp)^2 - \mathbf{k}_\perp^2}{2zM^2} \left( x f_T^\perp D_1 - \frac{m_h}{M} h_1^\perp \frac{\tilde{H}}{z} \right) + \frac{2(\hat{\mathbf{h}} \cdot \mathbf{P}_\perp)(\hat{\mathbf{h}} \cdot \mathbf{k}_\perp) - \mathbf{P}_\perp \cdot \mathbf{k}_\perp}{2zMm_h} \left( x h_T H_1^\perp + \frac{m_h}{M} g_{1T} \frac{\tilde{G}^\perp}{z} + x h_T^\perp H_1^\perp - \frac{m_h}{M} f_{1T}^\perp \frac{\tilde{D}^\perp}{z} \right) \right] \quad (3.23)$$

$$F_{LT}^{\cos(2\phi_h - \phi_S)} = \frac{2M}{Q} C \left[ \frac{2(\hat{\mathbf{h}} \cdot \mathbf{k}_\perp)^2 - \mathbf{k}_\perp^2}{2zM^2} \left( x g_1^\perp D_1 + \frac{m_h}{M} h_1^\perp \frac{\tilde{E}}{z} \right) - \frac{2(\hat{\mathbf{h}} \cdot \mathbf{P}_\perp)(\hat{\mathbf{h}} \cdot \mathbf{k}_\perp) - \mathbf{P}_\perp \cdot \mathbf{k}_\perp}{2zMm_h} \left( x e_T H_1^\perp - \frac{m_h}{M} g_{1T} \frac{\tilde{D}^\perp}{z} - x e_T^\perp H_1^\perp + \frac{m_h}{M} f_{1T}^\perp \frac{\tilde{G}^\perp}{z} \right) \right] \quad (3.24)$$

We remark that twist-3 structure functions in Eqs. (3.17-3.24) contain an explicit factor  $M/Q$ , and recall that we neglect two structure functions due to longitudinal virtual photon polarization which contribute, in the TMD factorization framework, at order  $\mathcal{O}(1/Q^2)$ , one being  $F_{UU,L}$  and the other contributing to the  $\sin(\phi_h - \phi_S)$  angular distribution [4].

### 3.2 Phenomenological information on the basis functions

WW-type approximations are applicable for two out of the 8 twist-2 structure functions and for all twist-3 structure functions (3.17-3.24). As a result, assuming WW-type approximations, all leading and subleading twist structure functions are described in terms of a "basis" which consists of 6 TMDs and 2 fragmentation functions, namely

$$\text{basis: } f_1^a, f_{1T}^a, g_1^a, h_1^a, h_{1T}^a, D_1^a, H_1^{\perp a}. \quad (3.25)$$

Phenomenological information is available for all of these functions at least to some extent. The four TMDs  $f_1^a$ ,  $g_1^a$ ,  $h_1^a$ ,  $D_1^a$  are related to twist-2 collinear functions. The other four TMDs  $f_{1T}^{1a}$ ,  $h_{1T}^{1a}$ ,  $H_{1T}^{1a}$  have no collinear counterparts, and we consider their (1)-moments which are of special interest as they are related to the so-called twist-3 collinear functions **AP: REFERENCE** and enter into the evolution of TMDs **AP: REFERENCE**.

In Fig. 3 we present plots with moments of all these functions. The details of the phenomenological extractions of the basis functions in Eq. (3.25) can be found in Appendix A.

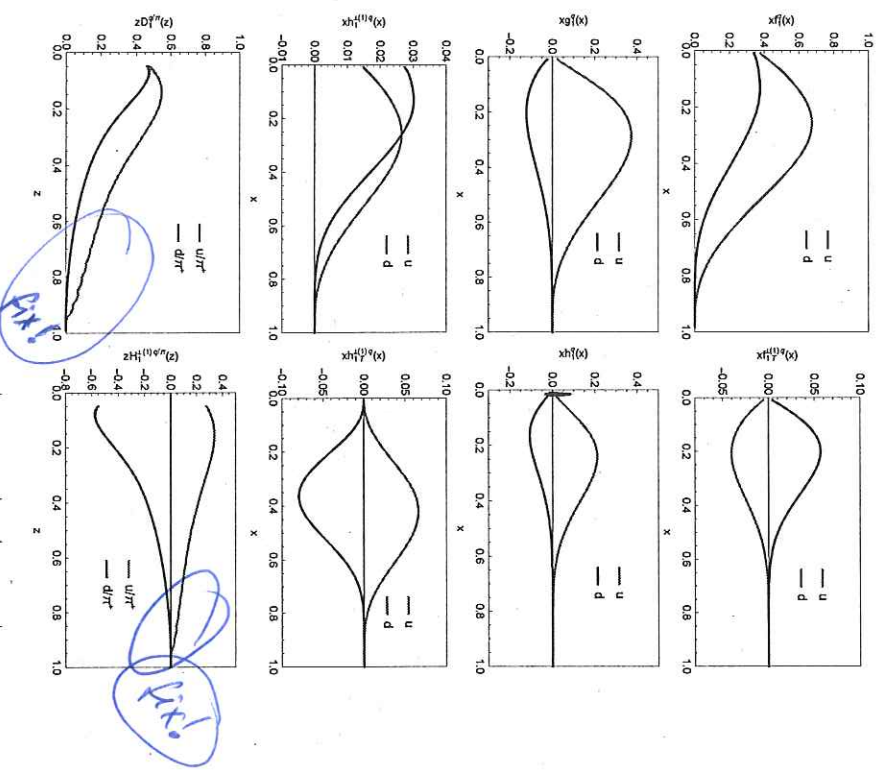


Figure 3. Moments of basis functions  $f_1^a$ ,  $f_{1T}^{1a}$ ,  $g_1^a$ ,  $h_1^a$ ,  $h_{1T}^{1a}$ ,  $D_1^a$ ,  $H_{1T}^{1a}$ .

### 3.3 Leading structure functions amenable to WW-type approximations

The WW- and WW-type approximations are useful for the twist-2 TMDs  $g_{1T}^a$  and  $h_{1L}^a$ , such that (notice that we use here the combinations of the classic WW-approximations and the WW-type approximations)

$$F_{LT}^{\cos(\phi_h - \phi_S)} \stackrel{\text{WW}}{=} C \left[ \frac{\hat{h} \cdot \mathbf{k}_\perp}{M} g_{1T} D_1 \right] \Big|_{g_1^a \rightarrow g_1^a} \quad (3.26)$$

$$F_{UL}^{\sin 2\phi_h} \stackrel{\text{WW}}{=} C \left[ \frac{2(\hat{h} \cdot \mathbf{P}_\perp)(\hat{h} \cdot \mathbf{k}_\perp) - \mathbf{P}_\perp \cdot \mathbf{k}_\perp}{z M m_h} b_{1L} H_1^\perp \right] \Big|_{h_{1L}^a \rightarrow h_1^a} \quad (3.27)$$

### 3.4 Subleading structure functions in WW-type approximations

In the case of the subleading twist structure functions the WW-type approximations in Eqs. (2.28–2.43) lead to considerable simplifications. We obtain the approximations for structure functions

$$F_{LU}^{\sin \phi_h} \stackrel{\text{WW}}{=} 0 \quad (3.28)$$

$$F_{LT}^{\cos \phi_S} \stackrel{\text{WW}}{=} \frac{2M}{Q} C \left[ -x g_T D_1 \right] \Big|_{g_1^a \rightarrow g_1^a} \quad (3.29)$$

$$F_{LL}^{\cos \phi_h} \stackrel{\text{WW}}{=} \frac{2M}{Q} C \left[ -\frac{\hat{h} \cdot \mathbf{k}_\perp}{M} x g_L^\perp D_1 \right] \Big|_{g_1^a \rightarrow g_1^a} \quad (3.30)$$

$$F_{LT}^{\cos(2\phi_h - \phi_S)} \stackrel{\text{WW}}{=} \frac{2M}{Q} C \left[ \frac{2(\hat{h} \cdot \mathbf{k}_\perp)^2 - \mathbf{k}_\perp^2}{2M^2} x g_T^\perp D_1 \right] \Big|_{g_1^a \rightarrow g_1^a} \quad (3.31)$$

$$F_{UL}^{\sin \phi_h} \stackrel{\text{WW}}{=} \frac{2M}{Q} C \left[ \frac{\hat{h} \cdot \mathbf{P}_\perp}{zm_h} x h_U H_1^\perp \right] \Big|_{h_U^a \rightarrow h_1^a} \quad (3.32)$$

$$F_{UU}^{\cos \phi_h} \stackrel{\text{WW}}{=} \frac{2M}{Q} C \left[ \frac{\hat{h} \cdot \mathbf{P}_\perp x h_H H_1^\perp - \hat{h} \cdot \mathbf{k}_\perp x f^\perp D_1}{zm_h} \right] \Big|_{f^\perp a \rightarrow f_1^a, h^a \rightarrow h_1^a} \quad (3.33)$$

$$F_{UT}^{\sin \phi_S} \stackrel{\text{WW}}{=} \frac{2M}{Q} C \left[ x f_T D_1 + \frac{\mathbf{P}_\perp \cdot \mathbf{k}_\perp}{2zMm_h} (x h_T - x h_T^\perp) H_1^\perp \right] \Big|_{f_T^a \rightarrow f_{1T}^a, h_T^a \rightarrow h_1^a} \quad (3.34)$$

$$\begin{aligned} F_{UT}^{\sin(2\phi_h - \phi_S)} &\stackrel{\text{WW}}{=} \frac{2M}{Q} C \left[ \frac{2(\hat{h} \cdot \mathbf{k}_\perp)^2 - \mathbf{k}_\perp^2}{2M^2} x f_T^\perp D_1 + \frac{2(\hat{h} \cdot \mathbf{P}_\perp)(\hat{h} \cdot \mathbf{k}_\perp) - \mathbf{P}_\perp \cdot \mathbf{k}_\perp}{2zMm_h} \right. \\ &\quad \times x(h_T + h_T^\perp) H_1^\perp \Big|_{f_T^a \rightarrow f_{1T}^a, (h_T^a + h_T^\perp a) \rightarrow h_1^a} \quad (3.35) \end{aligned}$$

### 4 Leading twist asymmetries and basis functions

In this section we review how the basis functions describe available SIDIS data. In the subsequent sections will present the predictions obtained from these basis functions in the framework of the WW-type approximation.

#### 4.1 Gauss Ansatz and $F_{UU}$ structure function

Throughout this work we use the so-called Gauss Ansatz for the transverse momentum dependent distribution and fragmentation functions. This Ansatz is popular not only because it considerably simplifies the calculations. In fact, all convolution integrals of the type (3.8) can be solved analytically with this Ansatz. Far more important is the fact that it works phenomenologically with a good accuracy in many practical applications [64–69]. It should be kept in mind that the Gauss Ansatz can, of course, be only a rough approximation. For instance, it is not consistent with general matching expectations when  $k_{\perp}$  becomes large [70]. Nevertheless, if one limits oneself to work in a region where the transverse momenta (of hadrons produced in SIDIS, dileptons produced in the Drell-Yan process, etc) are small with respect to the hard scale in the process, then the Ansatz works quantitatively very well. The most recent and detailed tests were reported in [67], where the Gauss Ansatz was shown to describe the most recent SIDIS data. No deviations could be observed within the error bars of the data provided one takes into account the broadening of the Gaussian widths with increasing energy [67] according with expectations from QCD [71]. Remarkably, the Gauss Ansatz is approximately compatible with the  $k_{\perp}$ -shapes obtained from evolution [71] or fits to high-energy Tevatron data on weak-boson production [72]. On the other end, effective models at low [37, 41] and intermediate [43] energies also support it approximately.

The Gaussian Ansatz for the unpolarized TMD and unpolarized FF is given by

$$f_1^a(x, k_{\perp}^2) = f_1^a(x) \frac{e^{-k_{\perp}^2/(k_{\perp}^2) f_1}}{\pi \langle k_{\perp}^2 \rangle}, \quad (4.1)$$

$$D_1^a(z, P_T^2) = D_1^a(z) \frac{e^{-P_T^2/(P_T^2) D_1}}{\pi \langle P_T^2 \rangle}, \quad (4.2)$$

The parameters  $\langle k_{\perp}^2 \rangle$  and  $\langle P_T^2 \rangle$  can be assumed to be flavor- and  $x$ - or  $z$ -dependent. But present data do not allow us to constrain too many parameters, see App. A.1 for a review.

The structure function  $F_{UU}$  needed for our analysis reads

$$F_{UU}(x, z, P_{hT}) = x \sum_q e_q^2 f_1^q(x) D_q^h(z) g_{UU}(x, z, P_{hT}), \quad (4.3)$$

where we introduce the notation  $g_{UU}(x, z, P_{hT})$  which is basically a Gaussian whose width and normalization are determined by the specific parameters introduced in (4.1, 4.2). Here, and for other structure functions appearing in collinear SIDIS, the normalization is  $\int d^3 p_{hT} g_{UU}(x, z, P_{hT}) = 1$  which correctly connects the structure function  $F_{UU}(x, z, P_{hT})$  with its  $P_{hT}$ -integrated counterpart

$$F_{UU}(x, z) \equiv \int d^2 p_{hT} F_{UU}(x, z, P_{hT}) = x \sum_q e_q^2 f_1^q(x) D_q^h(z) \quad (4.4)$$

This is step is trivial in our effective description, but one has to keep in mind that in QCD the connection of TMDs to PDFs is far more subtle [73].

To streamline the presentation we refer to the comprehensive Appendix for technical details on the used parametrizations for  $f_1^q(x)$  and  $D_1^q(z)$  (see App. A) or formulae for the Gaussians in  $F_{UU}(x, z, P_{hT})$  and other structure functions below (see App. B).



(a)

**Figure 4.** Examples of the description of transverse momenta of hadrons in unpolarized SIDIS.

(a) Differential cross section at  $\langle Q^2 \rangle = 2.37 \text{ GeV}^2$ ,  $\langle x \rangle = 0.24$ ,  $\langle z \rangle = 0.30$  measured at JLab with a 5.75 GeV beam [74]. Theoretical curve from Gauss model following Ref. [67]. (b) Example for HERMES multiplicities (to be created). (c) Example for COMPASS multiplicities (to be created).

#### 4.2 Leading twist $A_{LL}$ : first test of intrinsic $k_{\perp}$ beyond unpolarized case

In this Section we discuss the leading twist double spin asymmetry  $A_{LL} \propto g_{LL}^a D_1^a$  which does not require a WW-type approximation but is important for two reasons. First, we review one of our “basis functions”  $g_L^a(x)$ , and similarly we will review below also other “basis functions.” Second, throughout this work we use the Gaussian Ansatz demonstrated to provide good services in unpolarized case [64–69]. However, nothing is known about the applicability of the Gaussian Ansatz in polarized case. The JLab data [75] on  $A_{LL}(P_{hT})$  put us in the position to conduct a first “test” of our understanding of the  $k_{\perp}$ -behavior of polarized partons. To have an “informed idea” about the Gaussian width of  $g_{LL}(x, k_{\perp})$  we will explore information from the exploratory lattice QCD study of TMDs [55].

We assume Gaussian form for  $g_{LL}^a(x, k_{\perp}^2)$

$$g_{LL}^a(x, k_{\perp}^2) = g_{LL}^a(x) \frac{e^{-P_{hT}^2/(P_{hT}^2) g_{LL}^a}}{\pi \langle k_{\perp}^2 \rangle g_{LL}^a}, \quad (4.5)$$

and resort to the lattice QCD results [55] to gain an estimate on width  $\langle k_{\perp}^2 \rangle_{g_{LL}}$ , see App. A.2.

We will calculate the  $A_{LL}$  asymmetry using the structure functions  $F_{UU}$  and  $F_{LL}$  and compare our results to the experimental data from Ref. [75].

The structure function  $F_{LL}$  reads:

$$F_{LL}(x, z, P_{hT}) = x \sum_q e_q^2 g_L^q(x) D_q^h(z) g_{LL}(x, z, P_{hT}) \quad (4.6)$$

where the factor  $g_{LL}(x, z, P_{hT})$  is given in Eq. (B.9) of Appendix B.

The Double Spin Asymmetry  $A_{LL}$  is then

$$A_{LL}(x, z, P_{hT}) = \frac{F_{LL}(x, z, P_{hT})}{F_{UU}(x, z, P_{hT})}. \quad (4.7)$$

and  $P_{hT}$  integrated asymmetry reads:

$$A_{LL}(x, z) = \frac{\sum_q e_q^2 g_L^q(x) D_q^h(z)}{\sum_q e_q^2 f_1^q(x) D_q^h(z)}. \quad (4.8)$$

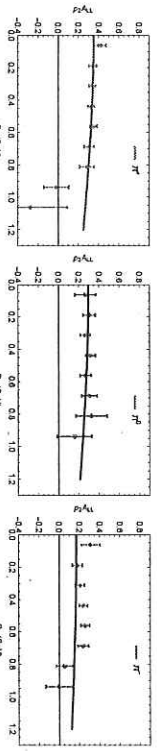


**Figure 5.**  $p_2A_{LL}$  asymmetry compared with Jefferson Lab experimental results Ref. [75] for  $\pi^+$  (left panel) and  $\pi^-$  (right panel). Solid lines are computations with mean values of kinematical variables  $\langle x \rangle = 0.25$ ,  $\langle z \rangle = 0.5$ ,  $\langle Q^2 \rangle = 1.7 \text{ GeV}^2$ .

Jefferson Lab presented experimental results in Ref. [75], and the definition of the asymmetry was:

$$A_{LL}(x, z, P_{hT}) = \frac{y(2-y)}{(1+(1-y)^2)} F_{UU}(x, z, P_{hT}), \quad (4.9)$$

which corresponds to our definition of  $p_2A_{LL}$ , where  $p_2 = y(2-y)/(1+(1-y)^2)$ . We compare results of Ref. [75] and our calculations of  $p_2A_{LL}$  in Fig. 5.

We conclude that lattice QCD results give appropriate description of the experimental data. Encouraged by these findings we will use results of Ref. [55] for  $g_{1T}^{(1)\mu}$  and  $h_{1L}^{\perp(1)\mu}$ , widths in the following sections. Of course, at this point one could argue that if assume the WW- and WW-type approximations allow us to  $g_{1T}$  and  $h_{1L}^{\perp}$  to express those TMDs in terms of  $g_1$  and  $h_1$ , then we could use for them also the same widths as for  $g_1$  and  $h_1$ . In fact, the lattice results for the respective widths are numerically similar, which can be interpreted as yet another argument in favor of the usefulness of the WW-type approximations. The practical predictions depend only weakly on the choice of parameters.

#### 4.3 Leading twist $A_{UT}^{\sin(\phi_h - \phi_S)}$ Sivers asymmetry

The structure function  $F_{UT}^{\sin(\phi_h - \phi_S)}$  reads

$$F_{UT}^{\sin(\phi_h + \phi_S)}(x, z, P_{hT}) = x \sum_q e_q^2 h_1^q(x) H_1^{\perp(1)q/h}(z) \frac{2zP_{hT}m_h}{M^2} G_{UT}^{\sin(\phi_h + \phi_S)}(x, z, P_{hT}) \quad (4.10)$$

where the factor  $G_{UT}^{\sin(\phi_h + \phi_S)}(x, z, P_{hT})$  is given in Eq. (B.14) of Appendix B.

If one calculates the asymmetry as a function of  $P_{hT}$  then the formula is the following

$$A_{UT}^{\sin(\phi_h + \phi_S)}(x, z, P_{hT}) = \frac{F_{UT}^{\sin(\phi_h + \phi_S)}(x, z, P_{hT})}{F_{UU}(x, z, P_{hT})}, \quad (4.14)$$

We can finally derive formulas for  $A_{UT}^{\sin(\phi_h + \phi_S)}$  asymmetry as a function of  $x, z$ :

$$A_{UT}^{\sin(\phi_h + \phi_S)}(x, z) = \frac{A_{UT}^{\sin(\phi_h + \phi_S)} \sum_q e_q^2 h_1^q(x) H_1^{\perp(1)q/h}(z)}{\sum_q e_q^2 f_1^q(x) D_q^h(z)}, \quad (4.15)$$

where the factor  $A_{UT}^{\sin(\phi_h + \phi_S)}$  is given in Eq. (B.15) of Appendix B.

Asymmetries  $A_{UT}^{\sin(\phi_h - \phi_S)}$  for Jefferson Lab 12 GeV are plotted in Fig. 7.

$$A_{UT}^{\sin(\phi_h - \phi_S)}(x, z) = -\frac{A_{UT}^{\sin(\phi_h - \phi_S)} \sum_q e_q^2 f_1^{\perp(1)q}(x) D_1^{q/h}(z)}{\sum_q e_q^2 f_1^q(x) D_q^h(z)}, \quad (4.12)$$

We can finally derive formulas for  $A_{UT}^{\sin(\phi_h - \phi_S)}$  asymmetry as a function of  $x, z$ :

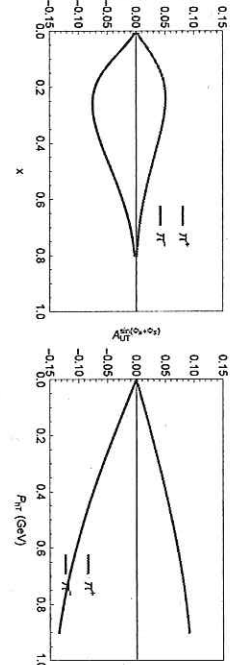


**Figure 7.**  $A_{UT}^{\sin(\phi_h + \phi_S)}$  as a function of  $x$  (left panel), and as a function of  $P_{hT}$  (right panel) at typical kinematics of Jefferson Lab 12 GeV,  $\langle x \rangle = 0.25$ ,  $\langle z \rangle = 0.54$ ,  $\langle Q^2 \rangle = 2.4 \text{ GeV}^2$ .

where the factor  $A_{UT}^{\sin(\phi_h - \phi_S)}$  is given in Eq. (B.17) of Appendix B.

Asymmetries  $A_{UT}^{\sin(\phi_h - \phi_S)}$  for Jefferson Lab 12 GeV are plotted in Fig. 6.

#### 4.5 Leading twist $A_{UU}^{\cos(2\phi_h)}$ Boer-Mulders asymmetry [ok]

The structure function  $F_{UU}^{\cos(2\phi_h)}$  reads

$$F_{UU}^{\cos(2\phi_h)}(x, z, P_{hT}) = x \sum_q e_q^2 h_1^{\perp(1)q}(x) H_1^{\perp(1)q/h}(z) \frac{4z^2 T^2 m_h}{M^3} g_{UU}^{\cos(2\phi_h)}(x, z, P_{hT}) \quad (4.16)$$

where the factor  $G_{UU}^{\cos(2\phi_h)}(x, z, P_{hT})$  is given in Eq. (B.20) of Appendix B. If one calculates the asymmetry as a function of  $P_{hT}$  then the formula is the following

$$A_{UU}^{\cos(2\phi_h)}(x, z, P_{hT}) = \frac{F_{UU}^{\cos(2\phi_h)}(x, z, P_{hT})}{F_{UU}(x, z, P_{hT})} \quad (4.17)$$

We can finally derive formulas for  $A_{UU}^{\cos(2\phi_h)}$  asymmetry as a function of  $x, z$ :

$$A_{UU}^{\sin(2\phi_h)} = A_{UU}^{\cos(2\phi_h)} \frac{\sum_q e_q^2 h_1^{\perp(1)q}(x) H_1^{\perp(1)q/h}(z)}{\sum_q e_q^2 f_1^q(x) D_q^h(z)}, \quad (4.18)$$

where the factor  $A_{UU}^{\cos(2\phi_h)}$  is given in Eq. (B.21) of Appendix B.

Asymmetries  $A_{UU}^{\cos(2\phi_h)}$  for Jefferson Lab 12 GeV are plotted in Fig. 8.

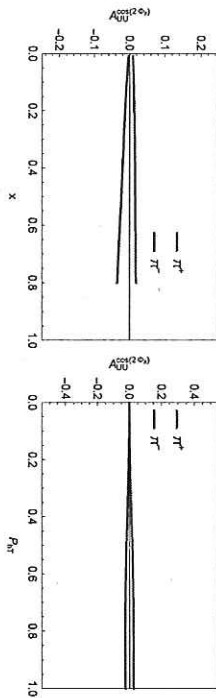


Figure 8.  $A_{UU}^{\cos(2\phi_h)}$  as a function of  $x$  (left panel), and as a function of  $P_{hT}$  (right panel) at typical kinematics of Jefferson Lab 12 GeV,  $\langle x \rangle = 0.25$ ,  $\langle z \rangle = 0.54$ ,  $\langle Q^2 \rangle = 2.4 \text{ GeV}^2$ .

## 5 Leading twist asymmetries in WW approximation

### 5.1 Leading twist $A_{LT}^{\cos(\phi_h - \phi_S)}$ [ok]

Following Ref. [22] we use the following parametrization for  $g_{LT}^{\perp}$

$$g_{LT}^{\perp}(x, k_\perp^2) = g_{LT}^{\perp(1)q}(x) \frac{2M^2}{\pi \langle k_\perp^2 \rangle^2 g_{LT}^{\perp}} e^{-k_\perp^2 / \langle k_\perp^2 \rangle g_{LT}^{\perp}}, \quad (5.1)$$

where  $g_{LT}^{\perp(1)q}(x)$  is computed using Eq. (2.45), and we assume that  $\langle k_\perp^2 \rangle g_{LT}^{\perp} = \langle k_\perp^2 \rangle g_1$  for our numerical estimates.

#### 4.6 Leading twist $A_{UT}^{\sin(3\phi_h - \phi_S)}$ asymmetry

The structure function  $F_{UT}^{\sin(3\phi_h - \phi_S)}$  reads

$$F_{UT}^{\sin(3\phi_h - \phi_S)}(x, z, P_{hT}) = x \sum_q e_q^2 h_{1T}^{\perp(1)q}(x) H_1^{\perp(1)q/h}(z) \frac{2z^3 P_{hT}^3 m_h}{M^4} G_{UT}^{\sin(3\phi_h - \phi_S)}(x, z, P_{hT}) \quad (4.19)$$

where the factor  $G_{UT}^{\sin(3\phi_h - \phi_S)}(x, z, P_{hT})$  is given in Eq. (B.18) of Appendix B. If one calculates the asymmetry as a function of  $P_{hT}$  then the formula is the following

$$A_{UT}^{\sin(3\phi_h - \phi_S)}(x, z, P_{hT}) = \frac{F_{UT}^{\sin(3\phi_h - \phi_S)}(x, z, P_{hT})}{F_{UU}(x, z, P_{hT})} \quad (4.20)$$

We can finally derive formulas for  $A_{UT}^{\sin(3\phi_h - \phi_S)}$  asymmetry as a function of  $x, z$ :

$$A_{UT}^{\sin(3\phi_h - \phi_S)}(x, z) = A_{UT}^{\sin(3\phi_h - \phi_S)} \frac{\sum_q e_q^2 h_{1T}^{\perp(1)q}(x) H_1^{\perp(1)q/h}(z)}{\sum_q e_q^2 f_1^q(x) D_q^h(z)}, \quad (4.21)$$

where the factor  $A_{UT}^{\sin(3\phi_h - \phi_S)}$  is given in Eq. (B.19) of Appendix B. Asymmetries  $A_{UT}^{\sin(3\phi_h - \phi_S)}$  for Jefferson Lab 12 GeV are plotted in Fig. 9.

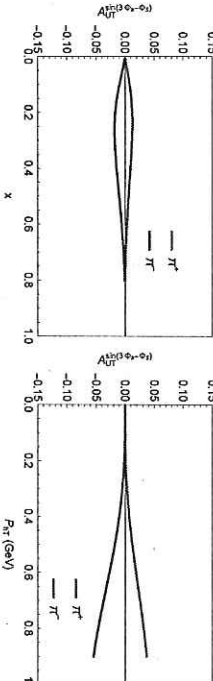


Figure 9.  $A_{UT}^{\sin(3\phi_h - \phi_S)}$  as a function of  $x$  (left panel), and as a function of  $P_{hT}$  (right panel) at typical kinematics of Jefferson Lab 12 GeV,  $\langle x \rangle = 0.25$ ,  $\langle z \rangle = 0.54$ ,  $\langle Q^2 \rangle = 2.4 \text{ GeV}^2$ .

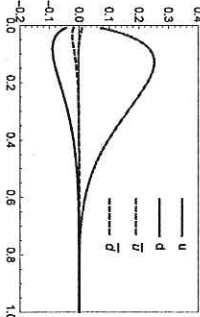
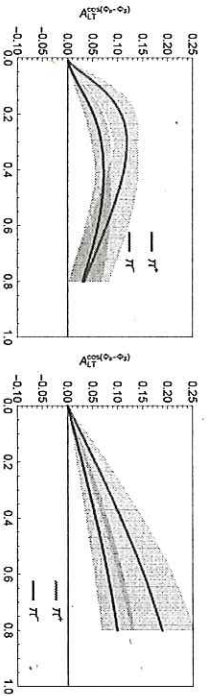


Figure 10.  $g_1^{\perp(1)q}(x)$  distributions.



**Figure 11.**  $A_{LT}^{\cos(\phi_h - \phi_S)}$  as a function of  $x$  (left panel), and as a function of  $P_{hT}$  (right panel) at typical kinematics of Jefferson Lab 12 GeV,  $\langle x \rangle = 0.25$ ,  $\langle z \rangle = 0.54$ ,  $\langle Q^2 \rangle = 2.4$  GeV $^2$ .

Let us remind that  $g_{hT}^q$  enters in the positivity bound [10] for the Sivers function  $f_{1T}^{1,q}$  [76]

$$\frac{k_1^2}{M^2} \left( (g_{1T}^{1,q}(x, k_1^2))^2 + (f_{1T}^{1,q}(x, k_1^2))^2 \right) \leq (f_1^q(x, k_1^2))^2, \quad (5.2)$$

so that it becomes important to measure  $g_{hT}^{1,q}$  in order to refine bounds for the Sivers function. The structure function  $F_{LT}^{\cos(\phi_h - \phi_S)}$  has the following form:

$$F_{LT}^{\cos(\phi_h - \phi_S)}(x, z, P_{hT}) = x \sum_q e_q^2 g_{hT}^{1(1)q}(x) D_q^h(z) \frac{2z P_{hT}}{M} \mathcal{G}_{hT}(x, z, P_{hT}) \quad (5.3)$$

where the factor  $\mathcal{G}_{hT}(x, z, P_{hT})$  is given in Eq. (B.10) of Appendix B.

We can finally derive the  $P_{hT}$  integrated formula for  $\cos(\phi_h - \phi_S)$  asymmetry:

$$A_{LT}^{\cos(\phi_h - \phi_S)}(x, z) = A_{LT}^{\cos(\phi_h - \phi_S)} \frac{\sum_q e_q^2 g_{hT}^{1(1)q}(x) D_q^h(z)}{\sum_q e_q^2 f_1^q(x) D_q^h(z)}, \quad (5.4)$$

where the factor  $A_{LT}^{\cos(\phi_h - \phi_S)}$  is given in Eq. B.11 of Appendix B.

If one calculates the asymmetry as a function of  $P_{hT}$  then the formula is the following

$$A_{LT}^{\cos(\phi_h - \phi_S)}(x, z, P_{hT}) = \frac{F_{LT}^{\cos(\phi_h - \phi_S)}(x, z, P_{hT})}{F_{UU}(x, z, P_{hT})}, \quad (5.5)$$

The helicity distributions  $g_1(x)$  are taken from Ref. [77]. Integrated parton distribution and fragmentation functions,  $f_{q/p}(x)$  and  $D_{h/q}(z)$ , are available in the literature; in particular, we use the GRV98LO PDF set [78] and the DSS fragmentation function set [79]. Resulting distributions  $g_{hT}^q$  are plotted in Fig. 10. The asymmetry  $A_{LT}^{\cos(\phi_h - \phi_S)}$  as a function of  $x$  and  $P_{hT}$  for Jefferson Lab 12 GeV is plotted in Fig. 11.

## 5.2 Leading twist $A_{LT}^{\sin(2\phi_h)}$ , Kotzinian-Mulders asymmetry

**DK**

We assume Gaussian form for Kotzinian-Mulders function  $h_{1L}^{1,q}$ :

$$h_{1L}^{1,q}(x, k_1^2) = h_{1L}^{\perp(1)q}(x) \frac{2M^2}{\pi(k_1^2)^2} e^{-k_1^2/(k_1^2 h_{1L}^{\perp})}, \quad (5.6)$$

We will use WW-type approximation from Eq. (2.46) for calculation of  $h_{1L}^{\perp(1)q}(x)$  and for the estimates of the asymmetry we will use  $\langle k_1^2 \rangle h_{1L}^{\perp} = \langle k_1^2 \rangle h_1 = 0.25$  (GeV $^2$ ).

Positivity bound [10] for  $h_{1L}^q$  includes also Boer-Mulders function  $h_1^{\perp q}$  [2]

$$\frac{k_1^2}{M^2} \left( (h_{1L}^q(x, k_1^2))^2 + (h_1^{\perp q}(x, k_1^2))^2 \right) \leq (f_1^q(x, k_1^2))^2. \quad (5.7)$$

The structure function  $F_{UL}^{\sin(2\phi_h)}$  reads

$$F_{UL}^{\sin(2\phi_h)}(x, z, P_{hT}) = x \sum_q e_q^2 h_{1L}^{\perp(1)q}(x) H_1^{\perp(1)q/h}(z) \frac{4z^2 P_{hT}^2 m_h}{M^3} \mathcal{G}_{UL}^{\sin(2\phi_h)}(x, z, P_{hT}) \quad (5.8)$$

where the factor  $\mathcal{G}_{UL}^{\sin(2\phi_h)}(x, z, P_{hT})$  is given in Eq. (B.12) of Appendix B. If one calculates the asymmetry as a function of  $P_{hT}$  then the formula is the following

$$A_{UL}^{\sin(2\phi_h)}(x, z, P_{hT}) = \frac{F_{UL}^{\sin(2\phi_h)}(x, z, P_{hT})}{F_{UU}(x, z, P_{hT})} \quad (5.9)$$

We can finally derive formulas for  $A_{UL}^{\sin(2\phi_h)}$  asymmetry as a function of  $x, z$ :

$$A_{UL}^{\sin(2\phi_h)} = A_{UL}^{\sin(2\phi_h)} \frac{\sum_q e_q^2 h_{1L}^{\perp(1)q}(x) H_1^{\perp(1)q/h}(z)}{\sum_q e_q^2 f_1^q(x) D_q^h(z)}, \quad (5.10)$$

where the factor  $A_{UL}^{\sin(2\phi_h)}$  is given in Eq. (B.13) of Appendix B. Resulting distributions  $h_{1L}^{\perp q}$  are plotted in Fig. 12.

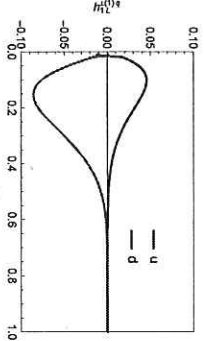


**Figure 12.**  $h_{1L}^{\perp(1)q}$  distributions.

Asymmetries  $A_{UL}^{\sin(2\phi_h)}$  for Jefferson Lab 12 GeV are plotted in Fig. 13.

## 6 Subleading twist azimuthal asymmetries in WW-type approximation

In this Section we will discuss the subleading twist asymmetries in the WW-type approximation. In view of the complex structure of subleading-twist structure functions, see Sec. 3, WW-type approximations might be particularly useful for the interpretation of twist-3 observables. The explicit formulas were worked out in Subsec. 3.4. For all 8 subleading-twist observables the WW-type approximations are useful.

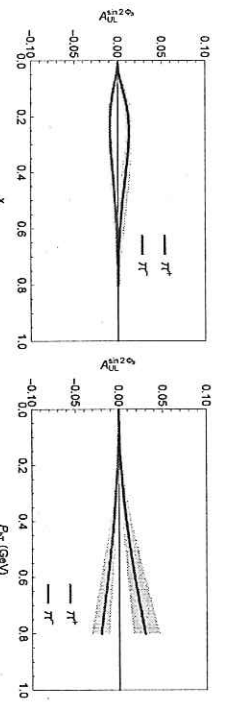


Figure 13.  $A_{LU}^{sin(2\phi_h)}$  as a function of  $x$  (left panel), and as a function of  $P_{hT}$  (right panel) at typical kinematics of Jefferson Lab 12 GeV,  $\langle x \rangle = 0.25$ ,  $\langle z \rangle = 0.54$ ,  $\langle Q^2 \rangle = 2.4$  GeV $^2$ .

### 6.1 Subleading twist $A_{LU}^{sin \phi_h}$ [Ok] (no expression to check → zero intro)

We start our discussion with the asymmetry  $A_{LU}^{sin \phi_h}$ , which at first glance looks like a failure of the WW-type approximation approach. However, we shall see that in fact this observable supports this approach. The asymmetry as given by Eq. (3.18) contains four terms. Two of them are proportional to the pure twist-3 fragmentation functions  $G^{\perp a}$  and  $E^a$  and we neglect them. The remaining two terms are proportional to the twist-3 TMDs  $e^a$  and  $g^{\perp a}$  which, upon the inspection of Eqs. (2.28, 2.39), turn out to be also given in terms of pure twist-3 interaction dependent terms only. Hence, after consequently applying the WW-type approximation we are left with no term. Our approximation predicts this observable to be zero.

Instead, data from Jefferson Lab and HERMES show a small but clearly non-zero effect of the order of magnitude of (2-3)% [80-83]. Does this mean a failure of the WW-type approximation? The answer is no. The important point is that in this (unfortunate, or rather fortunate) case, the entire effect is due to  $\bar{q}q$ -terms only. More precisely, the numerator of the asymmetry is proportional to  $\bar{q}q$ -correlators, while the denominator is of course give by  $f_1^a D_1^a$ , i.e. in terms of  $qq$ -correlators. Therefore we may formulate this approximation as follows

$$A_{LU}^{sin \phi_h} \propto \frac{\langle \bar{q}q \rangle}{\langle \bar{q}q \rangle} = \mathcal{O}((2-3)\%). \quad (6.1)$$

We should keep in mind several reservations. First, also kinematical prefactors and cuts are included in experimental result quoted in (6.1). Second, the denominator contains  $f_1^a$  and  $D_1^a$  which are the largest TMD and the largest fragmentation function because of positivity constraints. Third, the numerator is a sum of four terms, i.e. its smallness could also results from partial cancellations between different terms, rather than indicate that all 4 terms are small. Keeping all these reservations cautiously in mind, we may nevertheless consider the experimental observation of a (2-3)% asymmetry  $A_{LU}^{sin \phi_h}$  [80-83] as an encouraging indication that  $\bar{q}q$ -terms are smaller than  $qq$  terms.

To conclude, the WW-type approximation does not fail in the case of  $A_{LU}^{sin \phi}$ . It only is not well applicable in this case because there is no “leading order” (no  $\bar{q}q$  term) with respect to which the neglect of  $\bar{q}q$  terms would constitute a “reasonable” approximation [24, 25].

The beam spin asymmetry of the observed size, if it does not support it, is at least not in contradiction with our approximation. We notice that one obtains a zero result for this asymmetry in the parton model motivated approach limited to leading twist TMDs [63]. COMPASS: <https://arxiv.org/pdf/1401.6284.pdf>  
data: <https://hepdata.net/record/insl278730>

### 6.2

#### Subleading twist $A_{LT}^{\cos\phi_S}$

This double spin asymmetry actually does not require to use the TMD formalism. In fact, one may sum over all hadron transverse momenta, such that the structure function is given in terms of the collinear twist-3 PDF  $g_T^q(x)$  and the unpolarized fragmentation function, and if we sum over all final state hadron we obtain the DIS structure function discussed in detail in Sec. 2.6.

We present our estimates for  $F_{LT}^{\cos\phi_S}(x)$

$$F_{LT}^{\cos\phi_S} = \frac{2M}{Q} c \left[ -x g_T D_1 \right] \Big|_{g_T^a \rightarrow g_T^a} \quad (6.2)$$

in Fig. XYZ and a compare to preliminary COMPASS data [84, 85].

The structure function  $F_{LT}^{\cos\phi_S}$  reads

$$F_{LT}^{\cos\phi_S}(x, z, P_{hT}) = -\frac{2M}{Q} x \sum_q e_q^2 g_T^{1(1)q}(x) D_1^{q/h}(z) g_{LT}^{\cos\phi_S}(x, z, P_{hT}) \quad (6.3)$$

where the factor  $g_{LT}^{\cos\phi_S}(x, z, P_{hT})$  is given in Eq. (B.22) of Appendix B. If one calculates the asymmetry as a function of  $P_{hT}$  then the formula is the following

$$A_{LT}^{\cos\phi_S}(x, z, P_{hT}) = \frac{F_{LT}^{\cos\phi_S}(x, z, P_{hT})}{F_{UU}(x, z, P_{hT})} \quad (6.4)$$

We can finally derive formulas for  $A_{LT}^{\cos(\phi_S)}$  asymmetry as a function of  $x, z$ :

$$A_{LT}^{\cos\phi_S} = -\frac{2M}{Q} \sum_q e_q^2 g_T^{1(1)q}(x) D_1^{q/h}(z) \quad (6.5)$$

Asymmetries  $A_{LT}^{\cos\phi_S}$  for Jefferson Lab 12 GeV are plotted in Fig. 14.

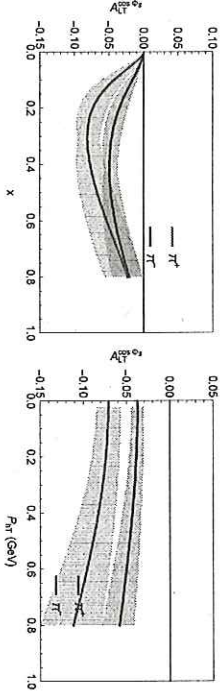


Figure 14.  $A_{LT}^{\cos\phi_S}$  as a function of  $x$  (left panel), and as a function of  $P_{hT}$  (right panel) at typical kinematics of Jefferson Lab 12 GeV,  $\langle x \rangle = 0.25$ ,  $\langle z \rangle = 0.54$ ,  $\langle Q^2 \rangle = 2.4$  GeV $^2$ .

### 6.3

#### Subleading twist $A_{LL}^{\cos\phi_h}$

We present our estimates for  $F_{LL}^{\cos\phi_h}$

$$F_{LL}^{\cos\phi_h} = \frac{2M}{Q} c \left[ \frac{\vec{h} \cdot \vec{k}_\perp}{M} x g_L^\perp D_1 \right] \Big|_{g_L^{1,a} \rightarrow g_L^a} \quad (6.6)$$

in Fig. XYZ and a compare to preliminary COMPASS data [84, 85].

The structure function  $F_{LL}^{\cos\phi_h}$  reads

$$F_{LL}^{\cos\phi_h}(x, z, P_{hT}) = -\frac{2M}{Q} x \sum_q e_q^2 g_L^\perp(x) D_1^{q/h}(z) \frac{z P_{hT}}{M} g_{LL}^{\cos\phi_h}(x, z, P_{hT}) \quad (6.7)$$

where the factor  $g_{LL}^{\cos\phi_h}(x, z, P_{hT})$  is given in Eq. (B.25) of Appendix B. If one calculates the asymmetry as a function of  $P_{hT}$  then the formula is the following

$$A_{LL}^{\cos\phi_h}(x, z, P_{hT}) = \frac{F_{LL}^{\cos\phi_h}(x, z, P_{hT})}{F_{UU}(x, z, P_{hT})} \quad (6.8)$$

We can finally derive formulas for  $A_{LL}^{\cos\phi_h}$  asymmetry as a function of  $x, z$ :

$$A_{LL}^{\cos\phi_h} = -\frac{2M}{Q} a_{LL}^{\cos\phi_h} \sum_q e_q^2 g_L^\perp(x) D_1^{q/h}(z) \quad (6.9)$$

Asymmetries  $A_{LL}^{\cos\phi_h}$  for Jefferson Lab 12 GeV are plotted in Fig. 15.

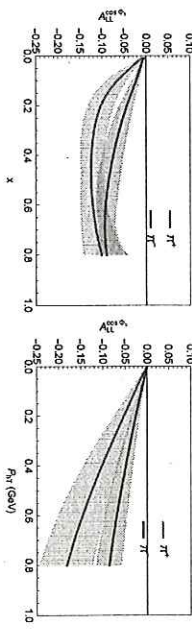


Figure 15.  $A_{LL}^{\cos\phi_h}$  as a function of  $x$  (left panel), and as a function of  $P_{hT}$  (right panel) at typical kinematics of Jefferson Lab 12 GeV,  $\langle x \rangle = 0.25$ ,  $\langle z \rangle = 0.54$ ,  $\langle Q^2 \rangle = 2.4$  GeV $^2$ .

### 6.4 Subleading twist $A_{LT}^{\cos(2\phi_h - \phi_S)}$

We present our estimates for  $F_{LT}^{\cos(2\phi_h - \phi_S)}$

$$F_{LT}^{\cos(2\phi_h - \phi_S)} = \frac{2M}{Q} C \left[ \frac{-2(\hat{h} \cdot \mathbf{k}_1) k_1^2}{2M^2} x g_T^{\perp} D_1 \right] \Big|_{\text{using Eqs (2.25, 2.31)}}$$

in Fig. XYZ and a compare to preliminary COMPASS data [84, 85].

The structure function  $F_{LT}^{\cos(2\phi_h - \phi_S)}$  has the following form:

$$F_{LT}^{\cos(2\phi_h - \phi_S)}(x, z, P_{hT}) = -\frac{2M}{Q} x \sum_q e_q^2 g_T^{\perp(1)q}(x) D_q^h(z) \frac{z^2 P_{hT}^2}{M^2} G_{LT}^{\cos(2\phi_h - \phi_S)}(x, z, P_{hT}) \quad (6.11)$$

where the factor  $G_{LT}^{\cos(2\phi_h - \phi_S)}$  is given in Eq. (B.27) of Appendix B.

We can finally derive the  $P_{hT}$  integrated formula for  $\cos(2\phi_h - \phi_S)$  asymmetry:

$$A_{LT}^{\cos(2\phi_h - \phi_S)}(x, z) = -A_{LT}^{\cos(2\phi_h - \phi_S)} \frac{\sum_q e_q^2 g_T^{\perp(1)q}(x) D_q^h(z)}{\sum_q e_q^2 f_1^l(x) D_q^h(z)}, \quad (6.12)$$

If one calculates the asymmetry as a function of  $P_{hT}$  then the formula is the following

$$A_{LT}^{\cos(2\phi_h - \phi_S)}(x, z, P_{hT}) = \frac{F_{LT}^{\cos(2\phi_h - \phi_S)}(x, z, P_{hT})}{F_{UL}(x, z, P_{hT})} \quad (6.13)$$

The asymmetry  $A_{LT}^{\cos(\phi_h - \phi_S)}$  as a function of  $x$  and  $P_{hT}$  for Jefferson Lab 12 GeV is plotted in Fig. 16.

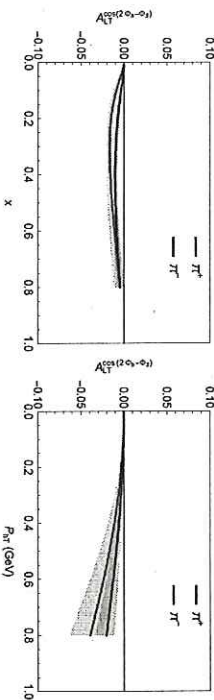


Figure 16.  $A_{LT}^{\cos(2\phi_h - \phi_S)}$  as a function of  $x$  (left panel), and as a function of  $P_{hT}$  (right panel) at typical kinematics of Jefferson Lab 12 GeV,  $\langle x \rangle = 0.25$ ,  $\langle z \rangle = 0.54$ ,  $\langle Q^2 \rangle = 2.4$  GeV $^2$ .

### 6.5 Subleading twist $A_{UL}^{\sin \phi_h}$

The first SSA in SIDIS ever measured! Seminal HERMES data on  $A_{UL}^{\sin \phi}$  [86–88]. See especially [89] where contaminations from transverse target polarization have been tediously removed! Have to compare to those VERY CLEAN data! See also the recent COMPASS data [90]. Lots of early studies, but remain unexplained! Also we will fail, I'm afraid ...

$$F_{UL}^{\sin \phi_h} = \frac{2M}{Q} C \left[ \frac{\hat{h} \cdot \mathbf{P}}{z m_h} x h_1 H_1^\perp \right]_{h_1^2 \rightarrow h_1^L} \text{according to Eq. (2.33)} \quad (6.14)$$

The structure function  $F_{UL}^{\sin \phi_h}$  reads

$$F_{UL}^{\sin \phi_h}(x, z, P_{hT}) = -\frac{2M}{Q} x \sum_q e_q^2 h_{1L}^{\perp(1)q}(x) H_1^{\perp(1)q/h}(z) G_{UL}^{\sin \phi_h}(x, z, P_{hT}) \quad (6.15)$$

where the factor  $G_{UL}^{\sin \phi_h}$  is given in Eq. (B.23) of Appendix B. If one calculates the asymmetry as a function of  $P_{hT}$  then the formula is the following

$$A_{UL}^{\sin \phi_h}(x, z, P_{hT}) = \frac{F_{UL}^{\sin \phi_h}(x, z, P_{hT})}{F_{UL}(x, z, P_{hT})} \quad (6.16)$$

We can finally derive formulas for  $A_{UL}^{\sin \phi_h}$  asymmetry as a function of  $x, z$ :

$$A_{UL}^{\sin \phi_h} = -\frac{2M}{Q} \sum_q e_q^2 h_{1L}^{\perp(1)q}(x) H_1^{\perp(1)q/h}(z) \frac{A_{UL}^{\cos \phi_h}(x, z, P_{hT})}{\sum_q e_q^2 f_1^l(x) D_q^{q/h}(z)} \quad * \text{of } \sin \phi_h \quad (6.17)$$

Asymmetries  $A_{UL}^{\sin \phi_h}$  for Jefferson Lab 12 GeV are plotted in Fig. 17.

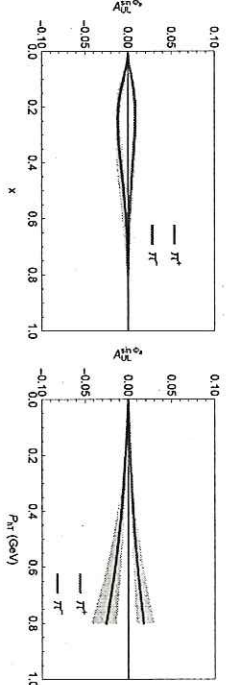


Figure 17.  $A_{UL}^{\sin \phi_h}$  as a function of  $x$  (left panel), and as a function of  $P_{hT}$  (right panel) at typical kinematics of Jefferson Lab 12 GeV,  $\langle x \rangle = 0.25$ ,  $\langle z \rangle = 0.54$ ,  $\langle Q^2 \rangle = 2.4$  GeV $^2$ .

$$A_{LT}^{\cos(2\phi_h - \phi_S)} = -\frac{\sum_q e_q^2 g_T^{\perp(1)q}(x) D_q^h(z)}{\sum_q e_q^2 f_1^l(x)} \cdot \frac{M_p^2 \langle p_T^2 \rangle z^2}{\Lambda} = -\frac{\sum_q e_q^2 \frac{\langle p_T^2 \rangle}{2m_h} g_T^{\perp(1)q}(x) D_q^h(z)}{\sum_q e_q^2 f_1^l(x)} \cdot \frac{2 M_p^4}{\Lambda} \cdot \frac{z^2}{\Lambda}$$

*different procedure*

## 6.6 Subleading twist $A_{UU}^{\cos\phi_h}$

The structure function  $F_{UU}^{\cos\phi_h}$  is given by Eq. (3.17) which reduces after applying the WW-type approximation to Eq. (3.33), which shows that it contains two contributions. One is due to a convolution of  $f_1^a$  and  $D_1^a$  and commonly referred to as the Calm effect [91]. The other is due to a convolution of the Boer-Mulders and Collins functions.

The asymmetry  $A_{UU}^{\cos\phi}$  was measured in several experiments, such as EMC [92], and more recently also at JLab [74, 93], HERMES [94] and COMPASS [95]. The asymmetry was also subject to several theoretical studies. In our context it is of interest to review two of them in some more detail, namely Refs. [64] and [67].

In Ref. [64] it was assumed that the EMC data on  $A_{UU}^{\cos\phi}$  is due to the Calm effect only, i.e. it arises solely from the transverse momentum dependences of  $f_1^a$  and  $D_1^a$ . On the basis of this assumption, the Gaussian widths of these functions were determined from the EMC data [92]. In the WW-type approximation, the EMC contain also contributions from the Boer-Mulders effect, see Eq. (3.33). There are two reasons, why one may neglect this contribution with a presumably good approximation [67]. First, one may expect it to be less dominant than the Calm effect contribution because the Boer-Mulders and Collins functions are required by positivity inequalities to be smaller than  $f_1^a$  and  $D_1^a$ , and phenomenologically  $h_1^{\perp a}$  and  $H_1^{\perp a}$  are both observed to be clearly smaller than the respectively allowed upper bounds. Moreover, EMC has not detected specific final state hadrons, but summed over all charged hadrons. In such sums the Collins effect for positive and negative pions tends to cancel with good accuracy. Charged pions yield the main part of charged hadrons, and the Collins effect for instance kaons is observed to be small. Therefore, the analysis of the EMC data of [64] gives insights mainly on the transverse momentum dependences of  $f_1^a$  and  $D_1^a$ , provided the WW-type approximation holds.

In contrast to this in [67] recent data on cross sections and mean transverse hadron momenta from Jefferson Lab [74, 93] and HERMES [96] were studied. The results from [67] were also shown to be compatible with COMPASS data, see [97]. The important point is that the analysis of [67] was free of any WW-type approximations. Nevertheless, the phenomenological numbers from the studies [64] and [67] are in good agreement (and both results are also supported by lattice QCD), see App. 4.1. The agreement of [64] and [67] indicates that the neglect of  $\bar{q}q$ -terms in  $A_{UU}^{\cos\phi}$  is, at least in the kinematics of the EMC experiment at within the accuracy of that data [92], a useful assumption.

It is necessary to make one cautious comment though. In the EMC experiment the data were taken with a 280 GeV muon beam, and one expects  $k_\perp$ -broadening effects [67, 71] as compared to HERMES or JLab energies. Without considering evolution effects, one obtains a good agreement of the descriptions of HERMES and EMC data with the same parameter set, see Fig. 18. If one takes these effects phenomenologically [67] or rigorously [71] into account, one would expect the theoretical curve in Fig. 18 to overshoot the data by about 30 %. This would indicate that the  $\bar{q}q$ -terms in this observable could about about 30 %. We stress that we would not expect WW-type approximations to work better than that.

To be considered: Compare also to JLab [74, 93] HERMES and COMPASS [94, 95]?

$$F_{UU}^{\cos\phi_h} = \frac{2M}{Q} C \left[ \frac{\hat{\mathbf{h}} \cdot \mathbf{P}_\perp}{z m_h} h_1^\perp - \frac{\hat{\mathbf{h}} \cdot \mathbf{k}}{M} x f_1^{\perp a} \right] f^{a \rightarrow f_1^a} h^a \rightarrow h_1^{\perp a} \quad \text{using Eqs. (2.29, 2.43)} \quad (6.18)$$

The structure function  $F_{UU}^{\cos\phi_h}$  reads

$$F_{UU}^{\sin\phi_h}(x, z, P_{hT}) = -\frac{2M}{Q} x \sum_q e_q^2 h_1^{\perp(1)q}(x) H_1^{\perp(1)q/h}(z) G_{UU1}^{\cos\phi_h}(x, z, P_{hT}) - \frac{2M}{Q} x \sum_q e_q^2 f_1^q(x) D_1^{q/h}(z) G_{UU2}^{\cos\phi_h}(x, z, P_{hT}) \quad (6.19)$$

where the factors  $G_{UU1}^{\cos\phi_h}(x, z, P_{hT})$  and  $G_{UU2}^{\cos\phi_h}(x, z, P_{hT})$  are given in Eqs. (B.29,B.31) of Appendix B. If one calculates the asymmetry as a function of  $P_{hT}$  then the formula is the following

$$A_{UU}^{\cos\phi_h}(x, z, P_{hT}) = \frac{F_{UU}^{\cos\phi_h}(x, z, P_{hT})}{F_{UU}(x, z, P_{hT})} \quad (6.20)$$

We can finally derive formulas for:  $A_{UU}^{\cos\phi_h}$  asymmetry as a function of  $x, z$ :

$$\begin{aligned} A_{UU}^{\cos\phi_h} &= \frac{2M}{Q} A_{UU1}^{\cos\phi_h} \frac{\sum_q e_q^2 h_1^{\perp(1)q}(x) H_1^{\perp(1)q/h}(z)}{\sum_q e_q^2 f_1^q(x) D_1^{q/h}(z)} - \\ &- \frac{2M}{Q} A_{UU2}^{\cos\phi_h} \frac{\sum_q e_q^2 f_1^q(x) D_1^{q/h}(z)}{\sum_q e_q^2 f_1^q(x) D_1^{q/h}(z)}, \end{aligned} \quad (6.21)$$

where the factors  $A_{UU1}^{\cos\phi_h}(x, z)$  and  $A_{UU2}^{\cos\phi_h}(x, z)$  are given in Eqs. (B.30,B.32) of Appendix B. Asymmetries  $A_{UU}^{\cos\phi_h}$  for Jefferson Lab 12 GeV are plotted in Fig. 19.

**Figure 18.** Azimuthal asymmetry  $A_{UU}^{\cos\phi}$  in charged hadron production in SIDIS of 280 GeV muons off protons as function of  $z$ . The data from EMC [92] refer to  $(Q) = 4.8$  GeV. The theoretical curve is the “WW-type and Calm-effect-only” approximation for this observable in the Gauss model with parameters fixed from HERMES data. From Ref. [67].

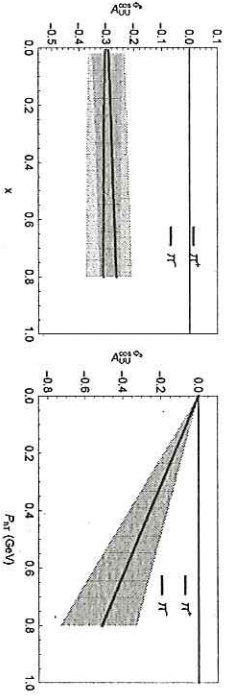


Figure 19.  $A_{UT}^{\cos\phi_h}$  as a function of  $x$  (left panel), and as a function of  $P_{hT}$  (right panel) at typical kinematics of Jefferson Lab 12 GeV,  $\langle x \rangle = 0.25$ ,  $\langle z \rangle = 0.54$ ,  $\langle Q^2 \rangle = 2.4$  GeV $^2$ .

### 6.7 Subleading twist $A_{UT}^{\sin\phi_S}$

Preliminary HERMES data in [98]. Nice and sizable asymmetry! Will provide an important test!

$$F_{UT}^{\sin\phi_S} = \frac{2M}{Q} C \left[ x f_T D_1 - \frac{\mathbf{P}_\perp \cdot \mathbf{k}_\perp}{2zMm_h} (x h_T - x h_T^\perp) H_1^\perp \right] f_T^\perp \rightarrow f_T^{\perp a}, (h_T^\perp - h_T^{a\perp}) \rightarrow h_1^a \text{ according to Eqs. (2.42, 2.34, 2.35)}$$

The structure function  $F_{UT}^{\sin\phi_S}$  reads

$$\begin{aligned} F_{UT}^{\sin\phi_S}(x, z, P_{hT}) = & -2Mx \sum_q e_q^2 f_{1T}^{\perp(1)q}(x) D_1^{q/h}(z) G_{UT1}^{\sin\phi_S}(x, z, P_{hT}) + \\ & \frac{2M}{Q} x \sum_q e_q^2 h_1^q(x) H_1^{\perp(1)q/h}(z) \frac{2z^2 m_h}{M} G_{UT2}^{\sin\phi_S}(x, z, P_{hT}) \end{aligned} \quad (6.23)$$

where the factors  $G_{UT1}^{\sin\phi_S}(x, z, P_{hT})$  and  $G_{UT2}^{\sin\phi_S}(x, z, P_{hT})$  are given in Eqs. (B.33,B.34) of Appendix B. If one calculates the asymmetry as a function of  $P_{hT}$  then the formula is the following

$$A_{UT}^{\sin\phi_S}(x, z, P_{hT}) = \frac{F_{UT}^{\sin\phi_S}(x, z, P_{hT})}{F_{UT}(x, z, P_{hT})} \quad (6.24)$$

We can finally derive formulas for  $A_{UT}^{\sin\phi_h}$  asymmetry as a function of  $x, z$ :

$$A_{UT}^{\sin\phi_h} = -\frac{2M}{Q} \frac{\sum_q e_q^2 f_{1T}^{\perp(1)q}(x) D_1^{q/h}(z)}{\sum_q e_q^2 f_1^q(x) D_1^{q/h}(z)} \quad (6.25)$$

Notice that our result for  $A_{UT}^{\sin\phi_h}$  integrated over  $P_{hT}$  differs from result of Ref. [4].

Asymmetries  $A_{UT}^{\sin\phi_S}$  for Jefferson Lab 12 GeV are plotted in Fig. 20.

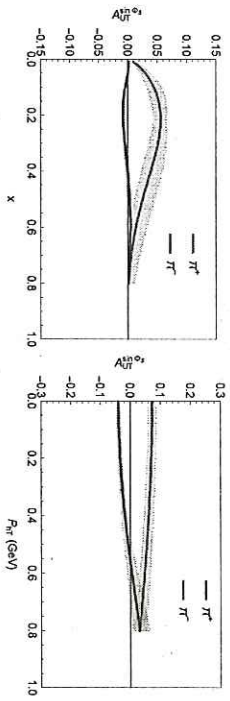


Figure 20.  $A_{UT}^{\sin\phi_S}$  as a function of  $x$  (left panel), and as a function of  $P_{hT}$  (right panel) at typical kinematics of Jefferson Lab 12 GeV,  $\langle x \rangle = 0.25$ ,  $\langle z \rangle = 0.54$ ,  $\langle Q^2 \rangle = 2.4$  GeV $^2$ .

### 6.8 Subleading twist $A_{UT}^{\sin(2\phi_h-\phi_S)}$

This twist-3 structure function contains a contribution of pretzelosity.

$$F_{UT}^{\sin(2\phi_h-\phi_S)} = \frac{2M}{Q} C \left[ \frac{2(\hat{\mathbf{h}} \cdot \mathbf{k}_\perp)^2 - \mathbf{k}_\perp^2}{2M^2} x f_T^\perp D_1 + \frac{2(\hat{\mathbf{h}} \cdot \mathbf{P}_\perp) - \mathbf{P}_\perp \cdot \mathbf{k}_\perp}{2zMm_h} \right]$$

The structure function  $F_{UT}^{\sin(2\phi_h-\phi_S)}$  reads

$$\begin{aligned} F_{UT}^{\sin(2\phi_h-\phi_S)}(x, z, P_{hT}) = & \frac{2M}{Q} x \sum_q e_q^2 f_{1T}^{\perp(1)q}(x) D_1^{q/h}(z) \frac{z^2 P_{hT}^2}{M^2} G_{UT1}^{\sin(2\phi_h-\phi_S)}(x, z, P_{hT}) - \\ & \frac{2M}{Q} x \sum_q e_q^2 h_1^q(x) H_1^{\perp(1)q/h}(z) \frac{z^2 P_{hT}^2 m_h}{M^3} G_{UT2}^{\sin(2\phi_h-\phi_S)}(x, z, P_{hT}) \end{aligned} \quad (6.27)$$

where the factors  $G_{UT1}^{\sin(2\phi_h-\phi_S)}(x, z, P_{hT})$  and  $G_{UT2}^{\sin(2\phi_h-\phi_S)}(x, z, P_{hT})$  are given in Eqs. (B.35,B.37) of Appendix B. If one calculates the asymmetry as a function of  $P_{hT}$  then the formula is the following

$$A_{UT}^{\sin(2\phi_h-\phi_S)}(x, z, P_{hT}) = \frac{F_{UT}^{\sin(2\phi_h-\phi_S)}(x, z, P_{hT})}{F_{UT}(x, z, P_{hT})} \quad (6.28)$$

We can finally derive formulas for  $A_{UT}^{\sin(2\phi_h-\phi_S)}$  asymmetry as a function of  $x, z$ :

$$\begin{aligned} A_{UT}^{\sin(2\phi_h-\phi_S)} = & -\frac{2M}{Q} \frac{\sum_q e_q^2 f_{1T}^{\perp(1)q}(x) D_1^{q/h}(z)}{\sum_q e_q^2 f_1^q(x) D_1^{q/h}(z)} - \\ & \frac{2M}{Q} \frac{A_{UT1}^{\sin(2\phi_h-\phi_S)} \sum_q e_q^2 h_1^{\perp(1)q}(x) H_1^{\perp(1)q/h}(z)}{\sum_q e_q^2 f_1^q(x) D_1^{q/h}(z)} \end{aligned} \quad (6.29)$$

where the factors  $A_{UT1}^{\sin(2\phi_h-\phi_S)}(x, z)$  and  $A_{UT2}^{\sin(2\phi_h-\phi_S)}(x, z)$  are given in Eqs. (B.36,B.38) of Appendix B. Asymmetries  $A_{UT}^{\sin(2\phi_h-\phi_S)}$  for Jefferson Lab 12 GeV are plotted in Fig. 21.

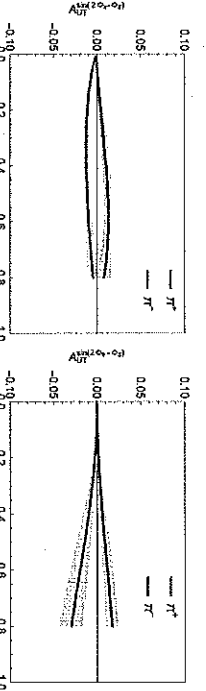


**Figure 21.**  $A_{UT}^{sin(2\phi_1 - \phi_2)}$  as a function of  $x$  (left panel), and as a function of  $P_{H\pi^0}$  (right panel) at typical kinematics of Jefferson Lab 12 GeV,  $\langle x \rangle = 0.25$ ,  $\langle z \rangle = 0.54$ ,  $\langle Q^2 \rangle = 2.4$  GeV $^2$ .

## 7 Conclusions (0 % okay, PS)

The following is just a collections of text fragments cut out from the main text and pasted here in the hope it might be useful.

the current knowledge. In the next subsections we will review and/or present new predictions for observables in SIDIS prepared on the basis of WW-type approximations. For our estimates we assume the WW-type approximations to hold within an accuracy of  $\varepsilon = \pm 40\%$ , which is motivated by the fact that data support the classic WW-approximation (2.25) within such (or better) accuracy, see Sec. 2.6 and [44]. Although the actual accuracy of WW-type approximations might be significantly different than that, by comparing our predictions to the size to the error bar projections for forthcoming experiments, we will obtain valuable hints on the sensitivity of the new data to the impact of  $q\bar{q}g$ -terms. In particular, in this way we will obtain important insights on whether future data will allow to ‘clearly resolve’ twist-3 contributions, or whether in the foreseeable future it will be possible to ‘completely’ understand and interpret the new data on the basis of the WW-type approximations.

In the dedicated study [44] it was shown that the error bars of the present data are compatible with a violation of the WW-approximation for  $g_T^p(x)$  up to 40 % in certain regions of  $x$ . Rephrased in a more optimistic way, one may interpret the findings of [44] as “the WW approximation works to an accuracy of 40 % or better,” and having an approximation with such a quality for TMDs would be very valuable. It would help to interpret first data, and allow us to make predictions for new experiments (JLab 12, EIC) where unknown TMDs contribute.

The aim of the presented study was to review what can be said about the quality of WW-(type-)approximations on the basis of results from theory, models, and phenomenology. In particular, we have presented a complete treatment of SIDIS observables in the WW-type-approximation. This is what we found out.

Bla, bla, bla.

## 8 Acknowledgments

This work was partially supported by the U.S. Department of Energy under Contract No. DE-AC05-06OR23177 (A.P.) and by the National Science Foundation under Contract No. PHY-1623454 (A.P.).

## A The “minimal basis” of TMDs and FFs

This Appendix describes the technical details of the parametrizations used in this work.

### A.1 Unpolarised distribution function $f_1^q(x, k_{\perp})$ , unpolarised fragmentation function $D_1(z, P_{\perp})$

In this work we use the leading-order parametrizations from [XX] for the unpolarized PDF  $f_1^q(x)$  and from [XX] for the unpolarized FF  $D_1^q(z)$ . If not otherwise stated the parametrizations are taken at the scale  $Q^2 = XX \text{ GeV}^2$  typical for many currently available SIDIS data. These parameterizations were used in [64] and other works whose extractions we adopt.

To describe the transverse momentum dependence of  $f_1^q(x, k_{\perp})$  and  $D_1(z, P_{\perp})$  we use the Gaussian Ansatz in Eqs. (4.1, 4.2). All early [64–67] and some recent [68] data could be well-described assuming the Gaussian widths  $\langle k_{\perp}^2 \rangle$  and  $\langle P_{\perp}^2 \rangle$  to be flavor and  $x$ - or  $z$ -independent. In the recent analysis [69] of HERMES multiplicities only flavour-independence of the widths was assumed. On long run one may anticipate that new precision data will require to relax these assumptions. However, one may also expect that the Gaussian Ansatz will remain a useful approximation as long as one is interested in describing data on transverse hadron momenta  $P_{\text{H}\gamma} \ll Q$ .

In this work we will explore the parameters described in Table 1. (What do we mean? Which parameters do we use?? All of them!!!?) Some comments are in order. In [64] no attempt was made to assign an uncertainty of the best fit result. The uncertainty of the numbers from [67] includes only the statistical error, but no systematic uncertainty. For comparison lattice results from [55] are included whose range indicates flavor-dependence (first number  $u$ -flavor, second number  $d$ -flavor). We will comment more on the lattice results in the next section. In view of the large (and partly underestimated) uncertainties and the fact that those parameters are anti-correlated the numbers from the different approaches quoted in Table 1 can be considered to be in good agreement.

study	$\langle Q^2 \rangle$ , $\langle x \rangle$ , $\langle z \rangle$ [GeV $^2$ ]	$\langle k_{\perp}^2 \rangle_{f_1}$ [GeV $^2$ ]	$\langle P_{\perp}^2 \rangle_{D_1}$ [GeV $^2$ ]	$\langle k_{\perp}^2 \rangle_{g_1^q}$ [GeV $^2$ ]
fit of [64]	XX, XX, XX	$\sim 0.25$	$\sim 0.2$	—
fit of [67]	2.5, 0.1, 0.4	$0.38 \pm 0.06$	$0.16 \pm 0.01$	—
fit of [69]	XX, XX, XX	$0.57 \pm 0.08$	$0.12 \pm 0.01$	—
fit of [68]	XX, 0.1, 0.5	$\sim 0.3$	$\sim 0.18$	—
lattice [55]	XX, —, —	0.14–0.15	—	0.11–0.15

**Table 1.** Gauss model parameters for  $f_1^q(x, k_{\perp})$ ,  $D_1^q(z, P_{\perp})$ ,  $f_{1L}^q(x, k_{\perp})$  from phenomenological and lattice QCD studies. The kinematics to which the phenomenological results and the renormalization scale of the lattice results are indicated. The range of lattice values indicates flavor dependence (first number refers to  $u$ -flavor, second number to  $d$ -flavor).

## A.2 Helicity distribution function $g_1^q(x, k_{\perp})$

For the helicity PDF  $g_1^q(x) \equiv g_{1L}(x) \equiv \int d^3k_{\perp} g_{1L}^q(x, k_{\perp})$  we use in this work the leading-order parametrization from [XX]. If not otherwise stated the parametrization is taken at the scale  $Q^2 = XX \text{ GeV}^2$ .

In lack of phenomenological information on the  $k_{\perp}$ -dependence of  $g_1^q(x, k_{\perp})$  we explore lattice QCD results from [55] to constrain the Gaussian width in Eq. (4.5). On a lattice with pion and nucleon masses  $m_{\pi} \approx 500 \text{ MeV}$  and  $M_N = 1.291(23) \text{ GeV}$  and with an axial coupling constant  $g_A^{(3)} = 1.209(36)$  reasonably close to its physical value  $1.2695(29)$  the following results were obtained for the mean square transverse parton momenta [55]. For the unpolarised TMDs it was found  $\langle k_{\perp}^2 \rangle_{f_1^q} = (0.3741 \text{ GeV}^2)$  and  $\langle k_{\perp}^2 \rangle_{g_1^q} = (0.3839 \text{ GeV}^2)$ . For the helicity TMDs it was found  $\langle k_{\perp}^2 \rangle_{g_1^d} = (0.327 \text{ GeV}^2)$  and  $\langle k_{\perp}^2 \rangle_{g_1^u} = (0.388 \text{ GeV}^2)$ . These values are quoted in Table 1.

The lattice values for  $\langle k_{\perp}^2 \rangle_{f_1^q}$  consistently underestimate the phenomenological numbers, see Table 1. The exact reasons for that are unknown, but it is natural to think it might be related to the fact that the lattice predictions [55] do not refer to TMDs entering in SIDIS (or Drell-Yan or other process) because a different gauge link was chosen, see Sec. 2.8. Still one may expect these results to bear considerable information on QCD dynamics.<sup>2</sup> To make use of this information we shall assume that the lattice results [55] provide robust predictions for the ratios  $\langle k_{\perp}^2 \rangle_{g_1^q}/\langle k_{\perp}^2 \rangle_{f_1^q} \approx 0.76$ . With the phenomenological value  $\langle k_{\perp}^2 \rangle_{f_1^q} = 0.25 \text{ GeV}^2$  we then obtain the estimate for the width of the helicity TMD  $\langle k_{\perp}^2 \rangle_{g_1^q} = 0.19 \text{ GeV}^2$ . In our phenomenological study we use this value for  $u$ -quarks and for simplicity also for  $d$ -quarks. Even though the lattice values indicate an interesting flavour dependence, see Table 1, for a proton target this is a very good approximation due to  $u$ -quark dominance. When precision data for deuterium and especially for  ${}^3\text{He}$  from Jefferson Lab become available, it will be interesting to re-investigate this point in detail.

### A.3 Sivers function $f_{1T}^q(x, k_{\perp})$

Sivers distribution function was studied in Refs. [63, 99–107]. We will use parametrization from Refs. [63, 100, 101]:

$$\langle k_{\perp}^2 \rangle_{f_{1T}} \equiv \frac{\langle k_{\perp}^2 \rangle M_1^2}{\langle k_{\perp}^2 \rangle + M_1^2} \quad (\text{A.1})$$

$$f_{1T}^q(x, k_{\perp}^2) = -\frac{M}{M_1} \sqrt{2e} N_q(x) f_{qT}(x, Q) \frac{e^{-k_{\perp}^2 \langle k_{\perp}^2 \rangle_{f_{1T}}}}{\pi \langle k_{\perp}^2 \rangle}, \quad (\text{A.2})$$

where  $M_1$  is a mass parameter,  $M$  the proton mass and

$$N_q(x) = N_q x^{\alpha} (1-x)^{\beta} \frac{(\alpha+\beta)!}{\alpha^{\alpha} \beta^{\beta}} \quad (\text{A.3})$$

The first moment of Sivers function is:

$$f_{1T}^q(1, q) = -\frac{\sqrt{\frac{e}{2}}}{M(\langle k_{\perp}^2 \rangle + M_1^2)^2} N_q(x) f_q(x, Q) \quad (\text{A.4})$$

<sup>2</sup> The results [55] refer also to pion masses above the physical value. This is caveat is presumably less critical and will be overcome as lattice QCD simulations are becoming feasible at physical pion masses.

$N_u = 0.40$	$\alpha_u = 0.35$	$\beta_u = 2.6$
$N_d = -0.97$	$\alpha_d = 0.44$	$\beta_d = 0.90$
$M_1^2 = 0.19 \text{ (GeV}^2)$		

**Table 2.** Best values of the fit of the Sivers functions. Table from Ref. [101]

We can rewrite parametrization of Sivers functions as

$$f_{1T}^{\perp q}(x, k_\perp) = f_{1T}^{\perp(1)q}(x) \frac{2M^2}{\pi \langle k_\perp^2 \rangle_{h_1}^2} e^{-k_\perp^2 / \langle k_\perp^2 \rangle_{h_1}}. \quad (\text{A.5})$$

The fit the HERMES proton and COMPASS deuteron data from including only Sivers functions for  $u$  and  $d$  quarks was done in Ref. [101], corresponding to seven free parameters, and parameters are shown in Table 2.

#### A.4 Transversity $h_1^q(x, k_\perp)$ and Collins fragmentation function $H_1^{\perp q}(x, P_\perp)$

These functions were studied in Refs. [46, 47, 108–111]. The following shape was assumed for parametrizations Refs. [46, 47, 108]:

$$h_1^q(x, k_\perp^2) = h_1^q(x) \frac{e^{-P_\perp^2 / \langle k_\perp^2 \rangle_{h_1}}}{\pi \langle k_\perp^2 \rangle_{h_1}}, \quad (\text{A.6})$$

$$h_1^q(x) = \frac{1}{2} N_q^T(x) [f_1(x) + g_1(x)], \quad (\text{A.7})$$

$$H_{1h/q}^\perp(z, P_\perp^2) = \frac{zm_h}{2P_\perp} \Delta^N D_{h/q}(z, P_\perp^2) = \frac{zm_h}{2m_q} e^{-P_\perp^2 / M_C^2} \sqrt{2e} H_{1h/q}^\perp(z) \frac{e^{-P_\perp^2 / M_C^2}}{\pi \langle P_\perp^2 \rangle}, \quad (\text{A.8})$$

with  $m_h$  produced hadron mass and

$$N_q^T(x) = N_q^T x^\alpha (1-x)^\beta \frac{(\alpha+\beta)^{(\alpha+\beta)}}{\alpha^\alpha \beta^\beta}, \quad (\text{A.9})$$

$$H_{1h/q}^\perp(z) = N_q^C(z) D_{h/q}(z), \quad (\text{A.10})$$

$$N_q^C(z) = N_q^C z^\gamma (1-z)^\delta \frac{(\gamma+\delta)^{(\gamma+\delta)}}{\gamma^\gamma \delta^\delta}, \quad (\text{A.11})$$

and  $-1 \leq NT \leq 1$ ,  $-1 \leq NC \leq 1$ . The helicity distributions  $g_1(x)$  are taken from Ref. [77], parton distribution and fragmentation functions are the GRV98LO PDF set [78] and the DSS fragmentation function set [79]. Notice that with these choices both the transversity and the Collins function automatically obey their proper positivity bounds. Note that as in Ref. [108] we use two Collins fragmentation functions, favored and disfavored ones, see Ref. [108] for details on implementation, and corresponding parameters  $N_u^C$  are then  $N_{fu}^C$  and  $NC_{ds}$ . For numerical estimates we use parameters extracted in Ref. [108], see Table 3. According to Eq. (B.7) we obtain the following expression for the first moment of Collins fragmentation function:

$$H_{1h/q}^{\perp(1)}(z) = \frac{H_{1h/q}^\perp(z) \sqrt{e/2} \langle P_\perp^2 \rangle M_C^3}{zm_h(M_C^2 + \langle P_\perp^2 \rangle)^2}. \quad (\text{A.12})$$

$NT = 0.46^{+0.20}_{-0.14}$	$NT = -1.0^{+1.17}_{-0.00}$
$\alpha = 1.11^{+0.89}_{-0.66}$	$\beta = 3.64^{+5.89}_{-3.37}$
$\langle k_\perp^2 \rangle_{h_1} = 0.25 \text{ (GeV}^2)$	
$NC_{ds} = 0.49^{+0.20}_{-0.18}$	$NC_{ds} = -1.00^{+0.38}_{-0.00}$
$\gamma = 1.06^{+0.45}_{-0.32}$	$\delta = 0.07^{+0.42}_{-0.37}$
$M_C^2 = 1.50^{+2.00}_{-1.12} \text{ (GeV}^2)$	

**Table 3.** Best values of the 9 free parameters fixing the  $u$  and  $d$  quark transversity distribution functions and the favoured and disfavoured Collins fragmentation functions. The table is from Ref. [108].

We also define the following variable:

$$\langle P_\perp^2 \rangle_{H_1^\perp} = \frac{\langle P_\perp^2 \rangle M_C^2}{\langle P_\perp^2 \rangle + M_C^2}. \quad (\text{A.13})$$

We can rewrite the parametrization of Collins FF as

$$H_1^\perp(z, P_\perp) = H_1^{\perp(1)}(z) \frac{2z^2 m_h^2}{\pi \langle P_\perp^2 \rangle_{H_1^\perp}^2} e^{-P_\perp^2 / \langle P_\perp^2 \rangle_{H_1^\perp}}. \quad (\text{A.14})$$

#### A.5 Boer-Mulders function $h_1^\perp(x, k_\perp)$

The Boer-Mulders function  $h_1^\perp$  [2] measures the transverse polarization asymmetry of quarks inside an unpolarized nucleon. The Boer-Mulders functions were studied phenomenologically in Refs. [112–114].

The following parametrization was used in Refs. [114]:

$$\langle k_\perp^2 \rangle_{h_1^\perp} = \frac{\langle k_\perp^2 \rangle M_{BM}^2}{\langle k_\perp^2 \rangle + M_{BM}^2}, \quad (\text{A.15})$$

$$h_1^\perp(x, k_\perp^2) = -\frac{M}{MBM} \sqrt{2e} N_q f_{1/p}(x, Q) \frac{e^{-k_\perp^2 / \langle k_\perp^2 \rangle_{h_1^\perp}}}{\pi \langle k_\perp^2 \rangle}, \quad (\text{A.16})$$

The first moment of Boer-Mulders function is:

$$h_1^{\perp(1)q}(x) = -\frac{\sqrt{\pi}}{M \langle k_\perp^2 \rangle + M_{BM}^2} N_q f_q(x, Q) = -\sqrt{\frac{e}{2}} \frac{1}{MBM} \frac{\langle k_\perp^2 \rangle_{h_1^\perp}^2}{\langle k_\perp^2 \rangle} N_q f_q(x, Q) \quad (\text{A.17})$$

We can rewrite parametrization of Boer-Mulders functions as

$$h_1^{\perp q}(x, k_\perp) = h_1^{\perp(1)q}(x) \frac{2M^2}{\pi \langle k_\perp^2 \rangle_{h_1^\perp}^2} e^{-k_\perp^2 / \langle k_\perp^2 \rangle_{h_1^\perp}}. \quad (\text{A.18})$$

$N_u$	$-0.49 \pm 0.15$	$N_d$	$-1 \pm 0.2$
$M_{BM}^2$	$0.1 \pm 0.2$	$(\text{GeV}^2)$	

Table 4. Fitted parameters of Boer-Mulders quark distributions. Values are from Ref. [114]

### A.6 Pretzelosity distribution $h_{TT}^\perp(x, k_\perp)$

Pretzelosity distribution function  $h_{TT}^\perp$  [115] describes transversely polarized quarks inside a transversely polarized nucleon. We use the following form of  $h_{TT}^\perp$  [115]:

$$h_{TT}^{\perp q}(x, k_\perp^2) = \frac{M^2}{M_{TT}^2} e^{-k_\perp^2/M_{TT}^2} h_{TT}^{1q}(x) \frac{e^{-k_\perp^2/\langle k_\perp^2 \rangle}}{\pi \langle k_\perp^2 \rangle} = \frac{M^2}{M_{TT}^2} h_{TT}^{1q}(x) \frac{e^{-k_\perp^2/\langle k_\perp^2 \rangle}}{\pi \langle k_\perp^2 \rangle}, \quad (\text{A.19})$$

where

$$h_{TT}^{1q}(x) = e N^a(x) (f_1^a(x, Q) - g_1^a(x, Q)), \quad (\text{A.20})$$

$$N^a(x) = N^a x^\alpha (1-x)^\beta \frac{(\alpha + \beta)^{\alpha + \beta}}{\alpha^\alpha \beta^\beta}, \quad (\text{A.21})$$

$$\langle k_\perp^2 \rangle h_{TT}^\perp = \frac{\langle k_\perp^2 \rangle M_{TT}^2}{\langle k_\perp^2 \rangle + M_{TT}^2}, \quad (\text{A.22})$$

where  $N^a$ ,  $\alpha$ ,  $\beta$ , and  $M_T$  are parameters fitted to data that can be found in Table 5.

We use Eq. (B.7) to calculate the first moment of  $h_{TT}^{\perp q}(x, k_\perp^2)$  of Eq. (A.19) and obtain:

$$h_{TT}^{\perp(1)q}(x) = \frac{h_{TT}^{1q}(x) M_{TT}^2 \langle k_\perp^2 \rangle}{2(M_{TT}^2 + \langle k_\perp^2 \rangle)^2} = \frac{h_{TT}^{1q}(x) \langle k_\perp^2 \rangle^2 h_{TT}^\perp}{2M_{TT}^2 \langle k_\perp^2 \rangle}. \quad (\text{A.23})$$

We can rewrite parametrization of pretzelosity functions as

$$h_{TT}^{\perp q}(x, k_\perp) = h_{TT}^{\perp(1)q}(x) \frac{2M^2}{\pi \langle k_\perp^2 \rangle^2} e^{-k_\perp^2/\langle k_\perp^2 \rangle} h_{TT}^\perp. \quad (\text{A.24})$$

### B.1 Notation for convolution integrals

Parton interpretation of structure functions can be obtained as convolution of distribution and fragmentation functions [1, 4, 63]

$$\mathcal{C}[wfD] = x \sum_a e_a^2 \int d^2 p_T d^2 k_T \delta^{(2)}(p_T - k_T - \mathbf{P}_{h\perp}/z) w(p_T, k_T) f^a(z, p_T^2) D^a(z, z^2 k_T^2), \quad (\text{B.1})$$

and the unit vector is defined as  $\hat{\mathbf{h}} = \mathbf{P}_{h\perp}/P_{h\perp}$ , here  $\mathbf{p}_T$  is the transverse momentum of quark with respect to the proton,  $\mathbf{k}_T$  is the transverse momentum of fragmenting quark with respect to the produced hadron, and  $-\mathbf{P}_{h\perp}/z \approx \mathbf{q}_T$  the transverse momentum of the virtual photon; these momenta are defined in “target - produced hadron” cm frame.

Fragmentation function have probabilistic interpretation with respect to transverse momentum of produced hadron with respect to the fragmenting quark

$$\mathbf{P}_\perp \simeq -z \mathbf{k}_T, \quad (\text{B.2})$$

so that for unpolarized fragmentation function one has

$$D_{1q/h}(z) \equiv \int d^2 \mathbf{P}_\perp D_{1q/h}(z, P_\perp^2) = z^2 \int d^2 k_T D_{1q/h}(z, z^2 k_T^2). \quad (\text{B.3})$$

Experimental measurements are usually given in the photon-proton cm frame in which we can rewrite Eq.(B.1) using “physical” vector  $\mathbf{P}_\perp$

$$\mathcal{C}[wfD] = x \sum_a e_a^2 \int d^2 \mathbf{k}_\perp d^2 \mathbf{P}_\perp \delta^{(2)}(z \mathbf{k}_\perp + \mathbf{P}_\perp - \mathbf{P}_{hT}) w\left(\mathbf{k}_\perp - \frac{\mathbf{P}_\perp}{z}\right) f^a(x, k_\perp^2) D^a(z, P_\perp^2), \quad (\text{B.4})$$

integrating  $\delta$  function we obtain

$$\mathcal{C}[wfD] = x \sum_a e_a^2 \int d^2 \mathbf{k}_\perp w\left(\mathbf{k}_\perp - \frac{(\mathbf{P}_{h\perp} - z \mathbf{k}_\perp)}{z}\right) f^a(x, k_\perp^2) D^a(z, (\mathbf{P}_{h\perp} - z \mathbf{k}_\perp)^2). \quad (\text{B.5})$$

The notations of our paper can be readily compared to notations of other papers, such as Ref. [63], for instance, where  $\mathbf{P}_\perp|_{our} \equiv \mathbf{P}_\perp|_{[63]}$  and  $\mathbf{k}_\perp|_{our} \equiv \mathbf{k}_\perp|_{[63]}$ .

We are using the following definitions of moments of TMDs

$$f^{(n)}(x) = \int d^2 \mathbf{k}_\perp \left(\frac{k_\perp^2}{2M^2}\right)^n f(x, k_\perp^2), \quad (\text{B.6})$$

$$D^{(n)}(z) = \int d^2 \mathbf{P}_\perp \left(\frac{P_\perp^2}{2z^2 m_h^2}\right)^n D(z, P_\perp^2). \quad (\text{B.7})$$

Table 5. Fitted parameters of the pretzelosity quark distributions. Table from Ref. [115]

### B Convolution integrals and expressions in Gaussian Ansatz

In this Appendix we explain the notation for convolution integrals of TMDs and FFs and give the explicit results obtained assuming the Gaussian Ansatz.

#### B.2 Gaussian factors

The gaussian factor for  $F_{UU}$ :

$$G_{UU}(x, z, P_{hT}) = \frac{1}{\pi \langle P_{hT}^2 \rangle} e^{-P_{hT}^2/\langle P_{hT}^2 \rangle}, \langle P_{hT}^2 \rangle = z^2 \langle k_\perp^2 \rangle + \langle P_\perp^2 \rangle. \quad (\text{E.8})$$

The gaussian factor for  $F_{LL}$ :

Good!

$$g_{LL}(x, z, P_{hT}) = \frac{1}{\pi \langle P_{hT}^2 \rangle_{g_1}} e^{-P_{hT}^2 / \langle P_{hT}^2 \rangle_{g_1}}, \langle P_{hT}^2 \rangle_{g_1} = z^2 \langle k_{\perp}^2 \rangle_{g_1} + \langle P_{\perp}^2 \rangle. \quad (\text{B.9})$$

The gaussian factors for  $F_{LT}^{\cos(2\phi_h - \phi_S)}$ :

$$g_{LT}(x, z, P_{hT}) = \frac{M^2}{\pi \langle P_{hT}^2 \rangle_{g_1}^2} e^{-P_{hT}^2 / \langle P_{hT}^2 \rangle_{g_1}}, \langle P_{hT}^2 \rangle_{g_1} = z^2 \langle k_{\perp}^2 \rangle_{g_1} + \langle P_{\perp}^2 \rangle. \quad (\text{B.10})$$

The gaussian factors for  $F_{UL}^{\sin(2\phi_h)}$ :

$$g_{UL}^{\sin(2\phi_h)}(x, z, P_{hT}) = \frac{M^1}{\pi \langle P_{hT}^2 \rangle_{h_L}^3} e^{-P_{hT}^2 / \langle P_{hT}^2 \rangle_{h_L}}, \langle P_{hT}^2 \rangle_{h_L} = z^2 \langle k_{\perp}^2 \rangle_{h_L} + \langle P_{\perp}^2 \rangle_{h_L}. \quad (\text{B.12})$$

$$\mathcal{A}_{UL}^{\sin(2\phi_h)} = \frac{4m_h M z^2}{\langle P_{hT}^2 \rangle_{h_L}}. \quad (\text{B.13})$$

The gaussian factors for  $F_{UT}^{\sin(2\phi_h)}$ :

$$g_{UT}^{\sin(2\phi_h)}(x, z, P_{hT}) = \frac{M^1}{\pi \langle P_{hT}^2 \rangle_{h_L}^2} e^{-P_{hT}^2 / \langle P_{hT}^2 \rangle_{h_L}}, \langle P_{hT}^2 \rangle_{h_L} = z^2 \langle k_{\perp}^2 \rangle_{h_L} + \langle P_{\perp}^2 \rangle_{h_L}. \quad (\text{B.14})$$

$$\mathcal{A}_{UT}^{\sin(2\phi_h)} = \frac{m_h z \sqrt{\pi}}{\sqrt{\langle P_{hT}^2 \rangle_{h_L}}}. \quad (\text{B.15})$$

The gaussian factors for  $F_{UT}^{\sin(\phi_h - \phi_S)}$ :

$$g_{UT}^{\sin(\phi_h - \phi_S)}(x, z, P_{hT}) = \frac{M^2}{\pi \langle P_{hT}^2 \rangle_{f_T}^2} e^{-P_{hT}^2 / \langle P_{hT}^2 \rangle_{f_T}}, \langle P_{hT}^2 \rangle_{f_T} = z^2 \langle k_{\perp}^2 \rangle_{f_T} + \langle P_{\perp}^2 \rangle_{f_T}. \quad (\text{B.16})$$

$$\mathcal{A}_{UT}^{\sin(\phi_h - \phi_S)} = \frac{M z \sqrt{\pi}}{\sqrt{\langle P_{hT}^2 \rangle_{f_T}}}. \quad (\text{B.17})$$

The gaussian factors for  $\tilde{F}_{UT}^{\sin(3\phi_h - \phi_S)}$ :

$$g_{UT}^{\sin(3\phi_h - \phi_S)}(x, z, P_{hT}) = \frac{M^4 \langle k_{\perp}^2 \rangle_{h_T}^3}{\pi \langle P_{hT}^2 \rangle_{h_T}^4} e^{-P_{hT}^2 / \langle P_{hT}^2 \rangle_{h_T}}, \langle P_{hT}^2 \rangle_{h_T} = z^2 \langle k_{\perp}^2 \rangle_{h_T} + \langle P_{\perp}^2 \rangle_{h_T}. \quad (\text{B.18})$$

$$\mathcal{A}_{UT}^{\sin(3\phi_h - \phi_S)} = \frac{3m_h \langle k_{\perp}^2 \rangle_{h_T} z^3 \sqrt{\pi}}{2 \sqrt{\langle P_{hT}^2 \rangle_{h_T}^3}}. \quad (\text{B.19})$$

The gaussian factors for  $F_{UU}^{\cos(2\phi_h)}$ :

$$g_{UU}^{\cos(2\phi_h)}(x, z, P_{hT}) = \frac{M^4}{\pi \langle P_{hT}^2 \rangle_{h_L}^3} e^{-P_{hT}^2 / \langle P_{hT}^2 \rangle_{h_L}}, \langle P_{hT}^2 \rangle_{h_L} = z^2 \langle k_{\perp}^2 \rangle_{h_L} + \langle P_{\perp}^2 \rangle_{h_L}. \quad (\text{B.20})$$

$$\mathcal{A}_{UU}^{\cos(2\phi_h)} = \frac{4m_h M z^2}{\langle P_{hT}^2 \rangle_{h_L}}. \quad (\text{B.21})$$

**Good!**

The gaussian factor for  $F_{LT}^{\cos(\phi_S)}$ :

$$g_{LT}^{\cos(\phi_S)}(x, z, P_{hT}) = \frac{z^2 \langle k_{\perp}^2 \rangle_{h_T}}{\pi \langle P_{hT}^2 \rangle_{h_T}^3}, \langle P_{hT}^2 \rangle_{h_T} = z^2 \langle k_{\perp}^2 \rangle_{h_T} + \langle P_{\perp}^2 \rangle. \quad (\text{B.22})$$

**Good!**

The gaussian factors for  $F_{LL}^{\sin(\phi_h)}$ :

$$g_{LL}^{\sin(\phi_h)}(x, z, P_{hT}) = \frac{4M^2 (z^2 \langle k_{\perp}^2 \rangle_{h_L})_{h_L} (P_{hT}^2 - z^2 \langle k_{\perp}^2 \rangle_{h_L}) + \langle P_{\perp}^2 \rangle_{h_L}^2}{\pi \langle P_{hT}^2 \rangle_{h_L}^4} e^{-P_{hT}^2 / \langle P_{hT}^2 \rangle_{h_L}}, \langle P_{hT}^2 \rangle_{h_L} = z^2 \langle k_{\perp}^2 \rangle_{h_L} + \langle P_{\perp}^2 \rangle_{h_L}. \quad (\text{B.23})$$

$$\mathcal{A}_{LL}^{\sin(\phi_h)} = \frac{m_h z \sqrt{\pi} (2 \langle P_{\perp}^2 \rangle_{h_L} + z^2 \langle k_{\perp}^2 \rangle_{h_L})}{\sqrt{\langle P_{hT}^2 \rangle_{h_L}^3}}. \quad (\text{B.24})$$

The gaussian factors for  $F_{LL}^{\cos(\phi_h)}$ :

$$g_{LL}^{\cos(\phi_h)}(x, z, P_{hT}) = \frac{\langle k_{\perp}^2 \rangle_{h_L}}{\pi \langle P_{hT}^2 \rangle_{h_L}^2}, \langle P_{hT}^2 \rangle_{h_L} = z^2 \langle k_{\perp}^2 \rangle_{h_L} + \langle P_{\perp}^2 \rangle_{h_L}. \quad (\text{B.25})$$

**Good!**

The gaussian factors for  $F_{LT}^{\cos(2\phi_h - \phi_S)}$ :

$$g_{LT}^{\cos(2\phi_h - \phi_S)}(x, z, P_{hT}) = \frac{M^2 \langle k_{\perp}^2 \rangle_{g_1}}{\pi \langle P_{hT}^2 \rangle_{g_1}^2} e^{-P_{hT}^2 / \langle P_{hT}^2 \rangle_{g_1}}, \langle P_{hT}^2 \rangle_{g_1} = z^2 \langle k_{\perp}^2 \rangle_{g_1} + \langle P_{\perp}^2 \rangle. \quad (\text{B.27})$$

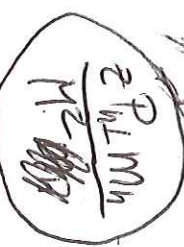
$$\mathcal{A}_{LT}^{\cos(2\phi_h - \phi_S)} = \frac{M^2 \langle k_{\perp}^2 \rangle_{g_1} z^2}{\langle P_{hT}^2 \rangle_{g_1}}. \quad (\text{B.28})$$

The gaussian factors for  $F_{UU}^{\cos(\phi_h)}$ :

$$g_{UU}^{\cos(\phi_h)}(x, z, P_{hT}) = \frac{4M^4 (\langle P_{\perp}^2 \rangle_{h_L})_{h_L} + z^2 \langle k_{\perp}^2 \rangle_{h_L} (\langle P_{hT}^2 \rangle_{h_L} - z^2 \langle k_{\perp}^2 \rangle_{h_L})}{\pi \langle P_{hT}^2 \rangle_{h_L}^4}, \langle P_{hT}^2 \rangle_{h_L} = z^2 \langle k_{\perp}^2 \rangle_{h_L} + \langle P_{\perp}^2 \rangle_{h_L}. \quad (\text{B.29})$$

**Good!**

**FIK**



different  
procedure

different procedure

## References

- [1] P. J. Mulders and R. D. Tangerman, *The complete tree-level result up to order  $1/Q$  for polarized deep-inelastic lepton production*, *Nucl. Phys.* **B461** (1996) 197–237, [[hep-ph/9510301](#)].
- [2] D. Boer and P. J. Mulders, *Time-reversal odd distribution functions in lepton production*, *Phys. Rev.* **D57** (1998) 5780–5786, [[hep-ph/9711485](#)].
- [3] K. Goeke, A. Metz and M. Schlegel, *Parameterization of the quark-quark correlator of a spin-1/2 hadron*, *Phys. Lett.* **B618** (2005) 90–96, [[hep-ph/0504130](#)].
- [4] A. Bacchetta et al., *Semi-inclusive deep inelastic scattering at small transverse momentum*, *JHEP* **02** (2007) 093, [[hep-ph/061265](#)].
- [5] S. Arnold, A. Metz and M. Schlegel, *Dilepton production from polarized hadron-hadron collisions*, [0809.2262](#).
- [6] A. Metz and A. Vossen, *Parton Fragmentation Functions*, *Prog. Part. Nucl. Phys.* **91** (2016) 136–202, [[1607.02521](#)].
- [7] G. A. Miller, *Densities, Parton Distributions, and Measuring the Non-Spherical Shape of the Nucleon*, *Phys. Rev.* **C76** (2007) 065209, [[0708.2297](#)].
- [8] M. Burkhardt, *Spin-orbit correlations and single-spin asymmetries*, [0709.2966](#).
- [9] M. Burkhardt, *The  $g(2)$  Structure Function*, *AIP Conf. Proc.* **1155** (2009) 26–34, [[0905.4079](#)].
- [10] A. Bacchetta, M. Boglione, A. Henneman and P. J. Mulders, *Bounds on transverse momentum dependent distribution and fragmentation functions*, *Phys. Rev. Lett.* **85** (2000) 712–715, [[hep-ph/9912490](#)].
- [11] S. Wandzura and F. Wilczek, *Sum Rules for Spin-Dependent Electroproduction: Test of Relativistic Constituent Quarks*, *Phys. Lett.* **B72** (1977) 195.
- [12] R. Jaffe and X-D. Ji, *Chiral odd parton distributions and Drell-Yan processes*, *Nucl. Phys. B* **375** (1992) 527–560.
- [13] R. Jaffe,  *$G(2)$ : The Nucleon's Other Spin Dependent Structure Function*, *Comments Nucl. Part. Phys.* **19** (1996) 239.
- [14] J. Balla, M. V. Polyakov and C. Weiss, *Nucleon matrix elements of higher twist operators from the instanton vacuum*, *Nucl. Phys.* **B510** (1998) 327–364, [[hep-ph/9707515](#)].
- [15] B. Dressler and M. V. Polyakov, *On the tourist - three contribution to  $h(L)$  in the instanton vacuum*, *Phys. Rev.* **D61** (2000) 097501, [[hep-ph/9912376](#)].
- [16] M. Gockeler, R. Horsley, W. Kurzinger, H. Oelrich, D. Pleiter et al., *A Lattice calculation of the nucleon's spin dependent structure function  $g(2)$  revisited*, *Phys. Rev.* **D63** (2001) 074506, [[hep-lat/0010091](#)].
- [17] M. Gockeler, R. Horsley, D. Pleiter, P. E. Rakow, A. Schäfer et al., *Investigation of the second moment of the nucleon's  $g(1)$  and  $g(2)$  structure functions in two-flavor lattice QCD*, *Phys. Rev.* **D72** (2005) 054507, [[hep-lat/0506017](#)].
- [18] E143 collaboration, K. Abe et al., *Measurements of the proton and deuteron spin structure functions  $g_1$  and  $g_2$* , *Phys. Rev.* **D58** (1998) 112003, [[hep-ph/9802357](#)].

- [19] E155 collaboration, P. L. Anthony et al., *Precision measurement of the proton and deuteron spin structure functions  $g_2$  and asymmetries  $A(2)$* , *Phys. Lett.* **B553** (2003) 18–24, [[hep-ex/0204028](#)].
- [20] A. M. Kotzinian and P. J. Mulders, *Longitudinal quark polarization in transversely polarized nucleons*, *Phys. Rev.* **D54** (1996) 1229–1232, [[hep-ph/9511420](#)].
- [21] A. M. Kotzinian and P. J. Mulders, *Probing transverse quark polarization via azimuthal asymmetries in lepto-production*, *Phys. Lett.* **B406** (1997) 373–380, [[hep-ph/9701330](#)].
- [22] A. Kotzinian, B. Pasquini and A. Prokudin, *Predictions for double spin asymmetry  $A(1T)$  in semi-inclusive DIS*, *Phys. Rev.* **D73** (2006) 114017, [[hep-ph/0603194](#)].
- [23] H. Avakian et al., *Are there approximate relations among transverse momentum dependent distribution functions?*, *Phys. Rev.* **D77** (2008) 014023, [[0709.3253](#)].
- [24] A. Metz, P. Schweitzer and T. Teckentrup, *Lorentz invariance relations between parton distributions and the Wandzura-Wilczek approximation*, *Phys. Lett.* **E680** (2009) 141–147, [[0810.5212](#)].
- [25] T. Teckentrup, A. Metz and P. Schweitzer, *Lorentz invariance relations and Wandzura-Wilczek approximation*, *Mod. Phys. Lett.* **A24** (2009) 2950–2959, [[0910.2567](#)].
- [26] H. Avakian, H. Matevosyan, B. Pasquini and P. Schweitzer, *Studying the information content of TMDs using Monte Carlo generators*, *J. Phys.* **G42** (2015) 034015.
- [27] J. C. Collins, *Leading-twist single-transverse-spin asymmetries: Drell-Yan and deep-inelastic scattering*, *Phys. Lett.* **B536** (2002) 43–48, [[hep-ph/0204004](#)].
- [28] J. P.Ralston and D. E. Soper, *Production of Dimuons from High-Energy Polarized Proton-Proton Collisions*, *Nucl. Phys.* **B152** (1979) 103.
- [29] A. Efremov and P. Schweitzer, *The chirally odd twist 3 distribution  $e(a)(x)$* , *JHEP* **0308** (2003) 006, [[hep-ph/0212044](#)].
- [30] R. L. Jaffe, *Spin, twist and hadron structure in deep inelastic processes*, [hep-ph/9602236](#).
- [31] R. Tangerman and P. Mulders, *Polarized twist - three distributions  $g(T)$  and  $h(L)$  and the role of intrinsic transverse momentum*, [hep-ph/9408305](#).
- [32] D. Diakonov and V. V. Petrov, *Instanton Based Vacuum from Reggeon Variational Principle*, *Nucl. Phys.* **B245** (1984) 259.
- [33] D. Diakonov, M. V. Polyakov and C. Weiss, *Hadronic matrix elements of gluon operators in the instanton vacuum*, *Nucl. Phys.* **B461** (1996) 539–550, [[hep-ph/9510232](#)].
- [34] E. V. Shuryak, *The Role of Instantons in Quantum Chromodynamics. 1. Physical Vacuum*, *Nucl. Phys.* **B203** (1982) 93.
- [35] M. Stratmann, *Bag model predictions for polarized structure functions and their  $Q^{**2}$  evolutions*, *Z. Phys.* **C80** (1993) 763–772.
- [36] A. Signal, *Calculations of higher twist distribution functions in the MIT bag model*, *Nucl. Phys.* **B497** (1997) 415–434, [[hep-ph/9610480](#)].
- [37] H. Avakian, A. Efremov, P. Schweitzer and F. Yuan, *The transverse momentum dependent distribution functions in the bag model*, *Phys. Rev.* **D81** (2010) 074035, [[1001.5467](#)].
- [38] R. Jakob, P. Mulders and J. Rodrigues, *Modeling quark distribution and fragmentation functions*, *Nucl. Phys.* **A626** (1997) 937–965, [[hep-ph/9704335](#)].
- [39] M. Wakamatsu, *Polarized structure functions  $g(2)(x)$  in the chiral quark soliton model*, *Phys. Lett.* **B487** (2000) 118–124, [[hep-ph/0006212](#)].
- [40] C. Lorce, B. Pasquini and M. Vanderhaeghen, *Unified framework for generalized and transverse-momentum dependent parton distributions within a 3Q light-cone picture of the nucleon*, *JHEP* **1105** (2011) 041, [[1102.4704](#)].
- [41] B. Pasquini, S. Cazzaniga and S. Bozzo, *Transverse momentum dependent parton distributions in a light-cone quark model*, *Phys. Rev.* **D78** (2008) 034025, [[0806.2298](#)].
- [42] P. Zavada, *The Structure Functions and parton momenta distribution in the hadron rest system*, *Phys. Rev.* **D55** (1997) 4280–4299, [[hep-ph/9609372](#)].
- [43] A. V. Efremov, P. Schweitzer, O. V. Teryaev and P. Zavada, *Transverse momentum dependent distribution functions in a covariant parton model approach with quarks orbital motion*, *Phys. Rev.* **D80** (2009) 014021, [[0903.3490](#)].
- [44] A. Accardi, A. Bacchetta, W. Melnitchouk and M. Schlegel, *What can break the Wandzura-Wilczek relation?*, *JHEP* **11** (2009) 093, [[0907.2942](#)].
- [45] A. V. Efremov, K. Goeke and P. Schweitzer, *Collins effect in semi-inclusive deeply inelastic scattering and in  $e^+ e^-$  annihilation*, *Phys. Rev.* **D73** (2006) 094025.
- [46] M. Anselmino et al., *Transversity and Collins functions from SIDIS and  $e^+ e^-$  data*, *Phys. Rev.* **D75** (2007) 054032, [[hep-ph/0701006](#)].
- [47] M. Anselmino et al., *Update on transversity and Collins functions from SIDIS and  $e^+ e^-$  data*, *Nucl. Phys. Proc. Suppl.* **191** (2009) 98–107, [[0812.4566](#)].
- [48] Y. Koike, K. Tanaka and S. Yoshiida, *Drell-Yan double-spin asymmetry  $A(1T)$  in polarized  $p$ -anti $p$  collisions: Wandzura-Wilczek contribution*, *Phys. Lett.* **B668** (2008) 286–292, [[0805.2289](#)].
- [49] R. Kundu and A. Metz, *Higher twist and transverse momentum dependent parton distributions: A Light front Hamiltonian approach*, *Phys. Rev.* **D65** (2002) 014009, [[hep-ph/0107073](#)].
- [50] M. Schlegel and A. Metz, *On the validity of Lorentz invariance relations between parton distributions*, [hep-ph/0405288](#).
- [51] K. Goeke, A. Metz, P. Polytis and M. Polyakov, *Lorentz invariance relations among parton distributions revisited*, *Phys. Lett.* **B567** (2003) 27–30, [[hep-ph/0302028](#)].
- [52] S. Meissner, A. Metz and K. Goeke, *Relations between generalized and transverse momentum dependent parton distributions*, *Phys. Rev.* **D76** (2007) 034002, [[hep-ph/0703176](#)].
- [53] A. Mukterjee, *Twist Three Distribution  $e(x)$ : Sum Rules and Equation of Motion Relations*, *Phys. Lett.* **B687** (2010) 180–183, [[0912.1446](#)].
- [54] A. Harindranath and W.-M. Zhang, *Examination of Wandzura-Wilczek relation for  $g_2(x, q^{**2})$  in  $p$ QCD*, *Phys. Lett.* **B408** (1997) 347–356, [[hep-ph/9706419](#)].
- [55] P. Hagler, B. U. Musch, J. W. Negele and A. Schäfer, *Intrinsic quark transverse momentum in the nucleon from lattice QCD*, *Eurphys. Lett.* **88** (2009) 61001, [[0908.1283](#)].
- [56] LHCb collaboration, LHCb et al., *Transverse structure of nucleon parton distributions from lattice QCD*, *Phys. Rev. Lett.* **93** (2004) 112001, [[hep-lat/0312014](#)].

- [57] LHPC COLLABORATIONS collaboration, P. Hagler et al., *Nucleon Generalized Parton Distributions from Full Lattice QCD*, *Phys.Rev.* **D77** (2008) 094502, [[hep-ph/0705.4295](#)].
- [58] QCDSF collaboration, M. Gockeler et al., *Quark helicity flip generalized parton distributions from two-flavor lattice QCD*, *Phys. Lett.* **B627** (2005) 113–123, [[hep-lat/0507001](#)].
- [59] M. Burkardt and Y. Konde, *Violation of sum rules for twist three parton distributions in QCD*, *Nucl.Phys.* **B632** (2002) 311–329, [[hep-ph/0111343](#)].
- [60] S. D. Bass, *Fixed poles, polarized glue and nucleon spin structure*, *Acta Phys.Polon.* **B34** (2003) 5893–5926, [[hep-ph/0311174](#)].
- [61] C. Lorce, B. Pasquini and P. Schweitzer, *Unpolarized transverse momentum dependent parton distribution functions beyond leading twist in quark models*, *JHEP* **01** (2015) 103, [[\[arXiv:1411.2550\]](#)].
- [62] C. Lorce, B. Pasquini and P. Schweitzer, *Transverse pion structure beyond leading twist in constituent models*, *Eur. Phys. J.* **C76** (2016) 415, [[\[arXiv:1505.00835\]](#)].
- [63] M. Amedelino, M. Boglione, U. D’Alesio, S. Melis, F. Murgia et al., *General Helicity Formalism for Polarized Semi-Inclusive Deep Inelastic Scattering*, *Phys.Rev.* **D83** (2011) 114019, [[\[arXiv:1101.1041\]](#)].
- [64] M. Amedelino et al., *The role of Collins and Sivers effects in deep inelastic scattering*, *Phys. Rev.* **D71** (2005) 074006, [[\[hep-ph/0501196\]](#)].
- [65] J. C. Collins et al., *Sivers effect in semi-inclusive deeply inelastic scattering*, *Phys. Rev.* **D73** (2006) 014021, [[\[hep-ph/0509076\]](#)].
- [66] U. D’Alesio and F. Murgia, *Azimuthal and Single Spin Asymmetries in Hard Scattering Processes*, *Prog. Part. Nucl. Phys.* **61** (2008) 394–454, [[\[arXiv:0712.4228\]](#)].
- [67] P. Schweitzer, T. Teckentrup and A. Metz, *Intrinsic transverse parton momenta in deeply inelastic reactions*, *Phys.Rev.* **D81** (2010) 094019, [[\[arXiv:1003.2190\]](#)].
- [68] A. Signori, A. Bacchetta, M. Radici and G. Schnell, *Investigations into the flavor dependence of partonic transverse momentum*, *JHEP* **11** (2013) 194, [[\[arXiv:1309.3507\]](#)].
- [69] M. Amedelino, M. Boglione, J. O. Gonzalez Hernandez, S. Melis and A. Prokudin, *Unpolarised Transverse Momentum Dependent Distribution and Fragmentation Functions from SIDIS Multiplicities*, *JHEP* **04** (2014) 005, [[\[arXiv:1312.5261\]](#)].
- [70] A. Bacchetta, D. Boer, M. Diehl and P. J. Mulders, *Matches and mismatches in the descriptions of semi-inclusive processes at low and high transverse momentum*, *JHEP* **08** (2008) 023, [[\[arXiv:0803.0227\]](#)].
- [71] S. M. Aybat and T. C. Rogers, *TMD Parton Distribution and Fragmentation Functions with QCD Evolution*, *Phys.Rev.* **D83** (2011) 1140402, [[\[arXiv:1101.5057\]](#)].
- [72] F. Landry, R. Brock, P. M. Nadolsky and C. Yuan, *Neutral-Ram-1 Z boson data and Collins-Soper-Sterman resummation formalism*, *Phys.Rev.* **D67** (2003) 073016, [[\[hep-ph/0212159\]](#)].
- [73] J. Collins, L. Gaumberg, A. Prokudin, T. C. Rogers, N. Sato and B. Wang, *Relating Transverse Momentum Dependent and Collinear Factorization Theorems in a Generalized Formality*, *Phys. Rev.* **D94** (2016) 034014, [[\[arXiv:1605.00671\]](#)].
- [74] CLAS COLLABORATION collaboration, M. Osipenko et al., *Measurement of unpolarized semi-inclusive pi+ electroproduction off the proton*, *Phys.Rev.* **D80** (2009) 032004, [[\[arXiv:0809.1153\]](#)].
- [75] CLAS collaboration, H. Avakian et al., *Measurement of Single and Double Spin Asymmetries in Deep Inelastic Pion Electroproduction with a Longitudinally Polarized Target*, *Phys. Rev. Lett.* **105** (2010) 262002, [[\[arXiv:0903.4549\]](#)].
- [76] D. W. Sivers, *Single spin production asymmetries from the hard scattering of point-like constituents*, *Phys. Rev.* **D41** (1990) 83.
- [77] M. Gluck, E. Reya, M. Stratmann and W. Vogelsang, *Models for the polarized parton distributions of the nucleon*, *Phys. Rev.* **D63** (2001) 094005, [[\[hep-ph/0011215\]](#)].
- [78] M. Gluck, E. Reya and A. Vogt, *Dynamical parton distributions revisited*, *Eur. Phys. J.* **C5** (1998) 461–470, [[\[hep-ph/9806404\]](#)].
- [79] D. de Florian, R. Sassot and M. Stratmann, *Global analysis of fragmentation functions for pions and kaons and their uncertainties*, *Phys. Rev.* **D75** (2007) 114010, [[\[hep-ph/0703242\]](#)].
- [80] CLAS COLLABORATION collaboration, H. Avakian et al., *Measurement of beam-spin asymmetries for pi+ electroproduction above the baryon resonance region*, *Phys.Rev.* **D69** (2004) 112004, [[\[hep-ex/0301005\]](#)].
- [81] HERMES COLLABORATION collaboration, A. Airapetian et al., *Beam-Spin Asymmetries in the Azimuthal Distribution of Pion Electroproduction*, *Phys.Lett.* **B648** (2007) 164–170, [[\[hep-ex/0612059\]](#)].
- [82] W. Gohn, H. Avakian, K. Joo and M. Ungaro, *Beam spin asymmetries from semi-inclusive pion electroproduction in deep inelastic scattering*, *AIP Conf.Proc.* **1149** (2009) 461–464.
- [83] M. Agnafyan, H. Avakian, P. Rossi, E. De Sanctis, D. Hesch et al., *Precise Measurements of Beam Spin Asymmetries in Semi-Inclusive pi^0 production*, *Phys.Lett.* **B704** (2011) 397–402, [[\[arXiv:1106.2293\]](#)].
- [84] COMPASS COLLABORATION collaboration, A. Kotzinian, *Beyond Collins and Sivers: Further measurements of the target transverse spin-dependent azimuthal asymmetries in semi-inclusive DIS from COMPASS*, **0705.2402**.
- [85] B. Parsanyan, *Transverse spin dependent azimuthal asymmetries at COMPASS*, *J.Phys.Conf.Ser.* **295** (2011) 012046, [[\[arXiv:1012.0155\]](#)].
- [86] HERMES COLLABORATION collaboration, A. Airapetian et al., *Observation of a single spin azimuthal asymmetry in semi-inclusive pion electro production*, *Phys.Rev.Lett.* **84** (2000) 4047–4051, [[\[hep-ex/9910062\]](#)].
- [87] HERMES COLLABORATION collaboration, A. Airapetian et al., *Single spin azimuthal asymmetries in electroproduction of neutral pions in semiinclusive deep inelastic scattering*, *Phys.Rev.* **D64** (2001) 097101, [[\[hep-ex/0104051\]](#)].
- [88] HERMES COLLABORATION collaboration, A. Airapetian et al., *Measurement of single spin azimuthal asymmetries in semi-inclusive electroproduction of pions and kaons on a longitudinally polarized deuteron target*, *Phys.Lett.* **B562** (2003) 182–192, [[\[hep-ex/0212039\]](#)].
- [89] HERMES COLLABORATION collaboration, A. Airapetian et al., *Subleading-twist effects in single-spin asymmetries in semi-inclusive deep-inelastic scattering on a longitudinally polarized hydrogen target*, *Phys.Lett.* **B622** (2005) 14–22, [[\[hep-ex/0505042\]](#)].

- [90] M. Aleshseev, V. Y. Alexakhin, Y. Alexanrov, G. Alexeev, A. Amoroso et al., *Azimuthal asymmetries of charged hadrons produced by high-energy muons scattered off longitudinally polarised deuterons*, *Eur. Phys. J.* **C70** (2010) 39–49, [[1007.1562](#)].
- [91] R. N. Cain, *Azimuthal Dependence in Leptoproduction: A Simple Parton Model Calculation*, *Phys. Lett.* **B130** (1983) 269.
- [92] EUROPEAN Muon Collaboration collaboration, J. Ahnert et al., *MEASUREMENT OF HADRONIC AZIMUTHAL DISTRIBUTIONS IN DEEP INELASTIC MUON PROTON SCATTERING*, *Phys. Lett.* **B130** (1983) 118.
- [93] H. Mkrchyan, P. Bosted, G. Adams, A. Almidouch, T. Angelescu et al., *Transverse momentum dependence of semi-inclusive pion production*, *Phys. Lett.* **B665** (2008) 20–25, [[0709.3020](#)].
- [94] HERMES COLLABORATION collaboration, F. Giordano and R. Lamb, *Measurement of azimuthal asymmetries of the unpolarized cross section at HERMES*, *AIP Conf. Proc.* **1149** (2009) 423–428, [[0901.2438](#)].
- [95] COMPASS COLLABORATION collaboration, R. Joosten, *Unpolarized azimuthal asymmetries from the COMPASS experiment at CERN*, *AIP Conf. Proc.* **1182** (2009) 585–588.
- [96] HERMES COLLABORATION collaboration, A. Airapetian et al., *Transverse momentum broadening of hadrons produced in semi-inclusive deep-inelastic scattering on nuclei*, *Phys. Lett.* **B684** (2010) 114–118, [[0906.2478](#)].
- [97] COMPASS COLLABORATION collaboration, J.-F. Rajotte, *Hadron transverse momentum distributions and TMD studies*, **1008**, 5125.
- [98] HERMES COLLABORATION collaboration, G. Schnell, *The Sivers and other semi-inclusive single-spin asymmetries at HERMES*, *PoS DIS2010* (2010) 247.
- [99] A. V. Efremov, K. Goeke, S. Meissel, A. Metz and P. Schweitzer, *Sivers effect in semi-inclusive DIS and in the Drell-Yan process*, *Phys. Lett.* **B612** (2005) 233–244, [[hep-ph/0412353](#)].
- [100] M. Anselmino et al., *Sivers Effect for Pion and Kaon Production in Semi-Inclusive Deep Inelastic Scattering*, *Eur. Phys. J.* **A39** (2009) 89–100, [[0805.2677](#)].
- [101] M. Anselmino, M. Boglione, U. D'Alesio, S. Melis, F. Murgia and A. Prokudin, *Distribution Functions and the Latest SIDIS Data*, in *19th International Workshop on Deep-Inelastic Scattering and Related Subjects (DIS 2011)* *Newport News, Virginia, April 11–15, 2011*, 2011, 1107, 4446.
- [102] S. M. Aybat, J. C. Collins, J.-W. Qiu and T. C. Rogers, *The QCD Evolution of the Sivers Function*, *Phys. Rev.* **D85** (2012) 034043, [[1110.6426](#)].
- [103] L. Gamberg, Z.-B. Kang and A. Prokudin, *Indication on the process-dependence of the Sivers effect*, *Phys. Rev. Lett.* **110** (2013) 232301, [[1302.3218](#)].
- [104] A. Bacchetta and M. Radici, *Constraining quark angular momentum through semi-inclusive measurements*, *Phys. Rev. Lett.* **107** (2011) 212001, [[1107.5755](#)].
- [105] M. Anselmino, M. Boglione and S. Melis, *A Strategy towards the extraction of the Sivers function with TMD evolution*, *Phys. Rev.* **D86** (2012) 014028, [[1204.1239](#)].
- [106] P. Sun and F. Yuan, *Energy Evolution for the Sivers Asymmetries in Hard Processes*, *Phys. Rev.* **D88** (2013) 034016, [[1304.5037](#)].
- [107] M. G. Edebarria, A. Idlibi, Z.-B. Kang and I. Vitev, *QCD Evolution of the Sivers Asymmetry*, *Phys. Rev.* **D89** (2014) 074013, [[1401.5078](#)].
- [108] M. Anselmino, M. Boglione, U. D'Alesio, S. Melis, F. Murgia and A. Prokudin, *Simultaneous extraction of transversity and Collins functions from new SIDIS and e+e- data*, *Phys. Rev.* **D87** (2013) 094019, [[1303.3822](#)].
- [109] Z.-B. Kang, A. Prokudin, P. Sun and F. Yuan, *Nucleon tensor charge from Collins azimuthal asymmetry measurements*, *Phys. Rev.* **D91** (2015) 071501, [[1410.4877](#)].
- [110] Z.-B. Kang, A. Prokudin, P. Sun and F. Yuan, *Extraction of Quark Transversity Distribution and Collins Fragmentation Functions with QCD Evolution*, *Phys. Rev.* **D93** (2016) 014009, [[1505.05889](#)].
- [111] M. Anselmino, M. Boglione, U. D'Alesio, J. O. Gonzalez Hernandez, S. Melis, F. Murgia et al., *Collins functions for pions from SIDIS and new e+e- data: a first glance at their transverse momentum dependence*, *Phys. Rev.* **D92** (2015) 114023, [[1510.05386](#)].
- [112] V. Barone, S. Melis and A. Prokudin, *The Boer-Mulders effect in unpolarized SIDIS: Analysis of the COMPASS and HERMES data on the cos 2 phi asymmetry*, *Phys. Rev. D81* (2010) 114026, [[0912.5194](#)].
- [113] V. Barone, S. Melis and A. Prokudin, *Azimuthal asymmetries in unpolarized Drell-Yan processes and the Boer-Mulders distributions of antiquarks*, *Phys. Rev.* **D82** (2010) 114025, [[1009.3423](#)].
- [114] V. Barone, M. Boglione, J. O. Gonzalez Hernandez and S. Melis, *Phenomenological analysis of azimuthal asymmetries in unpolarized semi-inclusive deep inelastic scattering*, *Phys. Rev. D91* (2015) 074019, [[1502.04214](#)].
- [115] C. Lefty and A. Prokudin, *Extraction of the distribution function  $n_T^{\perp}$  from experimental data*, *Phys. Rev.* **D91** (2015) 034010, [[1411.0580](#)].

$$\left\langle \frac{K_T^2}{P_{T^2}} \right\rangle + \frac{\left\langle K_T^2 \right\rangle \left( \frac{1}{P_T^2} + \frac{2}{P_{T^2}} \right)}{Z^2 P_T^2} -$$

next page

$$= \left( \frac{2P_T}{P_T^2 + P_{T^2}} \right) \left[ P_T^2 - \frac{2Z P_T \cdot P_{T^2}}{Z^2 P_T^2} \right] = \left( \frac{2P_T}{P_T^2 + P_{T^2}} \right)$$

$$- \text{ argument of exp} = \frac{P_T^2}{Z^2 P_T^2} + \frac{\left\langle K_T^2 \right\rangle}{Z^2 P_T^2} - \frac{P_T^2}{Z^2 P_T^2} + \frac{\left\langle K_T^2 \right\rangle}{Z^2 P_T^2}$$

cancel the

$$I(P_{T^2}) = \int dP_T \, w(P_T, ZP_T - P_{T^2}) \exp \left[ - \frac{\pi^2 C_P^2 \left\langle K_T^2 \right\rangle}{P_T^2} - \frac{\left\langle K_T^2 \right\rangle}{Z^2 P_T^2} \right]$$

$$\text{2nd step: integrate over } K_T. \text{ Notice } -K_T = ZP_T - P_{T^2}$$

$$\left( \frac{\pi^2 C_P^2 \left\langle K_T^2 \right\rangle}{P_T^2} - \frac{\left\langle K_T^2 \right\rangle}{Z^2 P_T^2} \right) \cdot \exp \left( - \frac{P_T^2}{Z^2 P_T^2} - \frac{K_T^2}{Z^2 P_T^2} \right).$$

$$\text{with } I(P_{T^2}) = \int dP_T \int dK_T \, g^{(2)}(ZP_T + K_T - P_{T^2}) \, w(P_T, -K_T)$$

$$(P_{T^2}) \, I(P_{T^2}) = x \sum_a f_a(x, P_T) \, g^{(2)}(x, K_T)$$

$$15^{\text{th}} \text{ step: substitute } K_T \rightarrow -\frac{Z}{P_T}$$

$$C[\omega f \circ \mathbb{D}] = x \sum_a f_a \int dP_T \int dK_T \, g^{(2)}(ZP_T - K_T - P_{T^2}) \, w(P_T, K_T)$$

Evaluating convolution integrals with Gauss model



$$\exp\left(-\frac{\langle P_2 \rangle \langle K_2 \rangle}{A} \left[ \frac{P_t}{P_{h_1}} - z \frac{P_t}{P_{h_2}} \right] \right) .$$

$$\left( \frac{1}{\langle P_2 \rangle} \int dP_t \omega(P_t, z) \frac{\pi \langle P_2 \rangle \langle K_2 \rangle}{A} \cdot \frac{\pi A}{e^{\frac{\langle P_2 \rangle \langle K_2 \rangle}{A}}} = \right. \\ \left. \left( \frac{\pi}{\langle P_{h_1} \rangle} - \right) \exp\left(-\frac{\langle P_2 \rangle \langle K_2 \rangle}{A} \right) . \right)$$

$$\left( \frac{1}{\langle P_2 \rangle} \int dP_t \omega(P_t, z) \exp\left(-\frac{\langle P_2 \rangle \langle K_2 \rangle}{A} \right) \right) \cdot \frac{\pi \langle P_2 \rangle \langle K_2 \rangle}{A} \\ \stackrel{z \rightarrow \infty}{=} I(P_t) = \int dP_t \omega(P_t, z) \left( \frac{\pi}{\langle P_{h_1} \rangle} - \right) \Leftarrow$$

$$\text{mother: } A = z \langle P_2 \rangle + \langle K_2 \rangle$$

$$(III) \quad \frac{\langle P_2 \rangle + \langle K_2 \rangle}{A} = \frac{\langle P_2 \rangle \langle K_2 \rangle}{A}$$

$$(III) \quad \frac{1}{\langle P_2 \rangle} = \frac{\langle P_2 \rangle (\langle P_2 \rangle + \langle K_2 \rangle)}{A} = \frac{\langle K_2 \rangle (\langle P_2 \rangle + \langle K_2 \rangle)}{A}$$

$$\frac{A}{\langle K_2 \rangle} = \frac{\langle K_2 \rangle + \langle P_2 \rangle + \langle K_2 \rangle}{\langle K_2 \rangle} = \frac{\langle P_2 \rangle + \langle K_2 \rangle}{\langle K_2 \rangle} \quad \downarrow (I)$$

$$\left( \frac{\langle P_2 \rangle + \langle K_2 \rangle}{\langle P_{h_1} \rangle} - 1 \right) \frac{\langle K_2 \rangle}{\langle P_{h_1} \rangle} +$$

$$Z^{(III)} \left( \frac{\left( \langle P_2 \rangle + \langle K_2 \rangle \right) \langle P_2 \rangle \langle K_2 \rangle}{\langle P_{h_1} \rangle} - \frac{P_t}{P_{h_1}} \right) \left( \frac{1}{\langle P_2 \rangle} + \frac{\langle K_2 \rangle}{\langle P_{h_1} \rangle} \right) =$$

$$\begin{aligned}
 & \text{Step 3:} \quad \text{insert specific expression for } \omega_{\text{left}} \text{ and perform integration} \\
 & \text{Integration over } d\mathbf{k}_1 \quad \text{Integration over } d\mathbf{k}_2 \\
 & \omega_1 = 1 \\
 & \omega_{2a} = \left[ -\frac{\hbar \cdot \mathbf{E}_1}{m_a} + \frac{\hbar \cdot \mathbf{K}_1}{m_a} \right]_{\text{muu-particle}} \\
 & \omega_{2b} = \left[ -\frac{\hbar \cdot \mathbf{E}_1}{m_b} \right]_{\text{muu-particle}} \quad \text{so } \hbar \cdot \mathbf{P}_1 = \mathbf{K}_1 \text{ in muu-particle} \\
 & \omega_A = \left[ -\frac{\hbar \cdot \mathbf{P}_1}{m_a} \right]_{\text{muu-particle}} \\
 & \omega_B = \left[ -\frac{\hbar \cdot \mathbf{P}_1}{m_b} \right]_{\text{muu-particle}} \\
 & \omega_C = \left( +\frac{\hbar \cdot \mathbf{P}_1}{m_b} \right)_{\text{muu-particle}} \\
 & \omega_D = \left( -\frac{\hbar \cdot \mathbf{P}_1}{m_a} \right)_{\text{muu-particle}} \\
 & \omega_{3a} = \left[ -\frac{2(\hbar \cdot \mathbf{K}_1)(\hbar \cdot \mathbf{P}_1)}{2H_m m_a} + \frac{2(\hbar \cdot \mathbf{K}_1)(\hbar \cdot \mathbf{P}_1)}{2H_m m_b} \right]_{\text{muu-particle}} \\
 & \omega_{3b} = \left[ -\frac{K_1 \cdot P_1}{H_m m_b} \right]_{\text{muu-particle}} \\
 & \omega_4 = \left( \frac{2(\hbar \cdot \mathbf{P}_1)(\hbar \cdot \mathbf{K}_1) + \mathbf{P}_1^2(\hbar \cdot \mathbf{K}_1) - 4(\hbar \cdot \mathbf{P}_1)^2(\hbar \cdot \mathbf{K}_1)}{2H_m^2 m_b} \right)_{\text{muu-particle}} \\
 & \omega_5 = \left( +\frac{2(\hbar \cdot \mathbf{P}_1)^2 - \mathbf{P}_1^2}{2H_m^2} \right)_{\text{muu-particle}} = \left[ \frac{2(\hbar \cdot \mathbf{P}_1)^2 - \mathbf{P}_1^2}{2H_m^2} \right]_{\text{muu-particle}}
 \end{aligned}$$

5th step: insert specific expression for  $\omega_{\text{left}}$  and perform integration

$$\begin{aligned}
 & \text{Step 4:} \quad \text{insert specific expression for } \omega_{\text{left}} \text{ and perform integration} \\
 & \text{Integration over } d\mathbf{k}_1 \quad \text{Integration over } d\mathbf{k}_2 \\
 & I(P_{h1}) = \exp\left(-\frac{\pi \alpha}{\Phi_{h1}}\right) \cdot \frac{\pi \alpha}{\Phi_{h1}} \cdot \int d\mathbf{k}_1 \frac{1}{\left(\frac{\hbar^2}{2m_a} \mathbf{K}_1^2 + \frac{\hbar^2}{2m_b} \mathbf{P}_1^2\right)^{1/2}} \cdot \exp\left(-\frac{\hbar \cdot \mathbf{E}_1}{m_a}\right)
 \end{aligned}$$

$$\text{4th step:} \quad \text{subst. } P_1' \rightarrow \left( \frac{\hbar}{\alpha} \frac{\mathbf{K}_1^2}{\mathbf{P}_1^2} \right)^{1/2} = \left( \frac{\hbar}{\alpha} \frac{\mathbf{K}_1^2}{\mathbf{P}_1^2} \right)^{1/2} \cdot \exp\left(-\frac{\hbar \cdot \mathbf{E}_1}{m_a}\right)$$

$$\begin{aligned}
 & \text{4th step:} \quad \text{substitution } P_1' \rightarrow \frac{\hbar}{\alpha} \frac{\mathbf{K}_1^2}{\mathbf{P}_1^2} = \frac{\hbar}{\alpha} - \frac{\hbar \cdot \mathbf{P}_1}{m_a} \frac{\mathbf{K}_1}{\mathbf{P}_1} \\
 & I(P_{h1}) = \frac{\pi \alpha}{\Phi_{h1}} \cdot \frac{\pi \alpha}{\left(\frac{\hbar^2}{2m_a} \mathbf{K}_1^2 + \frac{\hbar^2}{2m_b} \mathbf{P}_1^2\right)^{1/2}} \cdot \int d\mathbf{P}_{h1} \frac{\omega(P_{h1})}{\left(\frac{\hbar^2}{2m_a} \mathbf{K}_1^2 + \frac{\hbar^2}{2m_b} \mathbf{P}_{h1}^2\right)^{1/2}} \cdot \exp\left(-\frac{\hbar \cdot \mathbf{E}_1}{m_a}\right)
 \end{aligned}$$

$$\text{3rd step:} \quad \text{substitution } P_1' \rightarrow \frac{\hbar}{\alpha} - \frac{\hbar \cdot \mathbf{P}_1}{m_a} \frac{\mathbf{K}_1}{\mathbf{P}_1}$$

$$\left( \frac{V}{\epsilon^2 k} e^{-\frac{V}{kT}} - \frac{1}{2} \int_{\epsilon_1}^{\epsilon_2} \dots \right)$$

$$e^{-\frac{V}{kT}} = \left( \frac{P_n + n}{P_n} \right) e^{-\frac{V}{kT}}$$

$$(P_n + n) * \frac{V}{kT} \cdot \frac{1}{e^{-\frac{V}{kT}}} =$$

$$C \left[ \dots \omega(P_i, k_i) / \text{Ansatz, nach oben} \right]$$

general expression:

$$(II) \quad \frac{1}{\langle K_T^2 \rangle} = (I) \quad \frac{\int dK_T}{K_T^2} \frac{e^{-\frac{K_T^2}{2\sigma_{K_T}^2}}}{\langle K_T^2 \rangle}$$

$$\int dK_T \frac{e^{-\frac{K_T^2}{2\sigma_{K_T}^2}}}{\langle K_T^2 \rangle} = \int dx \frac{f(x)}{\int dx f(x)} e^{-\frac{x^2}{2\sigma_x^2}} = \int dx f(x) e^{-\frac{(x-\mu)^2}{2\sigma_x^2}}$$

$$= \int dx \frac{\int dp_T e^{-\frac{p_T^2}{2\sigma_{p_T}^2}}}{\int dp_T} e^{-\frac{(x-\mu)^2}{2\sigma_x^2}} = \int dp_T \int dx e^{-\frac{(x-\mu)^2}{2\sigma_x^2}}$$

$$(II) \quad f(x) = \int dp_T \frac{1}{2\pi} \int dx \frac{e^{-\frac{(x-\mu)^2}{2\sigma_x^2}}}{\int dx e^{-\frac{(x-\mu)^2}{2\sigma_x^2}}} = f(x) \quad \text{Definitions:}$$

$$(II) \quad \overbrace{\int dx \left[ \frac{x}{T} - \frac{x}{e} \right]}^{I=0} = \int dx \left[ \int_0^\infty e^{-y} dy - \int_0^\infty e^{-y} dy \right] = \int_0^\infty e^{-y} dy = I \quad (II)$$

$$I = \int_0^\infty \int_0^\infty e^{-x-y} dy dx = \int_0^\infty x e^{-x} dx = \int_0^\infty x e^{-x} dx = I \quad (I)$$

needed Gauss integrals:



$$x \leq e^{\int_{\alpha}^{\beta} m_u du} = e^{\frac{1}{2} \int_{\alpha}^{\beta} m_u du}$$

$$\frac{1}{e^{\frac{1}{2} \int_{\alpha}^{\beta} m_u du}} = \frac{1}{e^{-\frac{1}{2} \int_{\alpha}^{\beta} m_u du}} = e^{-\frac{1}{2} \int_{\alpha}^{\beta} m_u du}$$

$$(I) \text{ with } P_{y_1} = e^{-\frac{1}{2} \int_{\alpha}^{\beta} m_u du}$$

Let linear term in  $\zeta$  we see

$$e^{-\zeta} = \left( e^{-\frac{1}{2} \int_{\alpha}^{\beta} m_u du} + \zeta \cdot \frac{d}{d\zeta} e^{-\frac{1}{2} \int_{\alpha}^{\beta} m_u du} \right) \frac{1}{T} \int_{\alpha}^{\beta} m_u du =$$

$$\text{step 4} \quad \left( \left( e^{-\frac{1}{2} \int_{\alpha}^{\beta} m_u du} - \frac{1}{2} \frac{d}{d\zeta} e^{-\frac{1}{2} \int_{\alpha}^{\beta} m_u du} \right) \zeta + \dots \right) \frac{1}{T} \int_{\alpha}^{\beta} m_u du =$$

$$\text{step 3} \quad \left( \frac{h \cdot (2P_{y_1} - P_{y_1}^2)}{2m_u} \zeta - \dots \right) =$$

$$\text{step 2} \quad \left( \frac{h \cdot (2P_{y_1} - P_{y_1}^2)}{2m_u} \zeta - \dots \right) =$$

$$\text{step 1} \quad \dots \left( \frac{h \cdot K_T}{2m_u} \zeta + \dots \right) = [C + \frac{h \cdot K_T}{2m_u} \zeta]$$

$$(2a) \quad \omega = -\frac{h \cdot K_T}{2m_u} = +\frac{h \cdot K_T}{2m_u}$$

1 in  $F_{uu} \cos \theta$ ,  $F_{uu} \sin \theta$ ,  $F_{ul} \cos \theta$ ,  $F_{ul} \sin \theta$ ,  $F_{ur} \cos \theta$ ,  $F_{ur} \sin \theta$

(I) due to (I)

$$\underbrace{\exp \left( -\frac{1}{2} \int_{\alpha}^{\beta} m_u du \right)}_{\text{with } I, (P_{y_1})} = \exp \left( -\frac{1}{2} \int_{\alpha}^{\beta} m_u du \right)$$

$$[C] = x \leq e^{\int_{\alpha}^{\beta} m_u du} I, (P_{y_1})$$

1 in  $F_{uu} = F_{uu} \cos \theta$ ,  $F_{uu} \sin \theta$ ,  $F_{ul} = F_{ul} \cos \theta$ ,  $F_{ul} \sin \theta$ ,  $F_{ur} = F_{ur} \cos \theta$ ,  $F_{ur} \sin \theta$

$$\frac{V_n}{\left( \frac{V_n}{P_{n1}} + 2P_{n1} \right) M_n} \cdot \frac{V}{2eP_{n1}M_n} \text{exp}(-\int_{P_{n1}}^{P_n} f(x) dx) =$$

$$\frac{V_n}{P_{n1}} \cdot \frac{V}{M_n} - \frac{V}{2P_{n1}} \cdot \frac{\text{exp}(-\int_{P_{n1}}^{P_n} f(x) dx)}{M_n} =$$

... -  $\frac{V}{M_n} \text{exp}(-\int_{P_{n1}}^{P_n} f(x) dx)$  ...  
5th step with (II)

$\frac{V_n}{h \cdot \left( \frac{V_n}{P_{n1}} + 2P_{n1} \right) M_n}$  ...  
6th step

... -  $\frac{V_n}{h \cdot P_{n1}} \text{exp}(-\int_{P_{n1}}^{P_n} f(x) dx)$  ...  
3rd step

... -  $\frac{V_n}{h \cdot P_{n1}}$  ...  
1st step + 2nd step

(26)  $\omega = -\frac{V_n}{h \cdot P_{n1}} M_n$

in  $F_{uu}^{\cos}, F_{uu}^{\sin}, F_{uv}^{\cos}, F_{uv}^{\sin}, F_{vt}^{\cos}, F_{vt}^{\sin}$

$$\left( \frac{\lambda}{P_{42}} - \frac{1}{2} \right) \cdot \left( \frac{\lambda}{P_{42}} \right)_* \frac{\lambda}{P_{42}^2 < k_T^2} =$$

$$\left\{ 1 \cdot \frac{\lambda}{P_{42}^2 < k_T^2} - \frac{\lambda}{P_{41}^2 < k_T^2} \right\} \frac{\lambda}{P_{41}^2 < k_T^2} =$$

$$CL_{03a} = \left[ \frac{1}{T} \int d\phi \frac{\lambda}{P_{42}^2 < k_T^2} \left( h \cdot [L \cdot J_S + z P_{41} \frac{\lambda}{P_{42}^2}] \right) \right]$$

$$CL_{03a} = \left[ \frac{h_m m}{2 (h \cdot P_T) (h \cdot k_T)} \right] = CL_{03a}^{(v)}$$

$\text{Eq 36} \equiv \text{Eq 33}$  appears in  $F_{LT} \sin \theta$ ,  $F_{LT} \cos \theta$

$$= \frac{\langle P_{T2}^2 \rangle \langle K_T^2 \rangle}{2P_{T1}} + \frac{\langle P_{T2}^2 \rangle}{H_u m_b} + \frac{\langle P_{T2}^2 \rangle}{2P_{T1}}$$

$$\left[ \frac{\alpha}{P_{T1}^2} - 1 + \left[ \frac{\alpha}{H_u m_b} \right] \right] =$$

$$C[\alpha] = \left[ 1 - \left[ \frac{\langle P_{T2}^2 \rangle \langle K_T^2 \rangle}{1} \right] \right] = C[\alpha]$$

(3a + 36)

$$\left( \frac{\alpha}{P_{T1}^2} - 1 \right) \left( \frac{\alpha}{H_u m_b} \right) \langle P_{T2}^2 \rangle \langle K_T^2 \rangle * \dots =$$

$$C[\alpha] = \left\{ \frac{1}{2} \frac{\langle P_{T2}^2 \rangle \langle K_T^2 \rangle}{\alpha} - \frac{1}{2} \frac{\alpha}{P_{T1}^2} \right\} =$$

$$\frac{H_u m_b}{k_B P_T} + = R_C \quad (36)$$

$$\left[ \frac{V}{\Delta P_1} \right] \text{ vs } P_1 \quad \left[ \frac{V}{\Delta P_2} \right] \text{ vs } P_2 -$$

$$\frac{\chi^3}{\langle k^2 \rangle} - \frac{4}{\langle k^4 \rangle} + 4 \cdot \frac{\chi^3}{\langle k^2 \rangle} + 4 \cdot \frac{\chi}{\langle k^4 \rangle} \cdot \frac{\chi^3}{\langle k^2 \rangle} + 4 \cdot \frac{\chi^3}{\langle k^2 \rangle} = h$$

$$\frac{V_2}{V_1} = \frac{P_{H2}}{P_{H1}}$$

$$\frac{V}{\langle P_2 \rangle} = \frac{\sum_{i=1}^n \left( \frac{V_i}{\langle P_{2i} \rangle} \right) \frac{P_{2i}}{\sum_{j=1}^n P_{2j}}}{\sum_{i=1}^n \left( \frac{V_i}{\langle P_{2i} \rangle} \right)} - \frac{V}{\langle P_2 \rangle}$$

$$= -2 \cdot P_{H_1}^3 \cdot \left\langle P_2^2 \right\rangle \left\langle K_2^2 \right\rangle \text{All terms}$$

$$\left[ 2 \left( \frac{P_{\text{Tx}}}{P_{\text{Rx}}} \right)^2 < \frac{R_2}{A} < 2 P_{\text{Rx}} \right] \frac{P_{\text{Tx}}}{2 P_{\text{Rx}}}$$

$\leftarrow h_0$

$$\left\langle \begin{array}{c} K \\ \downarrow \end{array} \right\rangle = \frac{z}{\ln z} - \left\{ \begin{array}{c} \text{large} \\ \text{L} \end{array} \right\} \quad \leftarrow \quad h \cdot k$$

$$\frac{V}{Z} = \frac{V_1}{Z_1} + \frac{V_2}{Z_2} + \frac{V_3}{Z_3} + \dots$$

$$\frac{(\bar{y}_i \cdot p_i)^2}{\sum_{j=1}^n (\bar{y}_j \cdot p_j)^2} = \frac{\lambda}{\lambda + \sum_{j \neq i} \lambda_j} \quad (15.4)$$

$$\frac{P_{\text{in}}}{P_{\text{out}}} = \frac{1 - \alpha}{\alpha} + \frac{\alpha}{P_{\text{out}}} \left\{ \frac{1 - \alpha}{P_{\text{in}}} \right\}^2$$

$$\frac{P_{\text{d},k_t}}{P_{\text{t},k_t}} = \frac{\langle P_2^2(K_2) \rangle_{\text{d},k_t} - \langle P_{\text{u},1}^2 \rangle_{\text{d},k_t}}{\langle P_2^2(K_2) \rangle_{\text{t},k_t} - \langle P_{\text{u},1}^2 \rangle_{\text{t},k_t}}$$

$$\frac{\partial}{\partial t} \left( h \cdot \vec{P}_T \right) \left( h \cdot \vec{k}_T \right) + \vec{P}_T^2 \left( h \cdot \vec{k}_T \right) = -4 \left( h \cdot \vec{P}_T \right)^2 \left( h \cdot \vec{k}_T \right)$$

time:

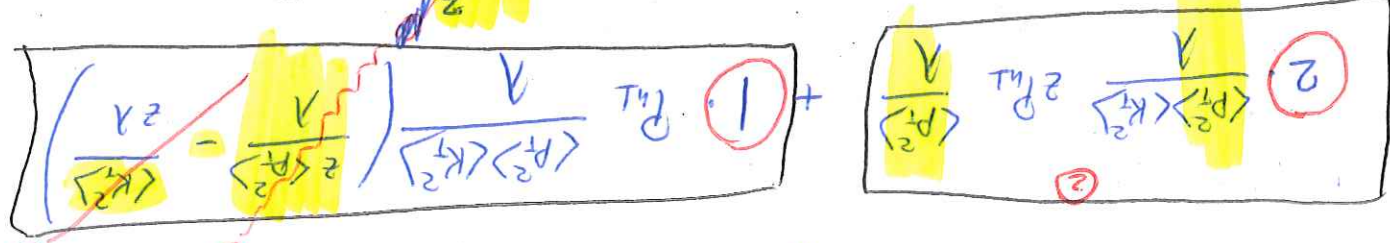
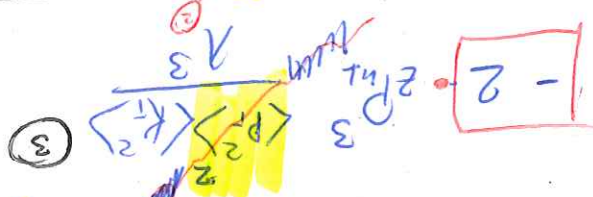
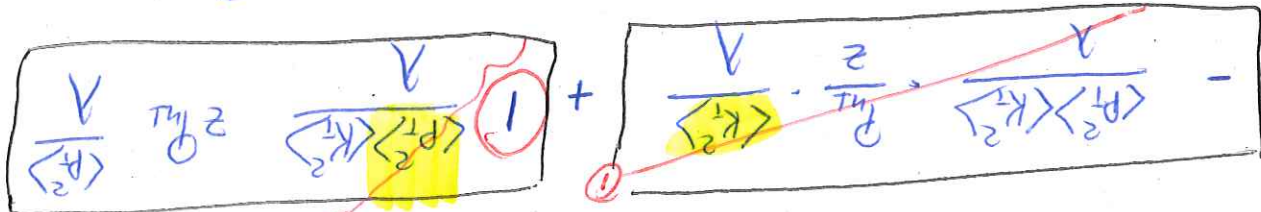
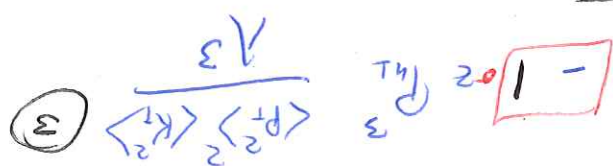
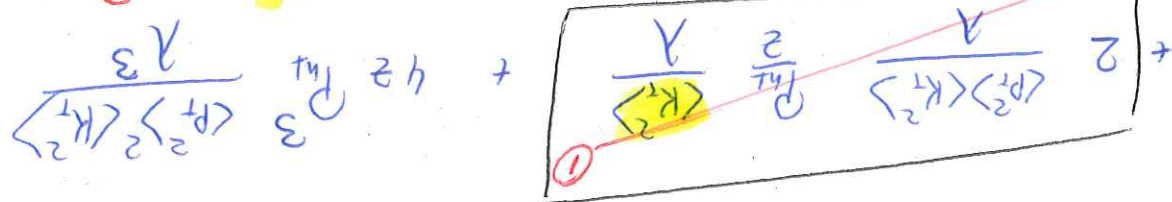
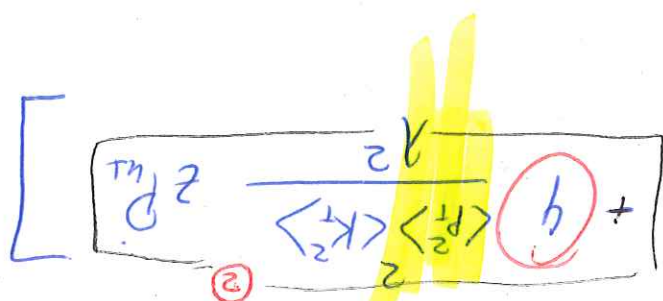
=  $\text{h}_{C1}$   
(3)

$$\frac{2H^2_{\mu_0}m_y}{2P^2_{\mu_1} < P^2_{\mu_1} < K^2_2}$$

$$= \frac{T}{2H^2_{\mu_0}m_y} \cdot \frac{A_3}{2P^2_{\mu_1} < P^2_{\mu_1} < K^2_2} = \frac{T}{2H^2_{\mu_0}m_y} \cdot (-2 - 1 + 3) = \frac{T}{2H^2_{\mu_0}m_y} \cdot 0 = 0$$

$$= +2 + 1 + 1 - 4 = 0$$

$$= 2 + 1 - 1 - 2 = 0$$



10

after integr.  $\mathcal{O}_4 \sim \frac{T}{2H^2_{\mu_0}m_y}$

$$\frac{1}{2H_0^2} \phi^2 \theta_{h_1}^2 \frac{\partial}{\partial z} =$$

$$\left[ \dots \cdot 1 - \frac{\partial}{\partial z} \right] \frac{1}{2H_0^2} \phi^2 \theta_{h_1}^2 + \frac{\partial}{\partial z} \frac{\partial}{\partial z} \frac{\partial}{\partial z} =$$

$$\left[ \dots + \text{linear in } \frac{\partial}{\partial z} \right] - \frac{\partial}{\partial z} \frac{\partial}{\partial z} \frac{\partial}{\partial z} -$$

$$= \left[ 2(\zeta \cdot \bar{\zeta}) \frac{\partial}{\partial z} \frac{\partial}{\partial z} \frac{\partial}{\partial z} \right] -$$

$$2 \left( \frac{\partial}{\partial z} \left( \frac{\partial}{\partial z} \frac{\partial}{\partial z} \right) + \frac{\partial}{\partial z} \frac{\partial}{\partial z} \frac{\partial}{\partial z} \right)$$

$$C[\omega_s] = - \frac{1}{T} \int d\zeta e^{-\zeta s} \cdot \frac{\partial}{\partial z}$$

$$\omega_s^{(2)} \equiv \frac{2(\zeta \cdot \bar{\zeta})^2 - p^2}{2H_0^2}$$

(5)

$\omega_3 \leftarrow \omega_4$

$\omega_{3a}, \omega_{3b}, \omega_5 \leftarrow \omega_4, \omega_8, \omega_3$

$\omega_{2a}, \omega_{2b} \leftarrow \omega_4, \omega_5$

for better modification: name  $\omega_i \rightarrow \omega_0$

higher induction  
power of  $\omega_1$

$$C[\omega_5] = \frac{H_0}{2P_{h1}} \cdot \frac{H_0}{2P_{h2}} \cdot \frac{\alpha}{\langle P_2 \rangle} \cdot \frac{\alpha}{\langle P_2 \rangle} \cdot \frac{1}{2}$$

$$C[\omega_4] = \frac{H_0}{2P_{h1}} \cdot \frac{H_0}{2P_{h2}} \cdot \frac{\alpha}{\langle P_2 \rangle} \cdot \frac{\alpha}{\langle P_2 \rangle} \cdot \frac{m_6}{2P_{h1}} \cdot \frac{m_6}{2P_{h2}} \cdot \frac{\alpha}{\langle P_2 \rangle} \cdot \frac{\alpha}{\langle P_2 \rangle} \cdot \frac{1}{2}$$

$$C[\omega_3] = \frac{2P_{h1}}{ZP_{h1}} \cdot \frac{2P_{h2}}{ZP_{h2}} \cdot \frac{\alpha}{\langle P_2 \rangle} \cdot \frac{\alpha}{\langle P_2 \rangle} \cdot \frac{m_6}{2P_{h1}} \cdot \frac{m_6}{2P_{h2}} \cdot \frac{H_0}{\langle P_2 \rangle} \cdot \frac{H_0}{\langle P_2 \rangle} \cdot *$$

$$C[\omega_3] = \frac{H_0 m_6 \alpha}{\langle P_2 \rangle \langle K_2 \rangle} \left( 1 - \frac{P_2}{P_{h1}} \right)$$

$$C[\omega_3] = \frac{H_0 m_6 \alpha}{\langle P_2 \rangle \langle K_2 \rangle} \left( -1 + \frac{\alpha}{2P_{h1}} \right)$$

$$C[\omega_{2b}] = \frac{\sqrt{V}}{2P_{h1}} \cdot \frac{\sqrt{H_0}}{\langle P_2 \rangle} \cdot *$$

$$C[\omega_{2a}] = \frac{\sqrt{V}}{2P_{h1}} \cdot \frac{\sqrt{H_0}}{\langle P_2 \rangle} \cdot *$$

$$C[\omega_1] = \sum_{i=1}^n f_m(\omega_i) G_i(P_2)$$

Summary of results

$$D_c^{(2)} = \frac{V}{4\pi^2 m_e^2}$$

$$(1) D_c = \frac{V}{2\pi^2} \left( \frac{\pi}{m_e^2} - 1 \right) \int d^2 p \int d^2 p' = D_c^{(1)}$$

$$\underbrace{\int_{-\infty}^{\infty} e^{-px} \int_{-\infty}^{\infty} e^{-px'} dx' dx}_{= 1} = \frac{1}{T} \cdot \frac{1}{T} \cdot \frac{V}{4\pi^2 m_e^2} =$$

$$- \int_{-\infty}^{\infty} e^{-px} \int_{-\infty}^{\infty} e^{-px'} \int_{-\infty}^{\infty} e^{-px''} dx' dx'' = \frac{1}{T} \cdot \frac{1}{T} \cdot \frac{V}{4\pi^2 m_e^2} =$$

$$\frac{V}{m_e^2} \cdot \frac{\pi}{e^2} \cdot \frac{V}{4\pi^2 m_e^2} \int d^2 p \int d^2 p' = D_c^{(1)} = D_c^{(2)}$$

$$H_n = \int d^4 p \delta(p^2) = D_c^{(1)}$$

$$\int_{-\infty}^{\infty} e^{-px} \int_{-\infty}^{\infty} e^{-px'} dx' dx'' = (-\frac{1}{e^p})^2 = \frac{1}{2m_p} \cdot \frac{\pi}{e^p} = D_c^{(1)} \cdot \frac{1}{2m_p} =$$

$$\frac{\pi}{2m_p} \int_{-\infty}^{\infty} e^{-px} \int_{-\infty}^{\infty} e^{-px'} dx' dx'' =$$

$$\frac{\pi}{2m_p} \cdot \frac{\pi}{e^p} = D_c^{(1)} \cdot \frac{1}{2m_p} \cdot \int d^2 p \int d^2 p' =$$

$$n = \frac{\pi}{e^p} = n \int d^2 p \int d^2 p' = \int d^2 p \int d^2 p' f_{(1)}$$

Integrating out transverse momenta:

$$\frac{V}{\epsilon} = \frac{\epsilon_0 A}{4\pi^2 m^2} \cdot \frac{1}{3!} \frac{1}{4!} =$$

$$\frac{V}{\epsilon} = \frac{\epsilon_0 A}{4\pi^2 m^2} \cdot \frac{1}{3!} \frac{1}{4!} =$$

$$\frac{V}{\epsilon} = \frac{\epsilon_0 A}{4\pi^2 m^2} \cdot \frac{1}{3!} \frac{1}{4!} =$$

$$\frac{V}{\epsilon} = \frac{\epsilon_0 A}{4\pi^2 m^2} \cdot \frac{1}{3!} \frac{1}{4!} =$$

$$\frac{V}{\epsilon} = \frac{\epsilon_0 A}{4\pi^2 m^2} \cdot \frac{1}{3!} \frac{1}{4!} =$$

11

$$\frac{V}{\epsilon} = \frac{\epsilon_0 A}{4\pi^2 m^2} \cdot \frac{1}{3!} \frac{1}{4!} =$$

$$\begin{aligned}
 & \text{in my notes!} \\
 & \text{definition of } u^{(3)} \\
 & \text{possibly incorrect} \\
 & u^{(3)} = \frac{\partial^3}{\partial t^3} \cdot \frac{m_1}{m_2 m_3} e^{3\sqrt{\mu}} \\
 & u^{(3)} = \frac{\partial^3}{\partial t^3} \cdot \frac{m_1}{m_2 m_3} e^{3\sqrt{\mu}} \\
 & u^{(3)} = \left[ u^{(2)} \cdot \frac{\partial^2}{\partial t^2} \cdot \frac{m_1}{2H_1} \right] = \\
 & u^{(2)} = \frac{1}{2} \frac{H_1}{m_1} \cdot \frac{H_2}{m_2} \cdot \frac{H_3}{m_3} \cdot \frac{\partial^2}{\partial t^2} \cdot \frac{m_1}{2H_1} \\
 & u^{(2)} = u^{(1)} \sin(\omega_T t - \phi_s) \quad (1)
 \end{aligned}$$

$$\begin{aligned}
 & \text{initial project} \\
 & u^{(1)} = \frac{1}{4H_1 m_3} \cdot \frac{\chi_2}{Z^2 P_{12}^2} \\
 & u^{(1)} = \frac{k}{2} \cdot \frac{1}{H_1} \cdot \frac{3}{H_2} \cdot \frac{1}{H_3} \cdot u^{(2)} \cdot G(P_{12}) = F_u \cos(\omega_T t) \quad (1)
 \end{aligned}$$

$$\begin{aligned}
 & u^{(1)} = - u^{(1)} G(P_{12}) = \\
 & u^{(1)} = - u^{(1)} G(P_{12}) \cdot \frac{H_2}{2ZP_{12}^2} \cdot \frac{\chi_2}{H_1} = F_u \sin(\omega_T t - \phi_s) \quad (1)
 \end{aligned}$$

$$\begin{aligned}
 & u^{(1)} = \frac{1}{2m_3} \cdot \frac{H_2}{H_1} \cdot \frac{1}{Z^2 m_2 H_2^2} \cdot \left( \frac{\chi_2}{Z^2 P_{12}^2} \right) \cdot G(P_{12}) = \\
 & u^{(1)} = \frac{1}{2m_3} \cdot \frac{H_2}{H_1} \cdot \frac{1}{Z^2 m_2 H_2^2} \cdot \left( \frac{\chi_2}{Z^2 P_{12}^2} \right) \cdot \left( \frac{\chi_2}{Z^2 P_{12}^2} \right) = 
 \end{aligned}$$

$$\begin{aligned}
 & F_u \sin(\omega_T t + \phi_s) = u^{(1)} \cdot \frac{H_2}{H_1} \cdot \frac{1}{Z^2 m_2 H_2^2} \cdot \frac{H_2}{H_1} \cdot e^{-\frac{P_{12}^2}{\chi_2}} \quad \text{initial project} \\
 & F_u \sin(\omega_T t + \phi_s) = F_u \sin(\omega_T t + \phi_s) \quad (1)
 \end{aligned}$$

Leading first de

and  $\left(\begin{matrix} AB \\ C \\ D \end{matrix}\right) = \frac{V}{2} \sqrt{m_1 m_2}$

$$4m_1 m_2 \underbrace{\left(\begin{matrix} V \\ 2P_{H_2} \\ 6(2) \\ 48 \end{matrix}\right)}$$

$$= \frac{V}{2} \sqrt{m_1 m_2} \cdot \frac{H_2}{H_1} \cdot \frac{f}{f} = \frac{V}{2} \sin 2\phi \quad (VII)$$

and  $\left(\begin{matrix} AB \\ C \\ D \end{matrix}\right) = \frac{V}{2} \sqrt{m_1 m_2}$

$$\frac{V}{2} \sqrt{m_1 m_2} \cdot \frac{H_2}{H_1} \cdot \frac{f}{f} \cdot \frac{H_1}{H_2} = \frac{V}{2} \sin 2\phi \quad (VIII)$$

16

$$(V) F_{LT} \cos(\phi_2 - \phi_1) - C_D \cdot$$

$$\text{left side} = \frac{\partial}{\partial x} \left( \frac{\partial u_{12}}{\partial x} \right) = \frac{\partial^2 u_{12}}{\partial x^2}$$

~~cosine~~

~~$\int \sin^2 x \cdot \sin^2(x+2\pi/3)$~~

~~$\int \sin^2 x \cdot \sin^2(x+2\pi/3) \cdot \frac{1}{2} \times \frac{\partial}{\partial x} =$~~

$$(x \int_0^{2\pi/3} x^2 dx)^2 = \left( \int_0^{2\pi/3} x^2 dx \right)^2 = \frac{1}{2} \int_0^{2\pi/3} x^4 dx = \frac{1}{2} \int_0^{2\pi/3} x^4 dx =$$

$$(\cos(2\phi - \phi)) = -\frac{1}{2} \times \int_0^{2\pi/3} x^4 dx = \frac{1}{2} \int_0^{2\pi/3} x^4 dx =$$

(ii)

$$\int_0^{2\pi/3} x^4 dx = -\frac{1}{2} \times \int_0^{2\pi/3} x^4 dx =$$

$$(x \int_0^{2\pi/3} x^2 dx)^2 = (x \int_0^{2\pi/3} x^2 dx)^2 \times x$$

$$\int_0^{2\pi/3} x^4 dx = \frac{1}{2} \int_0^{2\pi/3} x^4 dx =$$

$$R_{\text{left}} = \frac{1}{2} \int_0^{2\pi/3} x^4 dx = \frac{1}{2} \int_0^{2\pi/3} x^4 dx =$$

$$A_{\text{left}} = \frac{1}{2} \int_0^{2\pi/3} x^4 dx = \frac{1}{2} \int_0^{2\pi/3} x^4 dx =$$

{Z!}

A<sub>left</sub> ≈ 0 in WCD-type modelling to derive

different procedure

$$\int \left[ \cdots Q_T(x) \frac{d\omega}{h \cdot P} - \left( \frac{\partial}{\partial h} H_T \right) \right] = \text{(vi)} \quad F_{\text{diff}}^u = \frac{\partial}{\partial h} C - \frac{\partial}{\partial h} \left( x_h H_T \right)$$

$\omega_3$        $\omega_4$

(1)

different procedure

my calculation: keep original TTD (+ original  $P, k_T$ )  
and then use WO-type approximation!

and do integrations after  $P, k_T$

result after did: let use WO-type to replace  $h_L + h_R$

$\neq$  Allex, see Eq.(B23, B24)

$$\left| \frac{\partial}{\partial h} \int \left( \frac{\partial}{\partial h} H_T \right) f \right| = \frac{\partial}{\partial h} \left( \frac{\partial}{\partial h} \int h_L(x) H_T \right) \times \frac{\partial}{\partial h} =$$

$$\int \cdots \stackrel{\omega_A}{\mathcal{L}} \cdots =$$

$$\boxed{\text{(8)}} \quad \int \left[ \frac{\partial}{\partial h} H_T \right] \frac{\partial}{\partial h} + \int \frac{\partial}{\partial h} \left[ \cdots \right] = \text{(11)} \quad F_{\text{diff}}^u = \int \cdots \frac{\partial}{\partial h} C - \frac{\partial}{\partial h} \left( x_h H_T \right) + \cdots$$

19

Simplifying

$$F_{ut} = \frac{\partial H}{\partial t} C \left[ \omega_{03} \alpha - \frac{P_r \cdot K_r}{2 \pi n_0 m_u} (x_{h_r} - x_{l_r}) \right]$$

order  
in  $F_{H^+}$

0

1

2

3

4

5

6

7

8

9

10

order  
in  $F_{H^+}$

$$F_{nn} = F_{nn,T}$$

$$\ln \frac{Q^2}{Q_0^2}$$

$$\ln \frac{Q^2}{Q_0^2} + \frac{1}{2}$$

$$\ln \frac{Q^2}{Q_0^2} - \frac{1}{2}$$

$$\ln \frac{Q^2}{Q_0^2} - \frac{1}{2}$$

$$\ln \frac{Q^2}{Q_0^2} - \frac{1}{2}$$

$$\ln \frac{Q^2}{Q_0^2} + \frac{1}{2}$$

$$\ln \frac{Q^2}{Q_0^2} - \frac{1}{2}$$

1

2

3

4

5

6

7

8

9

10

$$\begin{aligned}
 & \text{denominator: } k_T^2 \\
 & = x \sum_a e_a^2 \int dp_T \int dk_T \left( 2p_T^2 + k_T^2 - p_{T_a}^2 \right) \partial f(x, p_T) \partial f(k_T) \\
 & \text{subst. } k_T^2 = -\frac{2}{K^2} \\
 & \text{with } C[0 \neq 1] = x \sum_a e_a^2 \int dp_T \int dk_T \left( p_T^2 - k_T^2 - \frac{p_{T_a}^2}{2} \right) \partial f(x, p_T) \partial f(k_T)
 \end{aligned}$$

$$\begin{aligned}
 & \text{function of } p_T, k_T, h_T \\
 & \text{with } h_T = \frac{p_{T_a}}{p_T} \\
 & \text{i.e. } B = \left( -h_T - \frac{2H_m}{p_T^2} h_{T_a}^2 + \dots + h_T - \frac{p_{T_a}^2}{p_T^2} h_{T_a}^2 \right) H_T
 \end{aligned}$$

$$\begin{aligned}
 & \text{zero in DIO} \\
 & x h_T - h_{T_a} - \frac{2H_m}{p_T^2} h_{T_a}^2 + \underbrace{m_a \frac{g_{T_a}}{H_T}}_{\text{zero in DIO}} - \frac{p_{T_a}^2}{p_T^2} h_{T_a}^2 = x h_T + h_{T_a} - \frac{2H_m}{p_T^2} h_{T_a}^2 \\
 & B = x h_T H_T + \underbrace{\frac{m_a}{H_T} g_{T_a}}_{\text{zero in DIO}} + \underbrace{\frac{2}{p_T^2} H_T^2}_{\text{zero in DIO}} - \frac{m_a}{H_T} h_{T_a}^2
 \end{aligned}$$

$$\begin{aligned}
 & \text{with: } A = x \cancel{f_{T_a}} - \underbrace{\frac{m_a}{H_T} h_{T_a}^2}_{\text{zero in DIO-type}} \cancel{f_{T_a}} = \\
 & \text{below } k_T^2 = -\frac{2}{K^2} \text{ so thus sign changes} \\
 & \boxed{B = \left[ \frac{2(h_T \cdot k_T)(h_T \cdot p_T) - k_T \cdot p_T}{2H_m m_a} \right] \frac{2(h_T \cdot k_T)(h_T \cdot p_T) - k_T \cdot p_T}{2H_m m_a}}
 \end{aligned}$$

$$\begin{aligned}
 & \sin(2\varphi - \varphi_0) = \frac{2H}{2H} C \left[ \frac{2(h_T \cdot p_T) - p_T^2}{2H_m^2} \cdot A \right]
 \end{aligned}$$

$$4\omega_0 + \left[ \frac{\langle K_T^2 \rangle / \langle P_T^2 \rangle}{2} - \frac{1}{P_T^2} \right] \cdot \left( \frac{\langle P_T^2 \rangle + \langle K_T^2 \rangle}{2} \right) =$$

$$\langle K_T^2 \rangle + \left[ \dots \right] =$$

$$\left[ \dots \right] + \left[ \frac{\left( \frac{\langle K_T^2 \rangle + \langle P_T^2 \rangle}{2} \right) \cdot \langle K_T^2 \rangle}{2 P_T^2} - \frac{1}{P_T^2} \right] \cdot \left( \frac{\langle P_T^2 \rangle + \langle K_T^2 \rangle}{2} \right) =$$

$$\frac{\langle K_T^2 \rangle}{P_T^2} + \frac{\langle K_T^2 \rangle}{2 P_T^2} - \frac{1}{2 P_T^2} \cdot \frac{\langle K_T^2 \rangle}{2 P_T^2} = \frac{\langle P_T^2 \rangle + \langle K_T^2 \rangle}{2}$$

now: - argument of exponential =  $\frac{\langle P_T^2 \rangle}{2} + \frac{\langle K_T^2 \rangle}{2 P_T^2} - \frac{1}{2 P_T^2} \cdot \frac{\langle K_T^2 \rangle}{2 P_T^2}$

$$\frac{\langle K_T^2 \rangle}{2 P_T^2} - \frac{\langle K_T^2 \rangle}{2 P_T^2} \cdot \exp \left( - \frac{\langle P_T^2 \rangle}{2 P_T^2} \right) = \int_0^{\infty} \frac{2 \pi R^2}{2 P_T^2} \cdot \frac{\langle K_T^2 \rangle}{2 P_T^2} \cdot \exp \left( - \frac{\langle P_T^2 \rangle}{2 P_T^2} \right) dR$$

$$C \cdot A = \int_0^{\infty} \frac{2 \pi R^2}{2 P_T^2} \cdot \frac{\langle K_T^2 \rangle}{2 P_T^2} \cdot \exp \left( - \frac{\langle P_T^2 \rangle}{2 P_T^2} \right) dR$$

solve series, integrals: [1st part]

B = analog

$$A = \int_{P_T}^{\infty} f_{\Gamma}(x, P_T) D(x, K_T) e^{-\frac{x^2}{2 P_T^2}} dx = \frac{\pi \langle K_T^2 \rangle}{2 P_T^2} e^{-\frac{\langle K_T^2 \rangle}{2 P_T^2}}$$

assume gaussian model:

$$\frac{\langle K_T^2 \rangle + \langle R_T^2 \rangle}{\langle P_T^2 \rangle} = P_T - \frac{P_{hT}}{\langle P_T^2 \rangle}$$

next step: substitute  $P_T \rightarrow P'_T = P_T - \frac{P_{hT}}{\langle P_T^2 \rangle}$

general result A similar finding! result depends on  $\log \eta$

$$\int \frac{\left( \frac{\langle K_T^2 \rangle + \langle R_T^2 \rangle}{\langle P_T^2 \rangle} + \frac{\langle K_T^2 \rangle}{\langle P_T^2 \rangle} \right) e^{-\left( \frac{\langle K_T^2 \rangle}{\langle P_T^2 \rangle} + \frac{\langle R_T^2 \rangle}{\langle P_T^2 \rangle} \right)} dP_T}{\langle P_{hT} \rangle} = \frac{\langle K_T^2 \rangle}{\langle P_T^2 \rangle} e^{-\frac{\langle K_T^2 \rangle}{\langle P_T^2 \rangle}}$$

with  $\ln f(P_{hT}) = \int dP_T \text{ weight}(P_T, P_{hT}) / \langle P_T^2 \rangle = P_{hT} - \frac{P_{hT}}{\langle P_T^2 \rangle}$

$$[\ln f(P_{hT})] = x \int \frac{e^{2 \int f_{hT}(x) dx}}{\langle P_{hT}^2 \rangle} e^{-\frac{\langle K_T^2 \rangle}{\langle P_{hT}^2 \rangle}}$$

therefore, this can be numerically easily after convolution integration only

$$\frac{\langle K_T^2 \rangle + \langle R_T^2 \rangle}{\langle P_{hT}^2 \rangle} = \frac{\langle K_T^2 \rangle}{\langle K_T^2 \rangle}$$

$$\left( \frac{E^2 + \frac{\langle K_T^2 \rangle}{\langle P_T^2 \rangle}}{E^2 + \frac{\langle K_T^2 \rangle}{\langle P_T^2 \rangle}} \right)$$

$$\left( 1 + \frac{\frac{\langle K_T^2 \rangle}{\langle P_T^2 \rangle}}{E^2} \right) - \frac{\langle K_T^2 \rangle}{\langle P_{hT}^2 \rangle} =$$

$$\left( \frac{\langle K_T^2 \rangle}{1} + \frac{\langle K_T^2 \rangle (\langle P_T^2 \rangle^2 + \langle E^2 \rangle)}{E^2} \right) - \frac{\langle K_T^2 \rangle}{\langle P_{hT}^2 \rangle} = 1$$

$$\frac{2H_0^2 (e^{2\langle P_T \rangle} + \langle K_T^2 \rangle)}{e^{2\langle P_T \rangle}} =$$

~~$$I_{n+1}(P_{h1}) = \frac{\pi \langle A \rangle \langle K_T^2 \rangle}{e^{2\langle P_T \rangle} + \langle K_T^2 \rangle} \cdot \frac{1}{e^{2\langle P_T \rangle} + \langle K_T^2 \rangle} \cdot \frac{2^2 P_{h1}}{2^2 \langle P_T \rangle}$$~~

$$\frac{\langle A \rangle \langle K_T^2 \rangle}{e^{2\langle P_T \rangle} + \langle K_T^2 \rangle} = \frac{\langle A \rangle \langle K_T^2 \rangle}{e^{2\langle P_T \rangle} + \langle K_T^2 \rangle} \cdot \frac{1}{e^{2\langle P_T \rangle} + \langle K_T^2 \rangle}$$

$$I_{n+1}(P_{h1}) = \frac{1}{e^{2\langle P_T \rangle}} \cdot \frac{2^2 H_0^2}{e^{2\langle P_T \rangle} + \langle K_T^2 \rangle} \int dP_T e^{-\left(\frac{1}{2} \langle P_T^2 \rangle + \frac{2^2}{2} \langle K_T^2 \rangle\right) P_T^2}$$

also notice that  $\langle h \cdot P_{h1} \rangle = P_{h1}$

due to:  $\int dP_T 2(h \cdot P_T)^2 = 2 \int dP_T h^2 P_T^2$

cancel out

$$= \frac{1}{e^{2\langle P_T \rangle}} \left\{ 2(h \cdot P_{h1})^2 + 2 \frac{e^2 \langle h \cdot P_{h1} \rangle^2}{e^{2\langle P_T \rangle} + \langle K_T^2 \rangle} - \frac{e^{-\left(\frac{1}{2} \langle P_T^2 \rangle + \frac{2^2}{2} \langle K_T^2 \rangle\right) P_{h1}^2}}{e^{2\langle P_T \rangle} + \langle K_T^2 \rangle} \right\}$$

$$= \int dP_T \frac{2 \left[ h \cdot (P_{h1} + \frac{e^2 P_{h1}}{e^{2\langle P_T \rangle}}) \right]^2 - (P_{h1} + \frac{e^2 P_{h1}}{e^{2\langle P_T \rangle}})^2}{e^{2\langle P_T \rangle}}$$

here:  $I_{n+1}(P_{h1}) = \int dP_T \frac{2 (h \cdot P_{h1})^2 - P_{h1}^2}{e^{2\langle P_T \rangle}} \cdot e^{-\left(\frac{1}{2} \langle P_T^2 \rangle + \frac{2^2}{2} \langle K_T^2 \rangle\right) P_{h1}^2}$

$$\int \left[ \begin{aligned} & + 2 \cdot 2 \frac{p_t}{p_{t1}} \cdot 2 \frac{p_t}{p_{t2}} \left( \frac{p_{t1}}{p_{t2}} \cdot \frac{p_{t2}}{p_{t1}} - 2z \cdot 2 \left( h \cdot \frac{p_t}{p_{t1}} \right) \cdot 2 \frac{p_{t1}}{p_{t2}} \cdot \frac{p_{t2}}{p_{t1}} \right) \\ & + 2z \frac{p_t}{p_{t1}} \cdot \frac{p_t}{p_{t2}} \left( \frac{p_{t1}}{p_{t2}} \cdot \frac{p_{t2}}{p_{t1}} - 2z \cdot 2 \left( h \cdot \frac{p_t}{p_{t1}} \right) \cdot 2 \frac{p_{t1}}{p_{t2}} \cdot \frac{p_{t2}}{p_{t1}} \right) \\ & + 2 \frac{p_t}{p_{t1}} + 2^3 \frac{p_t}{p_{t2}} \cdot \frac{p_{t1}}{p_{t2}} \end{aligned} \right] = \int d \frac{p_t}{p_{t1}} \left( \frac{p_{t1}}{p_{t2}} + 2^2 \frac{p_t}{p_{t2}} \cdot \frac{p_{t1}}{p_{t2}} - 2z \cdot 2 \left( h \cdot \frac{p_t}{p_{t1}} \right)^2 - 2^2 \frac{p_t}{p_{t2}} \cdot \frac{p_{t1}}{p_{t2}} \right) =$$

$$\begin{aligned} & + 2 \cdot \int \left( \frac{p_{t1}}{p_{t2}} + 2 \frac{p_t}{p_{t2}} \cdot \frac{p_{t1}}{p_{t2}} - 2z \left( h \cdot \frac{p_t}{p_{t1}} + 2 \frac{p_t}{p_{t2}} \cdot \frac{p_{t1}}{p_{t2}} \right) \right) e^{- \frac{1}{2} \left( \frac{p_t}{p_{t1}} + 2 \frac{p_t}{p_{t2}} \cdot \frac{p_{t1}}{p_{t2}} \right)^2} \\ & = \dots * \int d \frac{p_t}{p_{t1}} \left( \frac{p_{t1}}{p_{t2}} + 2^2 \frac{p_t}{p_{t2}} \cdot \frac{p_{t1}}{p_{t2}} \right) e^{- \frac{1}{2} \left( \frac{p_t}{p_{t1}} + 2^2 \frac{p_t}{p_{t2}} \cdot \frac{p_{t1}}{p_{t2}} \right)^2} = \\ & = \dots * \int d \frac{p_t}{p_{t1}} \left( \frac{p_{t1}}{p_{t2}} - 2z \left( h \cdot \frac{p_t}{p_{t1}} + 2^2 \frac{p_t}{p_{t2}} \cdot \frac{p_{t1}}{p_{t2}} \right) \right) e^{- \frac{1}{2} \left( \frac{p_t}{p_{t1}} - 2z \left( h \cdot \frac{p_t}{p_{t1}} + 2^2 \frac{p_t}{p_{t2}} \cdot \frac{p_{t1}}{p_{t2}} \right) \right)^2} = \end{aligned}$$

$$\begin{aligned} & = \dots * \int d \frac{p_t}{p_{t1}} \frac{p_{t1}}{p_{t2}} \left[ 2 \left( p_{t1} - 2 \frac{p_t}{p_{t1}} \cdot h \right) \left( h \cdot \frac{p_t}{p_{t1}} \right) - \left( p_{t1} \cdot \frac{p_t}{p_{t1}} - 2 \frac{p_t}{p_{t2}} \right) \right] = \\ & \quad \text{with } \text{int} \equiv \frac{\pi \langle p_t^2 \rangle \langle k_t^2 \rangle}{\langle p_t^2 \rangle + \langle k_t^2 \rangle} \end{aligned}$$

$$\begin{aligned} & \text{with } \text{int} \equiv \frac{\pi \langle p_t^2 \rangle \langle k_t^2 \rangle}{\langle p_t^2 \rangle + \langle k_t^2 \rangle} \\ & \text{WW-type!} \quad k_t = \frac{p_{t1} - 2 \frac{p_t}{p_{t1}} \cdot h}{h} \quad \int d \frac{p_t}{p_{t1}} \frac{p_{t1}}{p_{t2}} \left( 2 \left( h \cdot \frac{p_t}{p_{t1}} \right) \left( h \cdot \frac{p_t}{p_{t1}} \right) - \left( h \cdot \frac{p_t}{p_{t1}} \right)^2 \right) = \\ & = \int \frac{1}{\frac{p_{t1}}{p_{t2}} - 2 \frac{p_t}{p_{t1}} \cdot h} \left( -2 \int e^{2 \frac{h^2}{2} \text{H}_{\text{int}}^2(x) H_{\text{int}}^2} \cdot e^{-\frac{1}{2} \frac{(p_{t1} - 2 \frac{p_t}{p_{t1}} \cdot h)^2}{2 \text{H}_{\text{int}}^2}} \right) = \boxed{C \left[ \text{int} \right]} \end{aligned}$$

from  $k_t \leftarrow -\frac{k_t}{2}$ 

2nd part:

$$C_1 \cdot B = \frac{2H_N m_n}{\langle P_{h1}^2 \rangle^2} \cdot \frac{\langle P_{h1}^2 \rangle \langle k_{t1}^2 \rangle^2}{\langle P_{h1}^2 \rangle^2} \cdot (-2 \sum_{i=1}^n h_i L_a^i \ln L_a^i) \cdot e^{-\frac{A}{k_{t1}^2}}$$

$$\frac{2H_N^2 A^3}{\langle P_{h1}^2 \rangle^2 \langle k_{t1}^2 \rangle^2}$$

$$A = \frac{2 \pi \langle k_{t1}^2 \rangle \langle P_{h1}^2 \rangle}{2 H_N^2 A^2} \cdot \frac{\langle P_{h1}^2 \rangle \langle k_{t1}^2 \rangle^2}{\langle P_{h1}^2 \rangle^2} = \frac{\pi \langle k_{t1}^2 \rangle \langle P_{h1}^2 \rangle}{A^2}$$

II =

$$\begin{aligned} I = & \left[ -\frac{\partial}{\partial \alpha} \int dP_{h1}^2 e^{-\alpha k_{t1}^2} \right] = \\ & \left[ -\frac{\partial}{\partial \alpha} \int dP_{h1}^2 e^{-\alpha k_{t1}^2} \right] = \\ & \frac{1}{(\langle P_{h1}^2 \rangle + \frac{B^2}{k_{t1}^2})^2} \cdot \int dP_{h1}^2 k_{t1}^2 e^{-\frac{k_{t1}^2}{B^2}} \\ & \underbrace{\left( \int dP_{h1}^2 P_{h1}^2 \exp \left( -\left( \frac{1}{k_{t1}^2} + \frac{B^2}{k_{t1}^2} \right) P_{h1}^2 \right) \right)}_{\text{the integral}} = \\ & \frac{2 \pi \langle k_{t1}^2 \rangle \langle P_{h1}^2 \rangle}{2 H_N^2 A^2} \cdot \int dP_{h1}^2 P_{h1}^2 \left( \frac{1}{k_{t1}^2} + \frac{B^2}{k_{t1}^2} \right)^{-1} e^{-\frac{P_{h1}^2}{B^2}} \end{aligned}$$

$$+ 2 \pi \left( P_{h1}^2 \cdot P_{h1}^2 \right)^2 \frac{A}{\langle P_{h1}^2 \rangle} \left( \frac{A}{\langle P_{h1}^2 \rangle} - 1 \right) \int \left( \frac{A}{\langle P_{h1}^2 \rangle} - 1 \right)^2 e^{-\frac{P_{h1}^2}{B^2}}$$

$$\left[ \left( P_{h1}^2 + \frac{B^2}{k_{t1}^2} \right)^2 \cdot \frac{A}{\langle P_{h1}^2 \rangle} \left( \frac{A}{\langle P_{h1}^2 \rangle} - 1 \right) \int \frac{A}{\langle P_{h1}^2 \rangle} \cdot \int dP_{h1}^2 \right]$$

$$\int \frac{V}{M^3} \frac{d\tau}{dt} \frac{d\theta}{dt} \frac{d\phi}{dt} e^{-\frac{\phi}{A_2}} H_{T^4(a)}(z) - h_{T^4(a)}(x) H_{T^4(a)}(z)$$

$$\frac{\partial}{\partial x} \int \frac{V}{M^3} \frac{d\tau}{dt} \frac{d\theta}{dt} \frac{d\phi}{dt} e^{-\frac{\phi}{A_1}} H_{T^4(a)}(z) =$$

$$\int \frac{V}{M^3} \frac{d\tau}{dt} \frac{d\theta}{dt} \frac{d\phi}{dt} e^{-\frac{\phi}{A_2}} H_{T^4(a)}(z) - 2x \int \frac{V}{M^3} \frac{d\tau}{dt} \frac{d\theta}{dt} \frac{d\phi}{dt} e^{-\frac{\phi}{A_2}} H_{T^4(a)}(z)$$

$$\sin(\phi - \phi_s) = \frac{\partial}{\partial x} \left[ \int \frac{V}{M^3} \frac{d\tau}{dt} \frac{d\theta}{dt} \frac{d\phi}{dt} e^{-\frac{\phi}{A_2}} H_{T^4(a)}(z) \right]$$